

Experimental Studies on Co-pyrolysis of Biomass and Plastic Waste

Debalaxmi Pradhan



Department of Chemical Engineering

National Institute of Technology Rourkela

Experimental Studies on Co-Pyrolysis of Biomass and Plastic Waste

Dissertation submitted in partial fulfilment

of the requirements of the degree of

Doctor of Philosophy

in

Chemical Engineering

by

Debalaxmi Pradhan

(Roll Number: 511CH108)

based on research carried out

under the supervision of

Prof. R.K.Singh



August 4, 2017

Department of Chemical Engineering

National Institute of Technology Rourkela



Department of Chemical Engineering
National Institute of Technology Rourkela

August 4, 2017

Certificate of Examination

Roll Number: *511CH108*

Name: *Debalaxmi Pradhan*

Title of Dissertation: Experimental Studies on Co-pyrolysis of Biomass and Plastic Waste

We the below signed, after checking the dissertation mentioned above and the official record book (s) of the student, hereby state our approval of the dissertation submitted in partial fulfillment of the requirements of the degree of *Doctor of Philosophy* in *Chemical Engineering* at *National Institute of Technology Rourkela*. We are satisfied with the volume, quality, correctness, and originality of the work.

Prof R.K Singh
Principal Supervisor

Member, DSC

Member, DSC

Member, DSC

External Examiner

Chairperson, DSC

Head of the Department



Department of Chemical Engineering
National Institute of Technology Rourkela

Prof. R.K.Singh

Professor

August 4, 2017

Supervisor's Certificate

This is to certify that the work presented in this dissertation entitled “*Experimental studies on co-pyrolysis of biomass and plastic waste*” submitted by Roll Number 511CH108 is a record of original research carried out by her under my supervision and guidance in partial fulfilment of the requirements of the degree of Doctor of Philosophy in Chemical Engineering. Neither this dissertation nor any part of it has been submitted for any degree or diploma to any institute or university in India or abroad.

R.K.Singh
Professor

Dedication

**Dedicated to My Parents and my Son
(Raghunandan) for their Unconditional Love,
Constant Support and Sacrifice**

Declaration of Originality

I, Debalaxmi Pradhan, Roll Number- 511CH108 hereby declare that this dissertation entitled "*Experimental studies on co-pyrolysis of biomass and plastic waste*" represents my original work carried out as a doctoral student of NIT Rourkela and, to the best of my knowledge, it contains no material previously published or written by another person, nor any material presented for the award of any other degree or diploma of NIT Rourkela or any other institution. Any contribution made to this research by others, with whom I have worked at NIT Rourkela or elsewhere, is explicitly acknowledged in the dissertation. Works of other authors cited in this dissertation have been duly acknowledged under the section "Bibliography". I have also submitted my original research records to the scrutiny committee for evaluation of my dissertation.

I am fully aware that in case of any non-compliance detected in future, the Senate of NIT Rourkela may withdraw the degree awarded to me on the basis of the present dissertation.

August 4, 2017

Debalaxmi Pradhan

NIT Rourkela

Acknowledgment

This study would have never been accomplished without the support, assistance, and motivation provided by those around me.

In particular, I would like to thank my supervisor Prof. (Dr.) R. K. Singh for his help and guidance during the period of research. I feel indebted to my supervisor for giving abundant freedom to me for pursuing new ideas.

I express my deep sense of gratitude to the members of my Doctoral Scrutiny Committee Dr. H.M Jena, Dr. Santanu Paria and Dr. Abanti Sahoo of Chemical Engineering Department for thoughtful advice during discussion sessions. I express my gratitude and indebtedness to Prof. K. C. Biswal, Prof. P. Rath, Prof. S. K. Agarwal, Dr. Madhusree Kundu, Dr. Susmita Mishra, Dr. Basudeb Munshi, Dr. Arvind Kumar, Dr. Pradip Chowdhury, Dr. Sujit Sen and Dr.S.S. Mohapatra, of Chemical Engineering Department, for their valuable suggestions and instructions at various stages of the work.

My heartfully thanks to Dr. T.N Tiwari (Unique Research Center, Rourkela) for his valuable support during this work. My special thanks to Mr. Satyam Naidu Vasireddy, Mr Suresh chaluvadi, Mr Ravi, and Miss Bageshwari Sanga for their lots of support during the time of experiment and thesis writing.

I would like to also thank full to Prof. Murugan of Department of Mechanical Engineering and his student Mr. Harisankar Bendu, and supporting staff of mechanical engineering Mr Ramakrishna for their support in I. C. Engine lab, Mechanical Engineering Department.

I also thank to staff members of Chemical Engineering Department for their constant help throughout the work. This work also would not have been possible without the help of all the research group members. I would like to express my gratitude to my research group Namrata Kumari, Sowhm Swain Mohapatra, Arvind Kumar, and other research colleagues for their support and good wishes.

Finally, I express my humble regards to my parents, Father in-laws, Mother in-law, my husband, my brother, my sisters, sister in-laws, brother in-laws for their immense support, sacrifice and their unfettered encouragement at all stages.

August 4, 2017
NIT Rourkela

Debalaxmi Pradhan
Roll Number: 511ch108

Abstract

The depletion rate of non-renewable resources and their utility, which mostly ends up in polluting the environment, are the major reasons for which biomass usage has come into the limelight. Energy production from biomass is mostly done by thermo-chemical and biological conversion routes among which pyrolysis is considered as the most appropriate and efficient thermo-chemical method for biomass conversion. The present work is mostly based on the co-pyrolysis of Mahua seed (*Madhuca indica*) with plastic. Mahua seed is a widely available biomass, whose pyrolysis at different conditions of heating rate, temperature and residence time yields around 49% of bio-oil. But this bio-oil is highly viscous, unstable, and has high water content, which limit its application. Therefore, co-pyrolysis of Mahua seed (MS) with plastic (Polystyrene) has been done in a semi-batch reactor in the presence of inert atmosphere in different blending ratios (9:1, 3:1, 4:1 and 1:1) at a constant heating rate of 20 °C/min and temperature ranging from 400-600 °C. A maximum of 74.25% bio-oil has been obtained at 1:1 blend which is higher by about 25.25% than the oil yielded from the pyrolysis of Mahua seed alone.

Also, this bio-oil, obtained at 525 °C with 1:1 blend, possesses better quality and quantity in comparison to the bio-oil from Mahua seed. It had lower oxygen, higher carbon and higher hydrogen contents, having higher calorific value than Mahua bio-oil, which has been characterized through elemental analysis. Due to the addition of plastic in biomass, the physical properties such as viscosity, water content, flash point, pH, distillation temperature, and carbon residue are decreased near to petroleum based fuel. The FTIR, GCMS and ¹H-NMR analyses show that there is a significant decrease in phenolic, acidic compound; however most of the functional groups present in co-pyrolysis oil are aromatic compounds. The FTIR spectrum of the oil obtained from the co-pyrolysis closely resembles to that of Polystyrene (PS) pyrolysis oil rather than that of Mahua bio-oil. Further GC-MS analysis shows that most of the compounds present in co-pyrolysis oil are similar to those of Polystyrene pyrolysis oil. The aliphatic compound present in co-pyrolysis oil reduced as

compared to the Mahua bio-oil. The co-pyrolysis oil could be ranked as carbon chain range of C_6 – C_{18} , which is the mixture of gasoline and diesel.

In addition to that, the by-product (bio-char) obtained from Mahua seed pyrolysis and co-pyrolysis at an optimum temperature of 525 °C was also characterized and it was found that the calorific value of co-pyrolysis bio-char is more than that of Mahua seed bio-char; however both are more than that of Indian standard coal. The pH of Mahua seed and co-pyrolysis bio-char were 11.9 and 12.5 respectively, which is probably good for acidic soils. From the SEM images of Mahua seed and co-pyrolysis bio-chars it can be concluded that co-pyrolysis bio-char is more porous than that of Mahua seed bio-char. The obtained surface area of co-pyrolysis bio-char is more than that of Mahua seed bio-char.

The results of the thermal kinetic study of Mahua seed, Polystyrene and co-pyrolysis kinetics of Mahua seed:Polystyrene 1:1 blend shows that the behavior of the blends are quite different to the combination of the individual materials of biomass and Polystyrene. The Mahua seed and Polystyrene 1:1 blend exists good interaction and significant synergic effect between the plastic and biomass co-pyrolysis. The values of Activation energy (E_A) and pre-exponential factor (A) are higher for mixtures than for individual components in the Kissinger method, whereas the activation energy and pre-exponential factors obtained for FWO and KAS methods of mixture were lower than those of individual one. The obtained kinetic parameters from Kissinger, KAS and FWO methods are good in agreement, but KAS and FWO methods are more efficient in the description of the degradation mechanism of solid-state reactions.

To further evaluate the efficiency of this upgraded bio-oil, engine performance study was carried out where the oil has performed well up to 60% blend whereas bio-oil from Mahua seed oil ran up to 30% with diesel blend. This analysis further bolsters the potentiality of the obtained bio-oil from co-pyrolysis to be used as an alternative fuel in combustion devices after proper treatments.

Keywords: Mahua seed, Polystyrene, Co-pyrolysis, Bio-oil, Bio-char, Kinetic study, Engine test.

Table of Contents

Certificate of Examination	ii
Supervisor's Certificate	iii
Dedication	iv
Declaration of Originality	v
Acknowledgment	vi
Abstract	viii
List of Figures	xv
List of Table	xvii
Abbreviations	xviii
Nomenclature	xviii
Chapter 1	1
Introduction	1
1.1 Introduction	1
1.2 Problem Statement	2
1.3 Solution strategies	3
1.4 Motivation of the work	3
1.5 Scope of this study	4
1.6 Organizations of thesis	4
Chapter 2	6
Literature Review	6
2.1 Introduction	6
2.2 Bio-oil	6
2.3 Problems associated with bio-oil	7
2.3.1 Water content	7
2.3.2 Oxygen content	7
2.3.3 Ash content	7
2.3.4 Viscosity	8
2.3.5 Density	8
2.3.6 Calorific value	8
2.3.7 pH	9
2.3.8 Chemical composition of bio-oil	9

2.4 Hydrodeoxygenation (HDO).....	10
2.5 Catalytic cracking.....	10
2.6 Steam reforming.....	11
2.7 Emulsification	12
2.8 Supercritical fluids (SCFs).....	12
2.9 Solvent addition/Esterification.....	13
2.10 Significance of co-pyrolysis.....	14
2.11 Feedstock for co-pyrolysis process	15
2.12 Availability of plastic.....	16
2.13 Importance of plastics in co-pyrolysis process	19
2.14 Mechanism of co-pyrolysis	23
2.15 Pyrolysis of non-edible seeds.....	24
2.16 Advantages of Polystyrene as co-feed stock in pyrolysis	27
2.17 Reaction kinetics of co-pyrolysis of biomass and plastic blends.....	28
2.18 Performance and emission analysis of bio-oil in IC engine.....	31
2.19 Concluding remarks	32
2.20 Objectives of the research work.....	33
Chapter 3.....	34
Experimental Section.....	34
3.1 Introduction	34
3.2 Raw Materials	34
3.2.1 Collection of biomass and plastic materials	34
3.2.2 Preparation of raw materials.....	35
3.3 Characterization of raw materials	35
3.3.1 Proximate and ultimate analysis	35
3.3.2 Thermogravimetric analysis	36
3.3.3 Thermal pyrolysis of feedstock	36
3.3.3.1 Thermal pyrolysis of Mahua seed, polystyrene and their mixture.....	36
3.3.3.2 Thermal co-pyrolysis of Mahua seed: polystyrene blend.....	38
3.4 Characterization of pyrolytic oil	39
3.4.1. Density.....	39
3.4.2. Calorific value	39
3.4.3. Viscosity.....	39
3.4.4 Distillation temperature	39
3.4.5 Water content and pH analysis	40

3.4.6. Conradson carbon residue	40
3.4.7 Flash point, fire point, pour point	40
3.4.8 FTIR analysis of pyrolytic liquid.....	41
3.4.9 ¹ H-NMR analysis of pyrolytic oil.....	41
3.4.10 GC–MS analysis of pyrolytic liquid.....	41
3.5 Characterization of bio-char.....	41
Chapter 4.....	43
Thermal pyrolysis of Mahua seed, polystyrene and their mixture.....	43
4.1 Introduction	43
4.2 Experimental Section	43
4.3 Analysis of feedstock	43
4.3.1 Characteristics of feedstocks	43
4.4 Thermogravimetric analysis	45
4.4.1 Thermal decomposition profile of Mahua seed, polystyrene and their mixture.....	45
4.4.2.1 Influence of temperature on pyrolysis product yield of Mahua seed.....	47
4.4.2.2 Comparison of thermal pyrolysis product yield of Mahua seed, Polystyrene with Co-pyrolysis yield.....	48
4.5 Characterization of pyrolytic oil	51
4.5.1 Elemental analysis of Pyrolytic oils	51
4.5.2 Physical properties of pyrolytic oil.....	52
4.5.3 Chemical properties analysis	56
4.5.3.1 Functional group analysis	56
4.5.3.2 Comparison study on GCMS analysis of MSPS co-pyrolysis oil with MS and PS pyrolysis oils.....	60
4.5.3.3. GCMS analysis of MS and MSPS aqueous phase	70
4.5.3.4 ¹ H-NMR analysis of MS, PS and MSPS pyrolytic oil.....	73
4.6 Characterization of bio-char.....	76
4.6.1 Physical characterizations of bio-char	76
4.6.1.1 Proximate and ultimate analyses of bio-char	76
4.6.1.2 Bulk density and pH of bio-char	78
4.6.1.3 SEM and BET analysis of bio-char (morphological characteristics).....	79
4.5 Conclusion.....	80
Chapter 5.....	82
Thermal kinetics of Mahua seed, Polystyrene and their mixtures	82
5.1 Introduction	82

5.2 Experimental and materials	83
5.2.1 Feed stock preparation.....	83
5.2.2 Equipment and procedure detail	83
5.3 Results and discussion.....	84
5.3.1 Thermal decomposition characteristics of raw materials and their mixture.....	84
5.3.1.1 Thermal decomposition characteristic of Mahua seed.....	84
5.3.2 Thermal decomposition characteristic of Polystyrene.....	86
5.3.3 Thermal decomposition characteristics of biomass/ plastic mixture.....	87
5.4 Kinetic modelling	88
5.5 Model-free methods	90
5.5.1 Kissinger method	90
5.5.2 Flynn-Wall-Ozawa method	90
5.5.3 Kissinger-Akahira-Sunose Method	91
5.6 Kinetic analysis	93
5.7 Conclusion.....	99
Chapter 6.....	100
Mahua seed pyrolysis oil blends as an alternative fuel for light-duty diesel engines.....	100
6.1 Introduction	100
6.2 Materials and Methods	102
6.2.1 Characterization of raw material	102
6.2.2 Characterization of MPO.....	102
6.2.3 Engine experimental setup.....	102
6.2.4 Uncertainty analysis	104
6.3 Results and Discussion.....	105
6.3.1 Pyrolysis of Mahua seed.....	105
6.3.1.1 Characterization of Mahua seed.....	105
6.3.2 Production of Mahua bio-oil.....	106
6.3.3 Characterization of Mahua bio-oil.....	107
6.4 Performance Parameters.....	109
6.4.1 Brake thermal efficiency (BTE)	109
6.4.2 Brake specific energy consumption (BSEC)	110
6.5 Emission parameters	111
6.5.1 Carbon monoxide (CO) emission	111
6.5.2 Hydrocarbon (HC) emission.....	112
6.5.3 Nitric oxide (NO) emission	113

6.5.4 Smoke opacity	114
6.4 Conclusions	115
Chapter 7	116
Application of co-pyrolysis oil in a diesel engine	116
7.1 Introduction	116
7.2 Materials and methods	118
7.2.1 Characterization of raw materials	118
7.2.2 Co-pyrolysis oil production	118
7.2.3 Characterization of co-pyrolysis oil	118
7.2.4 Engine experimental setup	118
7.3 Results and Discussion	118
7.3.1 Co-pyrolysis of Mahua seed:Polystyrene 1:1	118
7.3.1.1. Characterization of MSPS	118
7.3.1.2 Co-pyrolysis of MSPS	118
7.3.2 Characterization of CPO	119
7.3.2.1 Physical characterization of CPO	119
7.3.3 Chemical characterization of CPO	122
7.4 Performance parameter	122
7.4.1 Brake thermal efficiency	122
7.4.2 Brake specific energy consumption	123
7.5 Emission parameters	124
7.5.1 Carbon monoxide (CO) emission	124
7.5.2 Hydrocarbon (HC) emission	125
7.5.3 Nitric oxide (NO) emission	126
7.5.4 Smoke opacity	127
7.6 Conclusions	128
Chapter 8	129
Conclusion and future scope	129
8.1 Conclusion	129
8.2 Future Scope	132
References	133
Dissemination	145

List of Figures

Figure No.	Figure Caption	Page No.
Fig. 3.1	Mahua seed	34
Fig. 3.2	Polystyrene	34
Fig. 3.3	Mahua seed Powder	35
Fig. 3.4	Polystyrene Powder	35
Fig. 3.5	Pyrolysis setup	37
Fig. 3.6	Centrifuge	37
Fig. 3.7	Mahua seed pyrolysis oil	38
Fig. 3.8	Polystyrene pyrolysis oil	38
Fig. 3.9	MSPS pyrolysis oil with different blends at 525 °C	38
Fig. 3.10	MSPS 1:1 blend pyrolysis oil with different temperature	38
Fig. 3.11	Mahua seed biochar	38
Fig. 3.12	MSPS bio-char	38
Fig. 4.1	TGA plot of MS, PS and MSPS blend	46
Fig. 4.2	DTG plot of MS, PS and MS: PS blend	47
Fig. 4.3	Influence of temperature on pyrolysis product yields of Mahua seed	48
Fig. 4.4	Pyrolysis product yield of Polystyrene	49
Fig. 4.5	Co-pyrolysis of different ratio of MS:PS at 525 °C	50
Fig. 4.6	Co-pyrolysis of 1:1 ratio of MS:PS at different temperature	50
Fig. 4.7	Distillation curve of MS, PS and MSPS pyrolysis oil with other conventional fuel	54
Fig 4.8 (A)	FTIR analysis of MS pyrolysis oil	56
Fig 4.8 (B)	FTIR analysis of PS pyrolysis oil	56
Fig 4.8 (C)	FTIR analysis of MSPS pyrolysis oil	57
Fig. 4.9	GC–MS chromatogram of MS pyrolysis oil	63
Fig. 4.10	GC–MS chromatogram of PS pyrolysis oil	64
Fig. 4.11	GC–MS chromatogram of MSPS pyrolysis oil	70
Fig 4.12	GC–MS chromatogram of MS aqueous phase	71
Fig 4.13	GC-MS chromatogram of MSPS aqueous phase	71
Fig. 4.14 (A)	¹ H-NMR analysis of MS pyrolysis oil	75
Fig. 4.14 (B)	¹ H-NMR analysis of PS pyrolysis oil	75
Fig. 4.14 (C)	¹ H-NMR analysis of MSPS pyrolysis oil	76

Fig. 4.15	SEM image of MS bio-char 1000x	74
Fig. 4.16	SEM image of MS bio-char 500x	74
Fig. 4.17	SEM image of MSPS bio-char 1000x	75
Fig. 4.18	SEM image of MSPS bio-char 500x	75
Fig. 5.1	TGA plot of Mahua seed at different heating rate	80
Fig. 5.2	DTG plot of Mahua seed at different heating rate	80
Fig. 5.3	TGA plot of Polystyrene at different heating rate	81
Fig. 5.4	DTG plot of Polystyrene at different heating rate	82
Fig. 5.5	TGA plot of MS:PS 1:1 blend at different heating rate	83
Fig. 5.6	DTG plot of MS:PS (1:1) at different heating rate	83
Fig. 5.7	Kissinger plot of MS	90
Fig. 5.8	Kissinger plot of PS	90
Fig. 5.9	Kissinger plot of MS:PS	91
Fig. 5.10	Activation energy as a function of conversion for MS	91
Fig. 5.11	Activation energy as a function of conversion for PS	92
Fig. 5.12	Activation energy as a function of conversion for MSPS	92
Fig. 6.1	Engine Experimental setup	99
Fig. 6.2	Distillation curves of diesel and MPO fuel	104
Fig. 6.3	Variation of viscosity, flash and fire point temperatures with MPO blend ratio.	104
Fig. 6.4	Brake thermal efficiency with brake power for diesel and the MPO-diesel blends	106
Fig. 6.5	Brake specific energy consumption with brake power for diesel and the MPO-diesel blends.	107
Fig. 6.6	Carbon monoxide emission with brake power for diesel and the MPO-diesel blends	108
Fig. 6.7	HC emission with brake power for diesel and the MPO-diesel blends	109
Fig. 6.8	Nitric oxide emission with brake power for diesel and the MPO-diesel blends	110
Fig. 6.9	Smoke opacity with brake power for diesel and the MPO-diesel blends	111
Fig. 7.1	Brake thermal efficiency with brake power for diesel and the CPO-diesel blends	121
Fig. 7.2	Brake specific energy consumption with brake power for diesel and the CPO-diesel blends	122
Fig. 7.3	Carbon monoxide emission with brake power for diesel and the CPO-diesel blends	123
Fig. 7.4	HC emission with brake power for diesel and the CPO-diesel blends	124
Fig. 7.5	Nitric oxide emission with brake power for diesel and the CPO-diesel blends	125
Fig. 7.6	Smoke opacity with brake power for diesel and the CPO-diesel blends	126

Table No	Table Caption	Page No
Table. 2.1	Different types of plastic and its application	17
Table. 2.2	Various work related on co-pyrolysis of biomass and plastic	19
Table. 2.3	Production of bio-oil and their characteristics from pyrolysis of different seeds	25
Table. 2.4	Different methods for solid kinetic study	29
Table. 4.1	Proximate and Ultimate analysis of raw materials	44
Table. 4.2	Elemental analysis of pyrolytic oils	51
Table. 4.3	Physical properties of pyrolytic oil	53
Table. 4.4	FTIR analysis of MS pyrolytic oil	56
Table. 4.5	FTIR analysis of PS pyrolysis oil	57
Table. 4.6	FTIR analysis of MSPS pyrolysis oil	57
Table. 4.7	GC-MS analysis of MS pyrolysis oil	59
Table. 4.8	GC-MS analysis of PS pyrolysis oil	63
Table. 4.9	GC-MS analysis of MSPS pyrolysis oil	65
Table 4. 10	GC-MS analysis of MS aqueous phase	71
Table 4.11	GC-MS analysis of MSPS aqueous phase	72
Table.4.12	¹ H-NMR integration of MS MSPS and PS pyrolytic oil	78
Table.4.13	Proximate and ultimate analysis of bio-char	73
Table.5.1	The kinetic parameters activation energy (EA) and pre-exponential factor (A) obtained by Kissinger, KAS and FWO for MS, PS and MS: PS (1:1) blend	93
Table.6.1	Test engine specifications	100
Table.6.2	Details of Instrumentation used in the study	101
Table.6.3	Proximate and Ultimate analysis of different biomass seed	102
Table.6.4	Pyrolysis yield of Mahua seed	103
Table.6.5	Physical properties of MPO in comparison with diesel	105
Table. 7.1	Physical properties of CPO	118

Abbreviations

MS	Mahua Seed
PS	Polystyrene
MSPS	Mahua seed: Polystyrene
FTIR	Fourier transform infrared spectroscopy
GC-MS	Gas chromatography – Mass spectroscopy
NMR	Nuclear magnetic resonance
SEM	Scanning electron microscopy
BET	Brunauer-Emmet-Teller
KAS	Kissinger-Akahira-Sunose
FWO	Flyn-Wall-Ozawa
HDO	Hydrodeoxygenation
SCFs	Supercritical fluids
CHNSO	Carbon hydrogen nitrogen sulfur oxygen
TGA	Thermogravimetric analysis
MPO	Mahua pyrolysis oil
BTE	Brake thermal efficiency
BSEC	Brake specific energy consumption
CO	Carbon monoxide emission
HC	Hydrocarbon emission
NO	Nitric oxide emission
CPO	Co-pyrolysis oil
GCV	Gross calorific value

Nomenclature

E _a	Activation Energy
A	Pre-exponential Factor
R	Universal gas constant
X	Conversion
T	Time (sec)
T	Temperature (°C)
T ₀	Initial temperature (°C)
m _i	Initial mass of the sample
m _t	Sample mass at time ‘t’
m _f	Final mass of the sample
N	Order of the reaction
B	Linear heating rate
K	Rate constant
T _m	Peak Temperature (°C)
α	Degree of conversion

Chapter 1

Introduction

1.1 Introduction

Global economy has been greatly affected by primary energy supplies like fossil fuel resources. On the other hand the world energy markets significantly dependent on fossil fuel resources such as coal, natural gas, and petroleum products. According to the world energy council, 82% of the fossil fuel resources are covering to the current World energy needs [1]. Indeed, these fossil fuel reserves have certain limits and they are subject to decline as they are consumed exponentially. From the scientific evidence, it has been predicted that the average temperature of the earth surface is rising due to increased concentration of carbon dioxide (CO₂), and other greenhouse gasses create environmental pollution [2–4].

For solving these major issues, an alternative to fossil fuels has been provided here. Several researchers have been considering renewable energy sources such as solar energy, hydropower, geothermal, wind, and so on to alternate the use of fossil fuel. In the meantime, renewable energy resources like liquid fuel from biomass is the only source which can be the best substitute for fossil fuel. Biomass energy is the world's largest sustainable energy due to its inexpensive nature, is readily available in large quantities and also environment friendly [5–7]. However, biomass utilization can be considered as the suitable option and have been receiving great attention due to its less pollution. Furthermore, it has a great potential to overcome the required energy demand and could supply the fuel for future. The worldwide production of biomass is projected at 146 billion metric tons per year, which is mostly wild plant growth. Other than that farm crops and trees can produce 20 metric tons per acre of biomass per year. But a few types of algae and grasses may produce 50 metric tons per year [4].

Recent researchers have taken the great challenge to convert these biomass sources into various forms of energy via developed technology, those include the thermochemical, biological and physical processes. Among them, the utmost challenging techniques proposed for biomass energy conversion is pyrolysis. However, each of these methods has its own limitation and can be adopted to a certain extent. Pyrolysis lies at the heart of all the thermo-chemical fuel conversion processes and is assumed to become a path to petroleum-type product from biomass resources and also one of the sustainable development technology because it leads to the formation of more liquid fuel and also it can provide a solution towards the energy crises. Other than that, the liquid fuels from biomass have versatile applications in combustion, engines, boilers, turbines, etc [8].

Biofuels obtained from different agricultural crops is a technical feasible alternatives for fossil-based gasoline or diesel. Moreover, their use fit perfectly in the present situation and technology of our mobility [1].

1.2 Problem Statement

Biofuels from biomass could become the most suitable alternative for reducing CO₂ emission in the transport sector, at the same time it also improves the fuel efficiency and electrification of the light vehicle fleet. For heavy-duty vehicles, marine vessels and airplanes, in particular, biofuels can play an increasing role to reduce CO₂ emissions since electric vehicles and fuel cells are not feasible for these modes of transport. Also they have been considered for various advantages including energy security reasons, environmental concerns, foreign exchange savings, and socioeconomic issues related to the rural sector. Increasing use of biofuels for energy generation purposes is of particular interest nowadays because they allow mitigation of greenhouse gases, provide means of energy independence, and may even offer new employment possibilities. Bio-oil is recognized as a future commodity to substitute petroleum based fuel. However, the extent of research and large scale production is still very limited. This research mainly focused on the production of bio-oil but it did not focus on storage and further upgradation. Unlike fossil fuels, use of this liquid has received positive reviews as being a more environment friendly fuel because of its minimal contribution to greenhouse gases emission [9–13]. However, the stability of bio-oil produced from pyrolysis of biomass is often too low due to its high fractions of water and oxygen, which reduce the calorific value, corrosion problems and instability [14,15].

Therefore, the approach for building the energy value of pyrolytic bio-oil is required. Numerous studies have been undertaken to obtain a high-grade pyrolysis oil with low oxygen content and high calorific value using various upgrading processes. The most commonly used upgrading processes are hydrodeoxygenation (HDO), catalytic cracking, steam reforming, emulsification, supercritical fluids, esterification, etc. The process of catalytic cracking is a cheaper method than HDO; however, their results are not effective as there is a high coke formation of (8-25 wt %) and the obtained fuel quality is poor. Upgrading method of HDO received special attention because of the significant increase in hydrocarbon fuel during conversion of low-grade pyrolysis oil [16–18]. However, the complicated equipment, need for catalysts and high pressure requirement for the reaction has made the method very complex and costly. Similarly, steam reforming, emulsification, supercritical fluids, and esterification have also some advantages and limitations. Somehow, these processes are too expensive, not cost effective and not suitable for large-scale production. Therefore, a new approach is sought after to reduce this cost [19].

1.3 Solution strategies

Simplicity, effectiveness and economy are the three key factors needed to be considered for the production of synthetic liquid fuel. Co-pyrolysis is the most promising technique, which can meet the aforementioned criteria while reducing the volume of the waste and environmental issues at the same time. Many studies have shown improvement in the quality and quantity of bio-oil without any modification of instruments or parameters of the process. The key feature of this technique is the synergistic effect between biomass and plastic which occurs during the process [20].

Co-pyrolysis of biomass and plastic can enhance the stability of bio-oil as a fuel since plastics can provide hydrogen that the biomass lacks. Plastics have higher hydrogen fraction than biomass and its pyrolysis produces a liquid with no water content. Despite their high potential as renewable energy source, waste plastics were discarded due to many social problems [21]. Co-pyrolysis has received much attention in recent years because it provides an alternative way to dispose of and convert waste plastics and biomass to high calorific value feed stock and fuels. Recent investigations have shown that biomass and plastic co-pyrolysis achieves a synergistic effect with increase in liquid yield products and improvement in the overall process efficiency.

1.4 Motivation of the work

The main motivation of the current study is the bio-oil upgrading process. Bio-oil is clean and environment friendly, but its properties are inferior to that of petroleum based fuels. Bio-oil is a very unstable fuel due the presence of higher oxygen and acid contents and the presence of high water content makes it more unstable. Therefore, further improvement in the properties of the bio-oil upgrading process is required. Henceforth, a recent upgrading process, viz. co-pyrolysis of biomass and plastic waste has been introduced. Many researchers have shown that co-pyrolysis of biomass and plastic waste provides encouraging results [22–26]. The major key factor for this process is the synergistic effect, which comes from the reaction of different materials during the process. Various studies have shown that the oil yield obtained from the co-pyrolysis process is higher than that from the individual biomass pyrolysis. This happens due to the interaction of hydrocarbon polymers during the process [15,27–29]. For the co-pyrolysis process, plastics have been chosen as a co-feedstock due to their various advantageous properties, as it has good thermal stability than that of biomass, higher hydrogen and carbon content, plastic being manufactured from petroleum residue and having higher calorific value, which helps to improve the quality of product yield. Plastic also consists of some polymers like paraffins, isoparaffins, olefins, naphthenes and aromatics, which help to improve the quantity of bio-oil during co-processing

[15,21,29]. In comparison to other feed stocks, solid waste plastic is the cheapest hydrogen-rich feedstock with economical and environmental advantages. Waste plastics are mainly formed by polymerization of olefins with H/C effective ratio of 2 which means that they are proper feedstocks for conversion with biomass [30]. Previously, various co-pyrolysis studies on lignocellulosic biomass with waste plastic have been conducted. But very few experiments have been conducted in co-pyrolysis of non-edible seed crops with waste plastic. The bio-oil obtained from non-edible seeds contains more unsaturated carbons with high acid content. Non-edible seed like Mahua seed having high oil content which indicates the suitability of use of this seed for industrial purpose. The presence of unsaturated fatty acid in Mahua seed is 65.9% and the presence of saturate fatty acid 32.7% [31]. The presence of these acids in Mahua seed will brake after thermal degradation and makes the oil acidic in nature. So, for reducing these characteristics in this study, we use Mahua seed (*Madhuca indica*) and Polystyrene for co-pyrolysis.

1.5 Scope of this study

The main interest to study the upgrading process, viz. co-pyrolysis of Mahua seed and Polystyrene is to improve the quality of Mahua seed oil. This study also gives an idea about interaction of Mahua seed with Polystyrene during co-pyrolysis and it helps to know how it improves the quality and quantity of the product yield. In this study, the obtained product yield from Mahua seed has been compared with co-pyrolysis yield and it shows their difference. The liquid product obtained from co-pyrolysis of Mahua seed and Polystyrene is the main product, whereas the char and gas are byproducts. The major analysis is focused on the liquid product. The use of other materials such as catalyst, solvent and additional pressure in the co-pyrolysis were beyond the scope of the present study. Mahua seed pyrolysis has been carried out with respect to various operating conditions such as time, temperature, inert gas and residence time. The same operating conditions with one more additional parameter i.e. blending ratio have been included in co-pyrolysis study. To understand the thermal pyrolysis kinetic of Mahua seed, Polystyrene and co-pyrolysis kinetics of Mahua seed: Polystyrene 1:1 blend have been studied. Application of liquid fuel in internal combustion (IC) engine has also been studied for future.

1.6 Organizations of thesis

The present work has been categorized in seven chapters, viz. Introduction, Literature Review, Experimentation, Co-pyrolysis study, Kinetic study, Engine Performance, Conclusion and Future scope of the work.

- Chapter 1 presents the introduction to the present study of the requirement of bio-oil and its various uses in different sector. This chapter also includes the drawback of bio-oil and further study about the bio-oil upgradation process for the production of upgraded bio-oil.
- Chapter 2 we discussed about bio-oil and its various physical and chemical properties, the advantages and disadvantages of the bio-oil properties are also included. Different related research works which have been studied earlier in the areas of bio-oil upgradation has been discussed in this chapter. Upgradation process like co-pyrolysis of biomass and plastic has been emphasized more in this work, therefore this chapter mainly included the various related work regarding co-pyrolysis of biomass and different types of plastic/polymer. Related discussion on co-pyrolysis study viz. influence of plastic with biomass during pyrolysis, advantages of co-pyrolysis process and the quality of the upgraded bio-oil obtained from co-pyrolysis process has been covered in this chapter. Various literature related to kinetics study of biomass, plastic and their mixture has been discussed in this chapter. Various research work related to engine performance and emission analyses study using bio-oil and various biofuel also presented in this section. Furthermore the main objective of the present work is also discussed in this chapter.
- Chapter 3 presents the collection of raw materials, preparation of raw materials, experimental setup and investigation of the product using various experimental procedures, scope of the experiment is also discussed in this section.
- Chapter 4 describes the thermal pyrolysis of Mahua seed, Polystyrene and co-pyrolysis of Mahua seed and Polystyrene. The obtained bio-oil and bio-char from pyrolysis of different raw materials physical and chemical characterization has been explained detail in this chapter as well as the comparison study of thermal pyrolysis with co-pyrolysis study also discussed in this chapter.
- Chapter 5 presents the thermal kinetics of biomass, plastic and their mixture using various models has been provided in this chapter.
- Chapter 6 we discussed the engine performance characteristics by using biomass pyrolysis oil.
- Chapter 7 the application of co-pyrolysis oil in diesel engine. Diesel engine testing procedure with these oil and provides the efficiency of oil, performance analysis and some characteristic with different blend has been presented in this chapter.
- Chapter 8 present the major conclusion of the study and future studies.

Chapter 2

Literature Review

2.1 Introduction

Recently bio-oil upgrading processes and various technologies have been studied for bio-oil upgrading. Bio-oils can replace fossil fuels, but some of the properties of bio-oils are inferior to fossil fuels. Generally, bio-oils are acidic, viscous, reactive and thermally unstable as compared to petroleum based fuel [16].

Therefore, various upgrading techniques such as hydrogenation, catalytic cracking, steam reforming, emulsification, supercritical fluids and solvent addition/esterification are used to improve the bio-oil properties and characteristics. These upgrading methods are not convenient often because many problems are associated with these methods due to their high equipment cost, expensive materials and not being cost effective.

Therefore, some recent investigations on the upgrading process like co-pyrolysis of biomass and plastic have attracted a great deal of attention in the current decade. However, this process has lot of advantages with the utilization of biomass and plastic waste as the forms of alternative energy resources. Co-pyrolysis is simple and effective since this process does not require any further modification of instruments.

This chapter presents the problems associated with bio-oil storage, transportation and its uses in various industries. This chapter also includes the various works related to upgrading techniques to improve the oil quality. Moreover, the limitations and drawbacks of bio-oil upgrading process have been explained in this study. One of the most suitable upgrading technology, viz. co-pyrolysis has been described with in-depth knowledge on co-pyrolysis of biomass and plastic in this chapter. The purpose for giving more importance to bio-oil upgrading process like co-pyrolysis of biomass and plastic is that the process provides the simple and effective way to produce the ideal synthetic liquid fuel. Further importance of co-pyrolysis, feedstock for co-pyrolysis, influence of plastic on co-pyrolysis, effect of plastic and biomass ratio on product yield, kinetics study of biomass and plastic with various literature works on co-pyrolysis of biomass and plastic have also been included in this chapter.

2.2 Bio-oil

The liquid product obtained rapidly and simultaneously depolymerizing and fragmenting the cellulose, hemicellulose, and lignin components of biomass is known as bio-oil or bio-crude. Bio-

oils are usually dark brown, free-flowing liquids with a distinctive smoky odor. The physical appearance of the bio-oil resembles crude oil, but its components are highly oxygenated in nature [16].

2.3 Problems associated with bio-oil

Biomass pyrolysis oil is environment friendly because it contributes minimum amount of greenhouse gas emissions. But its fuel characteristics remain poorer than fossil fuel, especially in relation to combustion efficiency. The problems associated with bio-oil are because of some undesirable properties for fuel application such as water content, oxygen content, ash content, viscosity, density, calorific value, acidity/pH, and chemical composition of bio-oil.

2.3.1 Water content

High water content in the biomass pyrolysis oil or bio-oil is one of the major drawbacks, which leads to lower calorific value, phase separation, increased ignition delay, and reduced combustion rate and flame temperature. Generally, the water content of bio-oil is 15-30% derived from the dehydration during pyrolysis reaction and storage. Due to these problems, it can be difficult to manage in various applications. Apart from that, water content in bio-oil has some positive aspects, which enhance the fluidity, which is good for combustion and atomization in engine. It also leads to a more uniform temperature distribution in diesel engine cylinder and lowers the NO_x emissions and thus reduces air pollution during combustion and emission [15,32,33].

2.3.2 Oxygen content

The difference between bio-oil and hydrocarbon fuel occurs due to the presence of higher amount of oxygen in bio-oil. Presence of high oxygen content creates lower energy density than the conventional fuel by 50% and makes it immiscible with conventional fuel. The high level of oxygen in the pyrolysis oil creates a low calorific value, corrosion problems and instability [33].

2.3.3 Ash content

The ash is the supplementary product in char production during pyrolysis. The presence of ash in bio-oil can cause erosion, corrosion and knocking problems in the engine and the valves and even deterioration when the ash content is higher than 0.1 wt.%. The char acts as a vapor cracking catalyst, so that rapid and effective removal or separation of product vapor from the char becomes very important. The presence of alkali metals in bio-oil are problematic elements of ash. Alkali metals such as sodium, potassium and vanadium are responsible for high temperature corrosion and deposition, while calcium is responsible for hard deposits [34,35].

2.3.4 Viscosity

Viscosity is one of the important properties of bio-oil, which helps to determine the flow quality of the liquid and plays major role in the manufacturing and design of engines where a liquid fuel is used. When the viscosity of bio-oil increases, it generates disturbance in pumping and poor atomization. Increase in viscosity also contributes to high pressure drop and increased equipment cost. The viscosity of the bio-oil varies in large range because of the different biomass feed stocks and process conditions. It can be decreased with the addition of some polar solvents like methanol or acetone. Also, the viscosity is reduced in bio-oil with the presence of water content and less water insoluble components. On the other hand, over the time the viscosity of the bio-oil increases with storage because of chemical reaction among various compounds present in the bio-oil leads to the formation of larger molecules [35–38].

2.3.5 Density

One of the most useful properties of bio-oil is its density. Density is used for the mass volume relationship of biofuel. The presence of water content in biofuel has effect on the density of the liquid fuel. Increase in water content of bio-oil raises the density of the bio-oil gradually. On the other hand, density of the bio-oil also affects the energy value of the oil or fuel. In general, the normal range of the density of pyrolysis oil from most common biomass feedstocks is found between 1000 and 1240 kg/m³ determined in between the temperatures of 15 °C and 40 °C. However, in a few biomass feedstocks like saw dust density may rise up to 1300 kg/m³ [39]. From the previous work, it was found that density of the bio-oil is around 1100-1300 kg/m³, due to the presence of some high molecular weight compounds such as guaiacols, syringols and sugar compounds [36,37].

2.3.6 Calorific value

Standard measurement of the energy content of any fuel can be determined through the heating value, which is one of the important parameters for the selection of fuel for a particular application. The oil becomes more efficient and useful if the oil has high calorific value. Calorific value of the bio-oil is mainly affected by the composition of the oil. Nevertheless, calorific value of the bio-oil is also affected by some other factors such as water content, oxygen content and the operating conditions of the pyrolysis process. According to the previous reports it was found that the heating values of most of the bio-oils are found between 15 and 36 MJ/kg, which are always lower than those of the conventional petroleum fuels (40-50 MJ/kg). Further upgrading process is required to improve the heating value of bio-oil [37–41].

2.3.7 pH

The pH of the bio-oil is acidic due to the presence of some organic acids such as acetic acid, and formic acid. Due to the presence of these acids, bio-oil pH occurs in lower range, i.e. 2-3. The acid in bio-oil is the main reason and accounts for corrosion of the materials in the storage and transport application process. Therefore, it requires upgrading to fulfil the requirement of fuels before application in various processes [5,16].

2.3.8 Chemical composition of bio-oil

The chemical composition of bio-oil is one of the major factors, which makes the bio-oil unusable and acidic. The 99.7% of bio-oil obtained from pyrolysis of biomass is a complex mixture of water and organic chemicals. Chemical composition of bio-oil consists of oxygenated hydrocarbons such as aliphatic compounds, alcohols, aldehydes, furanoids, paranoids, benzenoids, different types of acids, esters, ketones, sugar, phenols, and extractible terpene with multi-functional groups [5, 16, 41–43]. These complex chemicals have been found out as a result of many simultaneous and sequential reactions during biomass pyrolysis. Bio-oil is acidic in nature due to the presence of carboxylic acid, unstable due to the presence of reactive compounds and tends to deposit solid residue in pipes and reactors due to the presence of oligomer fragments. One of the major drawback of the chemical composition of bio-oil is very similar to that of original biomass and it is extremely different from the petroleum derived fuels and chemicals [42]. Wang et al. reported that the composition of bio-oil mainly consists of furfural, dimethyl phenol, 2-methoxy-4-methyl phenol eugenol, cedrol, furanone, etc., in large proportions. The major compounds found in the bio-oil are phenol with ketones and aldehydes groups, and almost all the functional groups showed the extensive existence of oxygen. In contrast, the author stated that abundant aldehyde and ketones make bio-oil hydrophilic and make it difficult to remove the water from bio-oil [43]. Capunitan et al. analyzed the composition of bio-oil obtained from corn stover pyrolysis, which mainly consists of phenolic compounds which are abundantly present in the bio-oil. Since they are present as monomeric units and oligomers from the lignin in the biomass feedstock, the author concluded that the aromatic and oxygenated compounds found in the bio-oil were due to the major components of the biomass feed stock such as cellulose hemicellulose and lignin [44]. Zhang et al. separated the bio-oil into four fractions, viz. aliphatic, aromatic, polar and non-volatile fragments through solvent extraction and liquid chromatography method. From the identification, it was revealed that high contents of acids and hydroxyacetones are found in water phase whereas and more polar with less aliphatic and aromatic hydrocarbons were detected in the oil phase [45].

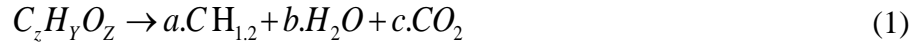
Considering the above discussion, bio-oil is associated with some problems due to the physical and chemical changes and immiscibility with fossil fuels. Various upgrading techniques for bio-oil production are as follows.

2.4 Hydrodeoxygenation (HDO)

Hydrodeoxygenation is a process in which the bio-oil can be upgraded by deoxygenating with H_2 in the presence of catalysts. During this process, the oxygenated compounds present in the bio-oil react with H_2 to form water and saturated C-C bonds. Catalysts are one of the key factors for bio-oil hydroprocessing. Previously many studies have focused on different types of catalysts such as CoMo and NiMo-based catalysts [46,47]. Especially, these catalysts are used for removal of oxygen from petrochemical feedstocks. Some other catalysts like zeolites and metals supported on zeolite have also been used previously, which are effective for upgrading the bio-oil through hydrodeoxygenation [48]. Bridgwater demonstrated that maximum stoichiometric yield of 56-86% by weight of liquid bio-oil through hydrodeoxygenation [49]. During hydrodeoxygenation, a number of reactions are observed such as hydrogenation, cracking and decarboxylation, cracking and hydrogenation [50]. However Huber et al [51] stated that hydrogenation is relatively expensive and the production of hydrogen from biomass is being slightly higher than that the market price of hydrogen. Hydrogenation is also sometimes considered as an unattractive process. Some other drawbacks of hydrogenation are the necessity of high pressures, high operating cost related to noble catalyst used, significant catalyst deactivation and considerable hydrogen consumption, which are also endured in the HDO process [52,53].

2.5 Catalytic cracking

It is one of the useful upgrading processes where the acid catalyst is used in the pyrolysis process under atmospheric pressure and in absence of hydrogen. During this process, the oxygen in bio-oil will be removed in the form of water and carbon dioxide. Catalytic cracking of bio-oil mainly produces, the liquid product in two phases: one is aqueous phase and another one is organic phase. The remaining gases and coke are deposited on the surface of the catalyst. Catalytic cracking of bio-oil in tubular fixed-bed reactor with HZSM-5 as catalyst has been carried out by Guo et al, From their result, it has been found that the organic distillate yields up to 45% and the oxygenated compound present in bio-oil are decreasing gradually [53]. Suchithra et al, reported that in zeolite cracking the oxygen in bio-oil can be removed in the form of CO_2 and H_2O . The authors also stated that in the cracking reaction, there is a splitting of C-C bonds associated with dehydration, decarboxylation, and decarbonylation; where dehydration is the main reaction. The reaction can be simplified is as follows:



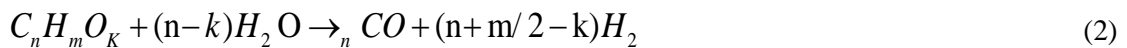
where, a,b,c depend on x, y and z. The aromatic yield is limited by hydrogen available in the bio-oil [36].

The zeolite catalysts such as HZSM-5, HY, etc. are very effective which is mainly used in bio-oil to convert the highly oxygenated compound to hydrocarbon fuel. The oxygenated compound presents in bio-oil are dominated by various light aromatic hydrocarbons of (benzene, toluene, xylene and naphthalene) [54,55]. On the other hand, catalytic cracking of bio-oil is not effective due to the production of low grade bio-oil with low carbon yield and high coke formation (of 8-25%) of the feed, resulting in a short catalyst lifetime. Moreover, this process is also not cost effective [48].

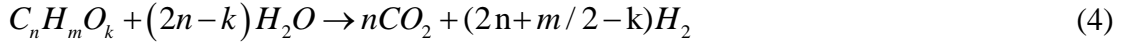
2.6 Steam reforming

Steam reforming is a well-studied technology currently used in industry to produce hydrogen. It is a process where the hydrocarbon fuels are used as a feed stock to produce hydrogen in the presence of nickel-based catalyst with a temperature range of 600-800 °C. The purpose to use the nickel-based catalyst in steam reforming is to obtain the maximum amount hydrogen from the feedstock and from the aqueous phase [41,56]. During steam reforming, many simultaneous reactions occur such as cracking, dehydrogenation and isomerization [48].

Czernik et al. [57] experimented the catalytic steam reforming of biomass-derived liquid and they found that the hydrogen yield in fluidized-bed reactor from the carbohydrate derived fraction of wood pyrolysis oil was about 80% of theoretical value, which corresponds to approximately 6 kg of hydrogen from 100 kg of wood used for pyrolysis. The major advantages of this process are that bio-oil is transferred much earlier and is less expensive than either biomass or hydrogen. Galdamez et al. have discussed the catalytic steam reforming of bio-oil for the production of hydrogen. These authors conducted the experiment in a fluidized-bed reactor with Ni-Al catalysts. Catalytic experiments showed a significant increase in total gas, H₂, and CO₂ yields, whereas CH₄ and C₂ (Note: C₂ = C₂H₂, C₂H₄, and C₂H₆.) yields decrease, when compared with those from non-catalytic experiments. The highest hydrogen yields are obtained with the Ni-Al catalyst. The addition of lanthanum in the catalyst composition diminishes the H₂ yield obtained with the Ni-Al catalyst [58]. It is an endothermic process in which the substrate is treated with steam in the presence of catalyst to produce carbon monoxide (CO), CO₂ and hydrogen (H₂). The chemical reactions for steam reforming of bio-oils are given below [59].



The CO can be further converted to CO₂ by the water gas shift reaction (equ 3)



But the main problem associated with steam reforming of bio-oil is the reaction, which is energetically demanding and some carbon cannot be eliminated by the simple addition of steam, which poses the problem of stability and long-term operation. Another problem is heavy coking of the catalyst leading to its deactivation. So the production of hydrogen by steam reforming of bio-oils obtained from the fast pyrolysis of biomass requires the development of efficient catalysts able to cope with the complex chemical nature of the reactant [48].

2.7 Emulsification

Emulsification is one of the upgrading process where the bio-oil can be emulsified with other fuel; however, the pyrolysis oils are not miscible with hydrocarbon fuels; therefore, addition of surfactants can be used for emulsifying the pyrolysis oil with other hydrocarbon fuel. Generally, upgrading of bio-oil through emulsion with diesel oil is relatively simple. It provides a short-term approach to the use of bio-oil in diesel engine. Cemek and Ogi et al. showed that the stable microemulsion with 5-30% of bio-oil in diesel has been developed. The authors proved that those emulsions are less corrosive and show promising ignition characteristics [60,61].

Emulsification of pyrolysis derived bio-oil in diesel fuel was investigated by Ikura et al. [62]. The obtained result was analyzed with statistical model. Costs for producing emulsions with zero stratification could be of the order of 2-6 cents/L for 10% emulsion, 3-4 cents/L for 20% emulsions and 4-1 cents/L for 30% emulsions. The physical properties of emulsified bio-oil are better than those of bio-oil. Therefore, this process can be considered for bio-oil emulsification as a possible approach to the wide use of these oils, reducing the investment in technologies. However, high cost and energy consumption inputs are needed in the transformations. The emulsions showed promising ignition characteristics, but fuel properties such as heating value, cetane index and corrosivity were still unsatisfied. Moreover, this process requires high energy for production. Design, production, testing of injection and fuel pump made from stainless steel or other materials are required [16,41,63].

2.8 Supercritical fluids (SCFs)

When the temperature and pressure of a fluid go above its critical point, then the fluid is considered as a supercritical fluid, which has unique transport property. It can effuse through gas and dissolved in liquid. In general, SCFs have the ability to dissolve materials not normally soluble in either liquid or gaseous phase of the solvent, and hence to promote the

gasification/liquefaction reactions. In this process, it promotes the reaction by its unique transport properties, viz. gas-like diffusivity and liquid-like density, thus dissolved materials not soluble in either liquid or gaseous phase of solvent. Recently, SCFs have been used to improve the oil quality and quantity with great potential. Xu et al. reported the hydro-liquefaction of a woody biomass (Jack pine powder) in sub-/super-critical solution of ethanol without and with iron-based catalysts (5 wt% FeS or FeSO₄) in stainless steel micro-reactor in a temperature range of 473–623 K and initial pressure of hydrogen varying from 2.0 to 10.0 MPa without catalyst. The results showed that the oil yield increases with reaction time and initial pressure of hydrogen. With catalysts, the oil yields significantly increased, while the yields of solid residue, gases and water decreased. A high oil yield of 63% was obtained with FeSO₄ at 623 K and 5 MPa of H₂ for 40 min [64]. Patel et al. used a mathematical model to characterize the supercritical extraction process for extraction of bio-oils from biomass. They proved that existing model is in better agreement with the experimental results [65]. Water is the cheapest and most commonly used supercritical fluid in hydrothermal processing, but utilizing water as the solvent for liquefaction of biomass has the following drawbacks: (1) Lower yield of the water-insoluble oil product, and (2) The obtained bio-oils are very viscous with high oxygen content. To enhance the oil yield and its qualities, the utilization of organic solvents such as ethanol, butanol, acetone, 2-propanol, n-hexanol, 1, 4-dioxane and methanol has been adopted. All these solvents have shown a significant effect on bio-oil yield and quality. Although SCFs can be produced at relatively low temperatures and the process is environment friendly, these organic solvents are too expensive to make it economically feasible on a large scale [46].

2.9 Solvent addition/Esterification

Esterification is a novel method. In this process, generally polar solvents such as methanol, ethanol and furfural have been used for many years to homogenize and to reduce the viscosity of biomass oils. While adding these polar solvents in bio-oil, it shows the immediate effects on physical properties of bio-oil, which decreases the viscosity and increase calorific value. The increase in calorific value of bio-oil during mixing with solvent occurs because the solvent has higher calorific value than that of most of the bio-oils. Addition of solvent also improves viscosity of the bio-oil, especially the reduction in viscosity is due to the following reasons: (1) physical dilution without affecting the chemical reaction rates; (2) Reducing the reaction rate by molecular dilution or by changing the oil microstructure; and (3) chemical reactions between the solvent and the oil components that prevent further chain growth. Xu et al synthesized and used a Zirconium-containing mesoporous catalyst in upgrading bio-oil through reactive rectification. His result

showed that two kinds of upgraded bio-oils (light oil and heavy oil) were obtained. The volatile organic acids were converted into esters under the action of the solid acid catalyst $\text{SO}_4^{2-}/\text{Zr-MCM}^{41}$, whereas, the heavy oil was composed of nonvolatile components in original bio-oil [66]. Upgrading of bio-oil using catalytic esterification of acetic acid and alkylation of acetaldehyde has been experimented from 40 to 140 °C by Ye June et al. The authors stated that at low temperature, catalyst dosage can lead to a restrained esterification reaction and the decomposition of acetals was successfully resolved by an alkylation reaction of acetaldehyde. The maximum yields of 2,2'-ethylidenebis (5-methylfuran) and butyl acetate were 84.5 and 74.4%, respectively [67]. However, several recent studies showed that reacting the oil with alcohol (e.g., ethanol) and acid catalysts (e.g., acetic acid) at mild conditions by using reactive distillation, resulted in a better bio-oil quality [68,69]. On the other hand, the cost of some solvents and catalysts will be more than that of the product itself and the mechanism involved in adding solvent is not quite understood yet [46].

From the above discussion on bio-oil upgrading via using various upgrading processes such as hydrogenation, catalytic cracking, steam reforming, emulsification, supercritical fluids and solvent addition or esterification, it is clear that they have some drawbacks like complexity and cost because of the complicated equipment, need to add catalyst, solvent and high pressure requirement for the reaction. Therefore, currently some research is focusing on the co-pyrolysis process. However, this process is simple and cost-effective and especially important to produce high-grade fuels [15].

2.10 Significance of co-pyrolysis

The simplicity and effectiveness are the two important parameters to develop a useful technique for the production of high-graded liquid fuel. Co-pyrolysis of biomass and synthetic polymer is one of the ideal processes, which satisfy the required criteria. Especially, this process can produce the effective liquid fuel which can be a better substitute for fossil fuel. Co-pyrolysis is a process where two or more different feedstocks can be combinedly pyrolysed. Previously, various studies have shown that co-pyrolysis of biomass with synthetic polymers has successfully improved the quality and quantity of liquid fuel without any additional modification of the system [28,70–72]. The previous bio-oil upgrading processes such as catalytic cracking, HDO, SCF, esterification, emulsification and steam reforming etc are less effective than the co-pyrolysis process [19]. However, co-pyrolysis technique has given a great attention to industrial utilization due to its attractive outcomes and effective performance/cost ratios. The major advantages of this technique are that this process is mainly concentrated on the synergistic effect between the reactions of the two feedstocks during the co-pyrolysis process. From the previous study, it was established that

the liquid product yield obtained from co-pyrolysis of biomass and plastic was more than that of the biomass alone [72]. Due to difference in nature of the biomass pyrolysis oil and plastic pyrolysis oil it is quite impossible for blending these oils and it will create phase separation after storage if these oils are mixed together. Moreover, it may increase the operating cost of liquid if the biomass and plastic were pyrolysed separately [15]. Previously, considerable attention has been paid to the co-pyrolysis technique because during co-pyrolysis process, the radical interaction between the feedstocks can promote the formation of stable pyrolysis oil and avoid the phenomenon of phase separation [71,73]. Thus co-pyrolysis technique is thought to be more reliable for the production of homogeneous pyrolysis oil instead of blending the pyrolysis oil. Moreover, it was found that polymer wastes like plastic wastes can be significantly consumed as a feedstock through the co-pyrolysis process, and it also reduces the polymer wastes in landfill. Manages the cost for waste treatment and solves a lot of environmental issues. However, disposal of polymer wastes in landfill is undesirable [21], hence the co-pyrolysis process is a suitable alternative for solid waste management system and further, it can enhance the energy security. Additionally, as per the economical point of view, co-pyrolysis process has been found to be more interesting than the pyrolysis of biomass alone. The synergistic effects of flash co-pyrolysis has been studied by Kuppens et al., the authors stated that use of co-pyrolysis process is more cost-effective than the pyrolysis of biomass alone and has good potentiality for the commercial development [74].

2.11 Feedstock for co-pyrolysis process

Biomass is one of the largest renewable energy sources, which can produce fuel in the form of solid, liquid and gas through pyrolysis. The characteristics of the fuel obtained from cellulosic biomass are lower than those of fossil fuels, consequently use of co-pyrolysis technologies improves the characteristics of the fuel. In this regard, the selection and availability of feedstock is necessary to explore and find the potentiality for application in co-pyrolysis process. Previously, various studies have been carried out in co-pyrolysis of biomass with other different polymers and show the potentiality of biomass to enhance the quality and quantity of pyrolysis oil. Particularly, for this purpose, the selection of biomass is becoming an important issue to be addressed in the current study. In general, biomass can be categorized into four groups, viz. agricultural residue, wood residue, municipal solid waste and dedicated energy crops.

Furthermore, the co-product used in co-pyrolysis technology like plastic are also categorized into two groups viz. industrial and municipal plastic waste, according to their origin. Generally, industrial plastics are more homogeneous and contamination-free, whereas municipal plastics are








more heterogeneous and have extraneous materials. Municipal plastics are mainly based on low density polyethylene (LDPE), high density polyethylene (HDPE), Polyethylene terephthalate (PET), Polypropylene (PP), Polystyrene (PS), Polyvinyl alcohol (PVA) and Poly(vinyl chloride) (PVC) [75]. Similarly, industrial plastic wastes are also called primary wastes, which are arising from the large plastics manufacturing, processing and packing industry. The industrial waste plastics mainly come from construction and demolition companies (e.g. Polyvinyl chlorides pipes and fittings, tiles and sheets), electrical and electronics industries (e.g. switch boxes, cable sheaths, cassette boxes, TV screens etc.) and the automotive industries spare-parts. During manufacturing process, the plastic wastes have deceased their characteristics and they have not been used in product application. However, this plastic can be repelletized and remolded to be simple and effective for recycling. But the heterogeneous plastic waste consists of mixed resins and is not suitable for reclamation. Therefore, thermal cracking into hydrocarbons may provide a suitable means of recycling, which is termed as chemical recycling [21].

2.12 Availability of plastic

The use of plastic in daily lives of human beings in the world is abundant because of the different uses of plastic in various sectors such as construction, healthcare, electronic, automotive, packing and others. The demand for the products made from plastic has been increasing due to rapid growth of world population. The continuous rising of plastic led to the growth of waste accumulation every year. From the statistical data, it was projected that the global plastic production from 1950 to 2014 is 1.5 to 311 million metric tons [76]. After the primary use of plastic, less than 10% of plastic can be recycled and over 60% of solid waste plastics is discarded in open space or landfills worldwide [75]. This indicates that the percentage of plastic waste discarded in the landfill is still very high, which occupies a large space. Furthermore, plastic may take up billions of years to degrade naturally. The gradual decomposition of plastic is due to the molecular bond of plastic, which consists of hydrogen, carbon and some other few elements such as nitrogen, chlorine and others, that makes the plastic very durable. It was estimated that the proportion of global waste plastic in MSW (Municipal solid waste) will increase to 9–13% in 2025 [72]. However, the disposal of these wastes becomes a major problem towards environment due to their non-biodegradable nature. Therefore, recycling by pyrolysis has been considered to reduce the waste and make it safe to the environment. But other recycling methods of plastic have proven difficult and are not cost effective due to the limitations of water pollution and inadequate separation [77]. To overcome above limitations, the abundantly available waste plastics have advantages in the future use as a co-feed in the co-pyrolysis process to minimize the disposal of

valuable plastic in landfills, and also it can be a substitute to the conventional fuel. Table 2.1 shows the different type of plastics and their various applications [78].

Table 2.1 Different types of plastics and their applications

Types of Plastics	Recycling structure	General properties	Uses of plastic
Polyethylene Terephthalate (PETE)		Good gas and moisture barrier properties, High resistance to heat, Microwave transparency, Solvent resistance.	Various food packing, Mineral water, Soft drink bottle, Electrical insulation, Printing sheets, Magnetic tapes, X-ray and other photographic film
High Density Polyethylene (HDPE)		Good chemical resistance, Good moisture barrier properties.	Detergent, Bleach and fabric conditioner bottle, Milk and non-carbonated drinks bottles, Toys, etc.
Polyvinyl chloride (PVC)		Long-term stability, Good chemical resistance, Stable electrical properties, Low gas permeability.	Wire, Cable insulation, Window frame, Credit card, Synthetic leather product, Food foil, Medical devices, Blood bags, etc.
Low density polyethylene (LDPE)		Tough and flexible, Stable electrical property, Good chemical resistance, Moisture resistance.	Plastic bags, Wrapping foils, Trash bags, Flexible bottles, Irrigation pipes, Shopping bags, wire and cable insulation
Polypropylene (PP)		Semi-rigid, Translucent, Good chemical resistance, Tough, Good fatigue resistance, Good heat resistance.	Bottles cap, Drinking straws, Strong hinged, lunch boxes, Refrigerator containers, Heavy duty bags, etc.
Polystyrene (PS)		Good impact resistance, Fatigue resistance, Moderate stiffness, Better heat stability, Good electrical insulator, Excellent optical clarity.	Food packing, Electronics, construction, Medical application and toys
Others Nylon (PA) Acrylonitrile butadiene styrene (ABS) Polycarbonate (PC)		Some other plastics have wide uses, particularly in engineering sectors. They are identified with number 7.	Used in baby bottles, Large water bottles, Compact discs, and medical storage containers. Recycled plastics in this category are used to make plastic lumber, among other products.

2.13 Importance of plastics in co-pyrolysis process

Petroleum resource has a major contribution in transportation sector. Since it is the end product, there will be an urgent need of other alternative resources. However, some petroleum products are still stored in other forms of plastic. Considerable amount of plastic cannot be recycled. Further, these plastics will come under the waste and require extra attention to the plastic waste management. By considering this fact, the challenge has been taken to resolve these issues through recycling of waste polymers to liquid fuel. Especially, plastics are synthetic polymers and they are rich in hydrogen and carbon. Thus, use of these plastics is a potential alternative for the production of hydrocarbon fuel to reduce the energy crisis to a large extent. During pyrolysis of plastic, the macromolecular structures of polymers are broken down into smaller molecules or oligomers and sometimes into monomeric units. Degradation of plastic depends on various types of operating conditions such as temperature, residence time, inert gas flow rate, and the presence of catalysts and other conditions [79]. The heating value of the plastic pyrolysis oil is nearly about conventional fuel, which is around 40MJ/Kg, with that it is also relatively clean and its fuel properties are similar to the petroleum fuels. Hence, the presence of plastic in the pyrolysis of biomass can make a positive contribution towards the co-pyrolysis yield [27]. Previously, many research works considered that plastic is one of the suitable co-feed with the aim of improving the quantity and quality of the oil. Table 2.2 summarizes the list of experiments performed in co-pyrolysis. Jeon et al. studied the co-pyrolysis of wood chips (WC) with block polypropylene (PP) to investigate the characteristics of liquid product yield. The authors suggested that the liquid product obtained from co-pyrolysis at 1:1 ratio of WC/PP has improved properties than those of the bio-oil obtained from individual biomass pyrolysis. From their GC-MS studies, it was found that some new compounds were observed, but they were not found in the biomass pyrolysis oil, which attributed to the interaction of WC and PP [27]. Abnisa et al. found that the oil yield obtained from co-pyrolysis of palm shell and polystyrene with 1:1 ratio increased the yield to about 61.63%, while the pyrolysis of palm shell alone only yielded oil about 46.13 wt%. From the physical properties analysis, it was found that the high heating value (HHV) of co-pyrolysis oil is more than that of the palm shell pyrolysis oil. Furthermore, the authors proved that the fuel obtained from co-pyrolysis has good impact to overcome the problem associated with environment and fossil fuel resources [19]. Onal et al. studied the co-pyrolysis of almond shell with high density polyethylene polymer to investigate the effect on product yield and composition. The result shows that the liquid yield obtained during co-pyrolysis increased to 23% as the weight ratio of HDPE mixture was increased.

Table 2.2 Various works related on co-pyrolysis of biomass and plastic

Types of raw materials		Reaction conditions				Results		Ref
Biomass	Plastic	Temp (°C)	Biomass to plastic ratio	Liquid yield of biomass	Co-pyrolysis yield	Quality of biomass pyrolysis oil HHV (MJ/kg), O content (wt %) and Water content (wt %)	Quality of co-pyrolysis yield HHV (MJ/kg), O content (wt %) and Water content (wt %)	
Wood chips	PP	600	1:1	39.3	63.1	HHV=19.9, O=42.3 Water=30.5	HHV=45.0,O=10.9, Water =6.9	[27]
Palm shell	PS	500	1:1	46.13	61.63	HHV=11.94,O=71.40, Water=53	HHV=38.01,O=7.82,Water=2.4	[19]
Almond shell	HDPE	500	1:1	21.12	41.39	O=27.75, Water =18.3	HHV increases 38% O=3.74, Water= 10.1	[29]
Pine cone	LDPE	500	1:1	47.5	63.9	N/A,O=67.79, Water=66.0	HHV=46.33, O=5.61,Water=0.09	[71]
	PP	500	1:1		64.1		45.58, O=1.55, Water=0.45	
	PS	500	1:1		69.7		HHV=46.43, O=6.54, Water=0.02	
Poplar wood	HDPE	625	1:1	N/A	64.80	Not reported	Not reported	[80]
Cellulose	PP	600	1:3	N/A	45	HHV=15.54,O=Not reported, Water=Not reported	HHV=41, O=Not reported, Water=Not reported	[81]

Cellulose	PS	500	1:1	45.5	58.8	Not reported	Not reported	[82]
Karanja, Niger	PS	550	2:1	32.90	57.81	HHV=37.65	HHV=42.18, water=11.06	[83]
		550	2:1	33.39	57.94	water=22.27, HHV=35.87, water=18.31,O= Not reported	HHV=41.42,water=10.69, O= Not reported	
Jatropha de-oiled cake	HDPE	450	1:1	49.8	79.2	HHV=17.6 O=41.40,water=12,	HHV=28.4,	[73]
	PP				85.5		O=Not reported	
	PS				88.2		Water= 5.10 HHV=30.8, O=Not reported Water=5.50 HHV=32.5, O=Not reported, Water= 6.50	
Willow	PHB	450	1:1	49.71	64.24	HHV=16.10, O=Not reported, water= 36.67	HHV=20.20, O=Not reported, water=15.95	[84]
Willow	PLA	450	1:2	48.85	55.53	HHV=16.13 O=Not reported, water=36.46	HHV=19.6 O=Not reported, water=8.3	[85]
Willow	Biopearls	450	1:1	50.10	52.79	HHV=16.1, Water=36.65	HHV=19.1	[86]
	Solanyl		1:1		59.24	O=Not reported	O=Not reported, water=15.53	
	Potato starch		1:1		51.52		HHV=15.7 O=Not reported, water=32.82 HHV=19.2 O=Not reported, water=16.17	

Lastly, the authors concluded that biomass co-pyrolysis with synthetic polymer has good prospects for integrated engine fuels, chemicals, taking into account of high bio-oil yield [29]. Co-pyrolysis of pine cone with various synthetic polymers has been studied by Brebu et al, the various synthetic polymers being LDPE, PP and PS. The oil yield obtained from the mixture of pine cone and polymers in the same weight ratio was increased to that of the pine cone. On the other hand the authors reported that the energy content of the oils from co-pyrolysis was higher than that of pyrolysis of pine cone [71]. Sun and his coworkers have studied the co-pyrolysis of poplar wood and high density polyethylene in a micro scale reactor using pyrolysis-gas chromatography/mass spectrometry. From their result, it was found that free radicals are formed from biomass pyrolysis and contribute in the reaction of plastic decomposition, and yields more light paraffins, since at the lower temperature biomass components were decomposed compared to that of polyolefin [80].

Vinu et al., studied fast co-pyrolysis of cellulose (C) and polypropylene (PP) using Py-GC/MS and Py-FT-IR. Their result showed that relating to the product distribution hydroxyl, hydrogen and methyl abstraction were dominated during interaction with PP during decomposition. They produce long-chain alcohols in the carbon range of C₈-C₂₀, with 36% alcohols and 45% hydrocarbons obtained during co-pyrolysis of C/PP (25:75) blend at 500 and 600 °C. Significantly higher heating value was observed for co-pyrolysis oil [81].

Rutkowski et al., observed the positive effect on co-pyrolysis product yield of polystyrene/cellulose mixture. The authors also stated that the influence of polystyrene during co-pyrolysis dominates the oxygen containing compound, and the addition of polystyrene to cellulose essentially changes the chemical structure of co-pyrolysis liquid product [82].

Co-pyrolysis of Karanja and Niger seed with PS was carried out to improve the quality and quantity of oil yield. The authors showed that biomass to plastic ratio of 2:1 is suitable to produce the higher calorific value oil with that low-carbon residue. Further, the authors also stated that co-pyrolysis is one of the important technique for the waste management, especially when the large amount of polystyrene waste is generated all over the world [83].

Rotliwala et al. studied thermal co-pyrolysis of jatropha deoiled cake and polyolefins like (HDPE, PP, and PS) were individually co-pyrolysed with jatropha deoiled cake at different temperature range of 400 and 450 °C in a batch reactor with inert atmosphere. With the addition of HDPE, PP and PS the co-pyrolysis yield increased from 2.0 to 4.9% at 450 °C. Co-pyrolysis afforded a reduction of paraffin and olefins in the liquid fraction for all the experiments. The reduction was found to be in the order of PS>PP>HDPE. Furthermore, the proportion of oxygenated compounds in the liquid product increased in order of PP>HDPE>PS [73].

Some other research work was also carried out for the utilization of biopolymer in co-pyrolysis process. Cornelissen et al. have performed many co-pyrolysis studies by using various biopolymers. The authors used various biopolymers in their studies, viz., polylactic acid (PLA), corn starch, polyhydroxybutyrate (PHB), biopearls, eastar, solanyl and potato starch, co-pyrolyzed with willow as selected biomass feed-stock [84–86]. The co-pyrolysis of willow and various biopolymers has been carried out in a semi-continuous pyrolysis reactor and the temperature was set around 723 K, they found that co-pyrolysis of willow/biopolymers blends generally results in improved pyrolysis characteristics, reduction of waste content in oil yield, increase in heating value, and the production of easily separable chemicals. PHB was found to be more suitable biopolymer than other polymers in co-pyrolysis process. The presence of PHB affords maximum oil yield and high heating value than that of others biopolymers.

Based on the above discussion and data in Table 2.2, it is seen that co-feeding of plastic in the pyrolysis of biomass can be appreciable to enhance the liquid and increase the quality of liquid product. For example, the energy content of the liquid products represented by calorific value showed a considerable increase in all co-pyrolysis oil compared to that of biomass pyrolysis oil. However, the production of energy from co-pyrolysis of biomass mixed with biopolymers was found to be lower than that of the oil production from co-pyrolysis of biomass with synthetic plastics.

Besides that, increase in plastic waste causes loss of natural resources, environmental pollution and reduction in space for landfills. Landfilling and incineration are not suitable options since these processes are creating various problems related to the environment. Therefore, utilization of such waste materials is indeed important with economical and environmental aspects. Thermochemical process like co-pyrolysis process is a suitable option to convert polyolefin and biomass materials into valuable feedstock, and the special benefits include recovery of valuable chemicals, waste reduction and substitution of fossil fuel [85].

2.14 Mechanism of co-pyrolysis

The synergistic effect during co-pyrolysis of biomass and plastic is the main factor, which is responsible for the improvement of quality and quantity of oil. This mechanism corresponds to co-pyrolysis of biomass and plastic and it has been discussed in various research works. During co-pyrolysis reaction, the synergistic effect can be achieved through radical interaction. It was reported that the biomass and plastic have different decomposition mechanisms in the thermal pyrolysis process. Pyrolysis of biomass occurs as a series of exothermic and endothermic reactions [88], while the thermal degradation of plastic takes place through a series of radical mechanisms

(initiation, propagation and termination) [29]. On the other hand, it has been said that the thermal stability of biomass is lower than that of plastic, which can affect their free radicals produced from the degradation of biomass during co-pyrolysis with plastic, further on the degradation mechanism by promoting the degradation of synthetic macromolecules [89,90].

The positive or negative synergy depends on the type and the contact of the components, residence time during pyrolysis, temperature and heating rate, removal or equilibrium of volatiles formed and addition of solvents, catalysts and hydrogen-donors. Among all these factors, the types of feed stock ratio is the major factor, which can significantly influence the synergistic effects [91,92].

Onal et al found that the hydrogen content of polyolefin materials is 14%, and the presence of hydrogen during thermal co-processing with biomass can lead to increase of liquid yields. This is one of the main reasons to increase the liquid yield of biomass with the addition of polymer. Their results shows that there is a synergistic effect on the co-pyrolysis of biomass and plastic mixture in the form of enhanced oil yield [87].

Flash co-pyrolysis of willow with polylacticacid (PLA) has been studied by Cornelissen et al. The authors reported that with the addition of PLA, there is an increment of bio-oil yield with lower water content. Synergistic effects were observed with addition of PLA to willow and they caused an increase of 28% in bio-oil yield and a decrease of 37% in water content [85].

Synergistic interaction of co-pyrolysis of pinecone with synthetic polymer has been studied by Brebu et al. They reported that in biomass/polymer mixtures, higher amounts of liquid product were obtained compared to the theoretical ones. The presence of cellulose improves, the degradation reaction mechanism, which leads to formation of more gas and less char which was more beneficial than in case of co-pyrolysis with the pine cone. The obtained product from co-pyrolysis has polar oxygenated compound. The char has high calorific value and ash content is below 1 wt % with very low sulphur concentration which makes them attractive to use as solid fuel or can be used as raw materials for the production of activated carbon [71]. Sun et al. explained the co-pyrolysis of poplar wood and high density polyethylene in a micro-scale reactor using pyrolysis GSMS. The authors reported that free radicals are formed from biomass pyrolysis and contribute in the reaction of plastic decomposition, yielding more light parafins due to the lower temperature decomposition of biomass component compared to polyolefins [80].

2.15 Pyrolysis of non-edible seeds

Tree seeds, rather than biomass or fuel crop plants, could represent an abundant source of renewable energy. However, biomass feed-stocks like non-edible seeds are very useful feedstock for biofuel production. In the year 2013-14, a total of 28.051 million hectares of land in India was

occupied by the oilseed crops as per Indian Institute of Oilseeds Research [93]. The rich forest resources and the favorable climatic conditions of India have promoted the harvesting of around 300 non-edible oil bearing plant species across the country such as Mahua (*Madhuca indica*), Sal (*Shorea robusta*), Jatropha (*Jatropha curcas*), Karanja (*Pongamia glabra*), Castor (*Ricinus communis*) etc, are important economic plants yielding significant quantity of oil. Among which Mahua (*Madhuca indica*) tree is an important economic seed plant, yielding significantly high quantity of oil [94]. The plant is extensively cultivated in central and southern India for its oil-bearing seeds, which have 35% oil content, 16% protein, desirable levels of oleic and stearic acids and are comparatively away from creating toxic effects. The annual production of Mahua seed in India is around 0.50 million tons with seed yield ranging from 20-200 kg per tree every year [31,95,96]. Such properties of Mahua seed can favor the high production of biofuel. Biofuel production from tree seeds in India will not only reduce the dependence on crude oil imports, but also reduce the environmental impact by transportation sector. Biofuel production through a thermochemical process like pyrolysis is more important than that of biochemical processes. Thermochemical pyrolysis is preferred presently because of the production of more fuel to feed ratio in the former case [7,97]. Pyrolysis is the thermal decomposition of biomass in an inert atmosphere to produce various products such as liquid fuel, solid residue and gas. These products have potential applications in boiler, diesel engine for power generation, and also they can be used as a source of pure chemicals [98]. Numerous research articles are available on the bio-oil production from non-edible seeds, which are shown in Table 2.3. From the table, it can be observed that the maximum yield of bio-oil is obtained within the temperature range of 400 to 600 °C in various non-edible seeds. From their physical and chemical analysis studies, it was found that most of them are acidic with some phenolic compounds, high viscosity and water content. From the above discussion, it can be stated that bio-oil has some limitations and drawbacks, so further upgradation is required. Therefore, in this current study, the discussion is included on the upgradation process of co-pyrolysis of different biomass with plastic and its application for various purposes.

Table 2.3 Production of bio-oil and its characteristics from pyrolysis of different seeds

Author	Different Types of Seed	Temperature (°C)	Bio-oil Yield (%)	Aqueous Phase (%)	Chemical Properties			Physical Properties			
					Phenol (%)	Acid (%)	O%	GCV (MJ/kg)	pH	Viscosity (cSt)	Water content (%)
Ucar et al. [99]	Pomegranate seed	600	22.23	31.97	22.89	1.58	23.13	34.19	–	–	–
Onay et al. [100]	Rape seed	600	75	–	–	–	13.1	37.9	3.2	36	–
Garg et al. [101]	Bobool seed	500	38.7	10.3	2	–					
Kader et al. [98]	Tamarind seed	400	45	–	–	–	–	25	NA	6.51	–
Nayan et al. [102]	Neem seed	475	38	–	–	–	–	32.3	3.9	22.6	30-35
Singh et al. [103]	Lin seed	550	68	–	–	–	–	33.83	3.1	1.97	–
Seal et al. [104]	Cotton seed	580	58.6	–	39.12	2.84	29.17	28.04	–	62.05	–
Singh et al. [105]	Caster seed	550	64.4	–	–	–	–	44.79	3.7	83.19	–
Panda et al. [106]	Kanar seed	600	79	2.2	–	–	–	35.99	5.9	27	–
Nayan et al. [107]	Karanja seed	500	57	–	–	77.96	–	33.9	–	27.9	–
Onoy et al. [108]	Saffower seed	600	54%	–	–	–	8.5	40.9	–	33	–

2.16 Advantages of Polystyrene as co-feed stock in pyrolysis

Plastic is a general common term for a wide range of synthetic or semi synthetic organic solid materials suitable for the manufacture of industrial products. Plastics are typically polymers of high molecular weight, and may contain other substances to improve performance and/or reduce costs. Plastics are also non-biodegradable polymers mostly containing carbon, hydrogen, and a few other elements such as chlorine, nitrogen etc. As it is non-biodegradable in nature, the plastic waste contributes significantly to the problem of Municipal Waste Management. Lazarevic et al, stated that landfilling is the least preferable method for plastic waste management [109].

Specifically, Polystyrene (PS) is a light-weight material, it contains 95% air with very good insulation properties and is used in all types of products from cups that keep beverages hot or cold to packaging material that keep electronics safe during shipping. Polystyrene is a petroleum-based plastic made from the styrene monomer. Many people know its name as ‘Styrofoam’, which is generally the trade name of a polystyrene foam product used for housing insulation. Therefore, it will occupy large volume in a landfill. According to 1986 EPA report on solid waste named the polystyrene manufacturing process is the 5th largest creator of hazardous waste. The National Bureau of Standards Centre for Fire Research identified 57 chemical byproducts released during the combustion of polystyrene foam. The process of making polystyrene pollutes the air and creates large amounts of liquid and solid wastes [108]. Previously, it was mentioned that PS waste creates a large carbon footprint when being transported to a landfill because of its low density [109].

Polystyrene is originally made from polymers and it is based on petroleum plastic, therefore it has a high heating value, which is near to fossil fuels. Thus energy recovery can be another option for managing the discarded plastic waste. Traditional thermal treatment like incineration for municipal solid waste has a lot of drawbacks such as technology costs, and emissions of polycyclic aromatic hydrocarbons and dioxins, formed as a result of oxidation [110].

Hence the only way the PS waste can be fully utilized is through the pyrolysis process in which it can be turned into more valuable liquid product rather than other traditional process and landfilling. Pyrolysis of polystyrene produces a substantial liquid product, which is more suitable for handling with less emissions [110]. According to United Nations Environment Program (2009), only PE, PP and PS are preferred for conversion into liquid fuel, based on the criteria such as effective conversion into fuel products, well controlled combustion and clean fuel gas in fuel user facilities [111]. Among these three plastics, PS resins are particularly attractive pyrolysis feedstock because they have the least percent recycled, based on municipal solid waste records

[112]. Due to uneconomical recycling cost, and finding difficulty in markets, most of the recycling stations do not accept PS waste. Furthermore, PS containers are more complicated to recycle because of the contamination. Interestingly, PS has quite high energy content, approximately 16,000 British thermal units (BTUs) per pound, which is twice that of coals [110]. Various studies have been focused on higher liquid product and low gas yield produced by PS pyrolysis compared to that of other plastics such as PP, PE, and PS under the same optimum conditions[111].

Pyrolysis of individual LDPE, HDPE, PP, PE and PS has been carried out at different temperatures (300–500 °C). From the results, it was found that the complete conversion of PS takes place compared to other plastics. Besides that, PS pyrolysis produces low gas without insoluble organic matter [113].

Onwudili et al., performed the pyrolysis of PS and LDPE between 300 and 500 °C. From the results they reported that PS produces an insignificant amount of gas, while LDPE produces higher quantities of gas. Moreover, they found that in pyrolysis, the mixture of LDPE and PS, PS influenced LDPE conversion by lowering degradation temperature and increasing the oil product compared with other individual plastics [114].

In the same way in co-pyrolysis of biomass and plastic waste, some authors showed that PS plastic increases the quantity of the bio-oil and also improves the quality of bio-oil compared to other plastics. Brebu et al. performed co-pyrolysis of pine cone with different plastics such as PE, PP and PS. From their results, it was found that the bio-oil obtained from co-pyrolysis of pine cone and PS is 52.3%, which is more than that of PC/PE and PC/PP co-pyrolysis oil, in the meantime the aqueous phase is 17.4 %, which is less than PC/PE and PC/PP co-pyrolysis oil [71].

Brebu et al. performed the co-pyrolysis of LignoBoost with synthetic polymers (such as Polyethylene, Polypropylene, Polystyrene and Polycarbonate) in a semi-batch reactor at 500 °C with self-generated pressure. The author showed that the co-pyrolysis yield of LignoBoost lignin/PS is more than that of other co-pyrolysis oils, while the water percentage is less than that of other co-pyrolysis oils. From their chemical analysis study, it was found that new polyaromatic compounds were obtained from the PS/LignoBoost. The co-pyrolysis oil obtained from the PC/LignoBoost is much simpler in composition and was more concentrated in phenol with its isopropyl- and isopropenyl derivatives and in bisphenol with its demethylated derivatives [22].

2.17 Reaction kinetics of co-pyrolysis of biomass and plastic blends

Basically, to understand the thermal decomposition or devolatilisation that occurs during co-pyrolysis of biomass with plastic mixture is very essential as kinetics is intrinsically related with

the decomposition mechanisms. Therefore, to study the kinetic mechanism of biomass and plastic mixture, thermogravimetric analysis (TGA) is important. TGA is commonly used to investigate the solid-phase thermal degradation and is also a useful technique to evaluate the kinetic parameters such as pre-exponential factor (A), activation energy (E_A), and order of reaction model (n). Kinetic evaluation involves measuring the amount of mass degraded versus the temperature at regular time intervals. There are many methods for determining non-isothermal solid-state kinetic data from TGA [115].

Further, to study the kinetic model, a rate law expression has been proposed, which obeys the fundamental Arrhenius rate expression model-fitting and model-free (isoconversional) methods, both presented in Table 2.4 [116]. In case of model fitting method, different models are used to find the best statistical fit as the model from which the kinetic parameters are calculated. Especially, model-fitting methods are widely used for solid state reactions because these methods have the ability to directly determine the kinetics parameters from a single TGA measurement. However, these methods suffer from several problems in their inability to uniquely determine the reaction model. Mainly for non-isothermal data; several models can be found as statistically equivalent, whereas the fitted kinetics parameters may differ by an order of magnitude and therefore, selection of an appropriate model can be difficult. Application of model-fitting methods for non-isothermal data gives higher values for kinetics parameters [117].

Similarly, model-free methods allow to estimate the kinetics parameters at specific extent of conversion for an independent model. Moreover, the advantages of model free methods are their simplicity and avoidance of errors connected with the choice of kinetic model [118].

Not all the methods are isoconversion: the Kissinger method is one of these exceptions because it does not calculate E_A values at progressive values but assume activation energy as constant [116].

Table 2.3 Different methods for solid state kinetic study [116]

Model fitting		Model free	
Isothermal	Non-isothermal	Isothermal	Non-isothermal
Conventional	Differential	Standard	Kissinger
	Freeman–Carroll	Friedman	Flynn–Wall and Ozawa
	Coats–Redfern	AIC	Vyazovkin and AIC
			Kissinger–Akahira–Sonuse

The various investigations have been studied previously in order to determine the degradation kinetics of biomass, plastic and their mixture. However, many research works described the devolatilisation characteristics of the biomass and showed the interaction of biomass and plastic during co-pyrolysis kinetics. The solid state kinetics have been described through Arrhenius equation as

$$k = A \exp\left(-\frac{E_A}{RT}\right) \quad (1)$$

where A is pre-exponential (frequency) factor. E_A is the activation energy and R is the universal gas constant and T is the absolute temperature.

Co-pyrolysis kinetics of rice husk, HDPE, LDPE, and PP mixture have been studied by using TGA. The kinetics parameters such as E_A activation energy and pre-exponential factor A of waste plastics (HDPE, LDPE and PP) decomposition are in the range of 279.0–455.1 KJmol⁻¹ and 4.95×10^{19} – 1.48×10^{31} min⁻¹, respectively. The author reported that E_A of plastic decomposition reaction is reduced when the plastic is mixed with rice husk. The E_A of the mixture is in the range of 221.2×10^{15} – 7.18×10^{21} min⁻¹ [119].

Rotliwala and Parikh studied the thermal degradation behavior of a mixture of rice bran and HDPE using TGA in nitrogen atmosphere and compared, with that of individual materials. From the results, it was found that there are three stages of decompositions occurring in HDPE/rice bran 1:1 mixture whereas two and one stage decompositions, are occurring for HDPE and rice bran, respectively. The activation energy for HDPE is in the range of 234.99–257.80 KJmol⁻¹, the E_A for rice bran in the first and second stage are in the range of 13.08–15.49 KJmol⁻¹ and 44.78–46.33 KJmol⁻¹, respectively. Meanwhile, the E_A for the mixture of HDPE and rice bran in the first, second, and third stages are 11.62–14.54 KJmol⁻¹, 33.51–33.57, KJmol⁻¹ and 165.76–174.96 KJmol⁻¹ respectively. From this study the author concluded that the activation energy of mixture is less compared to that of individual plastics [120].

Oyedun et al. studied the pyrolysis characteristics and kinetics of plastic with biomass (bamboo, empty fruit bunch and sawdust). The individual devolatilisation characteristics of the fuel shows that the thermal decomposition of the materials occurred at a single stage reaction whereas the blends can be characterized by two decomposition reaction stages. The authors proposed that the co-pyrolysis characteristic of the blends are quite different from the combination of the individual materials so, consequently, the possible synergistic effect has been observed during the co-pyrolysis reaction [121].

Co-pyrolysis of polystyrene and bamboo waste kinetics and its modeling approach has been carried out by Hui et al. The samples were mixed in the ratio of 1:3, 1:1 and 3:1 before TGA/DTA

analysis and then heated from 25 °C to 800 °C in a nitrogen environment at a heating rate of 10 and 30 °Cmin⁻¹. The authors reported that the used modeling approaches shows an effective synergistic effect of the reduction in overall energy during the co-pyrolysis of bamboo and polystyrene. The second modeling approach allows the interaction between two feedstocks and gives more reduction in the overall energy usage up to 6.2%, depending on the ratio of PS in the mixed blend [122].

Aboulkas et al. studied the kinetics mechanism of Tarfaya (Morocco) oil shale and LDPE mixture with different heating rates of 2 to 50 Kmin⁻¹. Kissinger–Akahira–Sunose method, Friedman’s method, and Flynn–Wall–Ozawa method have been used in their study to determine the activation energies of the materials. From their results, it was found that the most possible model for the pyrolysis of oil shale kerogen agrees with the diffusion model (D4 mechanism) and the thermal degradation process of LDPE goes to a mechanism involving “Contracting cylinder” model (R2mechanism), whereas the mixture degrades following a kinetic model of D4. The authors also proved that a significant synergistic effect during pyrolysis of oil shale mixed with LDPE has been occurred [123].

From the above, it can be suggested that the co-pyrolysis kinetics had gained a lot of importance in the last decades due to the certain synergistic effects such as higher quantity and better quality of product, limited supply of certain feedstocks and improving the overall pyrolysis process.

2.18 Performance and emission analysis of bio-oil in IC engine

Bio-oil has been considered as a renewable liquid fuel, therefore it can be served as a substitute for fuel oil or diesel in many static applications including boilers, furnaces, engines and turbines for electricity generations. However, direct application of bio-oil in engines is complicated due to its acidic nature, low heating value and poor ignition properties. It can be advantageous to upgrade the bio-oil to certain extent to simplify its use in engines. Therefore, previously various authors have carried out the use of bio-oil with diesel blend through emulsification and some have mixed the bio-oil with diesel fuel in IC engine application.

Yang et al., studied the application of biomass pyrolysis oil in diesel engine. The oil obtained from pyrolysis of coffee bean residue was mixed with diesel fuel through emulsification. Three different proportions of bio-oil viz. CPO 0, CPO 5 and CPO 10 blends have been carried out with respect to various loads and engine rotational speeds to evaluate the performance indices for diesel engines. From the results, it was analyzed that the CPO 5 and CPO 10 had reduced the combustion efficiency, but the presence of water content in bio-oil partially enhanced the combustion

characteristics. Increased proportions of added bio-oil efficiently reduced NO_x emissions, but in certain situations, denser smoke was produced [124].

Vikrant et al. studied the Mustard cake pyrolytic oil (MCPO) in diesel engine with different blends of MCPO 10%, MCPO 20%, MCPO 30%, MCPO 40% and MCPO 50% were carried out to determine the engine performance and emission characteristics. They showed that the efficiency of MCPO blends was higher than that of diesel and it was increased to 4.7% for MCPO 30% blend. Un-burnt hydrocarbon emissions for B30 were lower than those for MCPO 40% but slightly higher than those of diesel fuel. Lastly, they concluded that MCPO 30% blend is a suitable blend for the substitute of diesel fuel [125].

De-linked sludge pyrolysis oil (DSPO) was blended with biodiesel and tested in multi cylinder indirect type of Internal Combustion (IC) engine. Performance, emission and combustion characteristics were compared against diesel fuel and biodiesel and at a constant speed of 1500 rpm. The author showed that there were a few differences in the results from the engine performance test of DSPO 20% and DSPO 30% oil. However, when compared with diesel fuel and biodiesel with DSPO- biodiesel blend, a number of small but significant differences was observed. Brake thermal efficiency was about 3-6% lower than that for biodiesel and was similar to diesel fuel. Exhaust emissions of the blends contained 4% higher CO₂ and 6-12% lower NO_x as compared to diesel fuel. At full load, the peak burn rate of combustion from the 30% blend was about 26% and 12% higher than that for diesel and biodiesel fuel respectively. In comparison to diesel fuel, the combustion duration was decreased for both blends, whereas for 30% blend at full load, the duration was almost 12% lower. The author concluded that up to 20% blend of de-linked sludge pyrolysis oil with biodiesel can be used in an indirect injection IC engine without adding any ignition additives or surfactants [126].

2.19 Concluding remarks

From the above discussion on previous research works related to various bio-oil upgradating technology, it is implied that co-pyrolysis is one of the promising and economically feasible technologies to produce the upgraded bio-oil. Related to co-pyrolysis, various research works have been done on the potentiality of co-pyrolysis techniques using mostly lignocellulosic biomass with different types of plastics waste. From their research works, it can be concluded that the obtained results are encouraging. Some investigations have been established to obtain high quantity and quality of oil without the presence of any catalyst or solvent and hydrogen pressure, which follows the various available standards. Co-pyrolysis process also provides various advantages such as reducing consumption of fossil fuels, solving some environmental issues, enhancing energy

security and improving waste management systems. Apart from this, co-pyrolysis process also provides simplicity in design and feasibility with respect to economical point of view.

There are some important factors before performing co-pyrolysis process which need to be emphasized in the feed system. To obtain a high grade liquid, adjustments of the types and feedstock ratios are important. The suitable combination of the feedstock in co-pyrolysis should be included. Many research works have stated that these combinations can provide improvements in pyrolysis oil through synergistic effects.

Co-pyrolysis process can be done with low cost, and no special equipment need to be designed and constructed for this process. Some minor modification may be required for feed preparation system. Moreover, this process also benefits to enhance the calorific value of byproducts. It is one of the optional solutions to increase the energy security of the nation and reduce dependence on fossil fuel.

However, previous various research works have been carried out on the upgradation of bio-oil from lignocellulosic biomass and different plastic wastes. A few literatures have been used to upgrade the bio-oil using non-edible seeds with plastic waste. On the other hand, kinetics of co-pyrolysis of non-edible seeds with plastic waste and the application of co-pyrolysis oil in engine have not been found.

Considering the above facts the main objectives of the current works are as follows.

2.20 Objectives of the research work

The research has attempted to obtain from several scientific overviews the use of Mahua seed to produce bio-oil, and the use of co-pyrolysis technique with regards to improving the pyrolysis oil. The specific objectives and approaches are as follows:

1. To study the potentiality of Mahua seed as a feed stock for pyrolysis oil and to optimized the conditions for maximum yield.
2. To characterize the liquid and solid products obtained from thermal pyrolysis of Mahua seeds as per their physical and chemical characterization.
3. Further improving the quality of bio-oil by co-pyrolysis of Mahua seed and polystyrene with different conditions.
4. Study the physical and chemical properties of co-pyrolysis liquid and solid products.
5. To study the thermal kinetics of Mahua seed, Polystyrene and their mixture by using various isoconversion with model free methods to evaluate the kinetic parameters.
6. To study the engine performance and emission analysis of Mahua bio-oil and co-pyrolysis oil separately.

Chapter 3

Experimental Section

3.1 Introduction

This chapter includes the collection of different types of raw materials. Before performing the experiment, the pretreatment methods are explained in detail. The procedure followed to determine the raw material characterization such as proximate and ultimate analysis, thermogravimetric analysis, and pyrolysis procedure are explained. Further, the liquid and the solid product obtained from thermal pyrolysis/co-pyrolysis studies has been described. The methods used for the liquid and solid product analysis are physical properties studies, chemical properties studies (like GCMS, FTIR and NMR, etc) for liquid product analysis and for solid product SEM, BET and bulk density are mentioned in this chapter.

3.2 Raw Materials

3.2.1 Collection of biomass and plastic materials

The used raw materials for this study are biomass Mahua seed (MS) and waste plastic Polystyrene (PS) which were collected from National Institute of Technology (Rourkela) campus waste yards, India, Odisha, and used for experiment. The high-grade chemicals used during the experimental analysis are KCL, chloroform-d and n-hexane, which were obtained from Fisher Scientific, Merck, and Sigma Aldrich. Fig. 3.1, Fig. 3.2, Fig. 3.3 and Fig 3.4 show the pictorial representation of raw materials.



Fig. 3.1 Mahua seed



Fig. 3.2 Polystyrene



Fig. 3.3 Mahua seed powder



Fig. 3.4 Polystyrene powder

3.2.2 Preparation of raw materials

Collected raw materials Mahua seeds were sun dried for 15 days to get them free from moisture. Before performing the experiment, Mahua seed were kept in the hot air oven at 105 ± 5 °C for one hour and then crushed in the grinder to get powder form. The Mahua seed powder was sieved using BSS standard sieve to collect the average particle size of $550 \mu\text{m}$. The Mahua seed powder samples were kept in air tight plastic bottle to get them free from moisture for remaining experiment. In the same way, the polystyrene waste was made into powder with the average size of less than 1 mm, for making it into powder to reduce its volume by heating in hot air oven for 2 hours at 100 °C. Before performing pyrolysis, the powdered samples of Mahua seed and polystyrene (MS: PS) were blended by tumbling for 30 min in order to achieve homogeneity.

3.3 Characterization of raw materials

3.3.1 Proximate and ultimate analysis

The characterization of raw materials was very important to check the suitability for thermochemical conversion. The major criteria for thermal pyrolysis are high volatile matter with low ash and sulfur content [127]. The sample of raw material was oven dried for further analyses and pyrolysis experiments. The proximate analysis of MS, PS and MS: PS 1:1 blend with its bio-char was performed according to the ASTM D 3172-07a, which provides the information on moisture content, volatile matter, fixed carbon and ash content. The ultimate analysis of the samples were carried out by CHNSO elemental analyzer (Variael CUBE Germany). It provides the elemental composition of carbon, hydrogen, nitrogen and sulfur percentages, while oxygen percentage was determined by difference. The calorific values of MS:PS, MS/PS 1:1 blend and bio-char were determined using ASTM D 4809-95 standard method. The major constituents of Mahua seeds are hemicellulose, cellulose, lignin and oil content, which were also determined by using the previous standard method [95,128].

3.3.2 Thermogravimetric analysis

Pyrolysis is thermal cracking of a substance under inert atmosphere. Hence, the effective pyrolysis temperature of MS, PS, and MS/PS (1:1) blend had to be determined. For this purpose, thermogravimetric analysis (TGA) of the raw materials were performed using a SHIMADZU model DTG-60/60H instrument. The samples were grinded into powder and sieved to a size of $<100\ \mu\text{m}$. The initial weight of the sample was approximately 10 to 12 mg with $<100\ \mu\text{m}$ size. They were taken in an Al_2O_3 crucible and heated up to $600\ ^\circ\text{C}$ at $20\ ^\circ\text{C}/\text{min}$ heating rate. High purity nitrogen gas at around 100 mL/min flow rate was used as an inert purge gas to displace air in the pyrolysis zone for avoiding unwanted oxidation of the sample. Thermal degradation depends on the amount of cellulose, hemicellulose and lignin content of that biomass sample. Thermo-gravimetric weight loss curve was plotted against temperature. The maximum range of thermal degradation of MS, PS and MS: PS 1:1 blend can be obtained from TGA.

3.3.3 Thermal pyrolysis of feedstock

3.3.3.1 Thermal pyrolysis of Mahua seed, polystyrene and their mixture

Fig 3.5 shows the schematic diagram of pyrolysis setup. The feedstock of MS and PS were fed individually into the stainless steel semi-batch reactor of 17.5 cm length with the inside and outer diameter 4.7 and 5 cm, respectively. Air was purged from reactor with a nitrogen flow rate of 30 mL/min for 15 min to create an inert atmosphere to perform all the experiments. The reactor was heated by electrical furnace and the temperature of the pyrolysis reactor was measured with Cr-Al (K type) thermocouple (error $\pm 2\ ^\circ\text{C}$) and controlled by using high sensitive PID controller. The temperature was maintained from $450\text{--}600\ ^\circ\text{C}$ in steps of $25\ ^\circ\text{C}$ at constant heating rate of $20\ ^\circ\text{C}/\text{min}$ and the maximum yield of the liquid product was obtained at $525\ ^\circ\text{C}$. The volatiles from the pyrolysis reactor were condensed with water cooled condenser at room temperature and the non-condensable gasses were vented out. After pyrolysis, the reactor was cooled down to room temperature and weighed to estimate the weight percentage of char (solid residue). The weight percentage of gas (non-condensable volatiles) was determined from the difference of condensable aqueous product and char. The total liquid product consisted of two phases, i.e., aqueous and oil phase. Separation of pyrolysis oil from the aqueous phase was done by centrifuging at 5000 rpm and then both were weighed individually. The centrifuge is shown in the Fig 3.6. The optimum temperature for maximum pyrolytic oil produced from MS and PS thermal pyrolysis was decided on the basis of highest weight percentage yield of the pyrolytic oil. The following 3.1, 3.2 and 3.3 equations were used to determine the weight percentage of liquid, solid and gaseous products obtained from pyrolysis of MS and PS.

$$\text{Liquid yield \%} = (\text{Weight of the liquid product} / \text{Weight of the feed}) \times 100 \quad (3.1)$$

$$\text{Char yield \%} = (\text{Weight of the char} / \text{Weight of the Feed}) \times 100 \quad (3.2)$$

$$\text{Gas yield \%} = 100 - (\text{Total liquid yield \%} + \text{Char yield \%}) \quad (3.3)$$

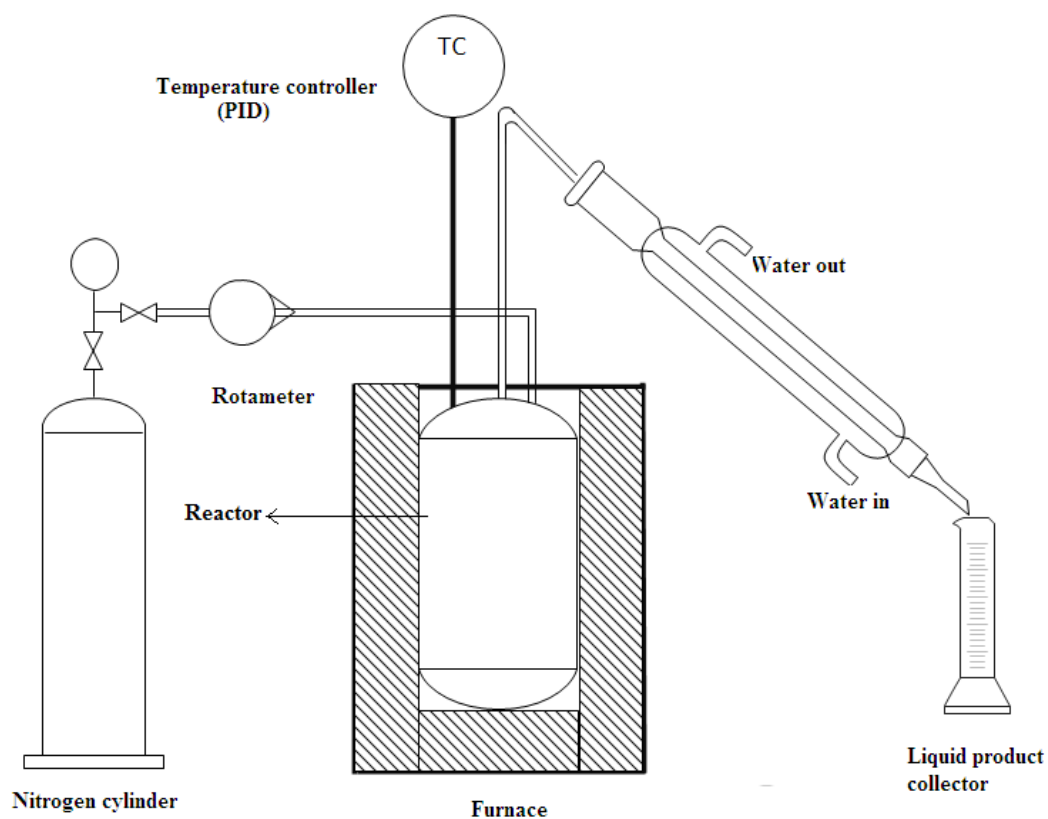


Fig. 3.5 Pyrolysis setup



Fig. 3.6 Centrifuge



Fig. 3.7 Mahua seed pyrolysis oil



Fig. 3.8 Polystyrene pyrolysis oil

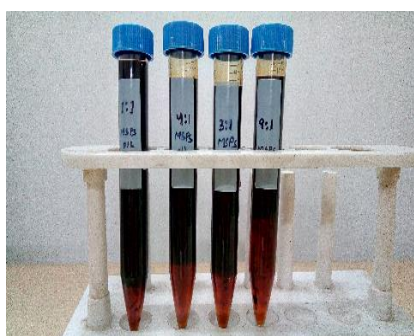


Fig. 3.9 MSPS pyrolysis oil with different blends at 525 °C

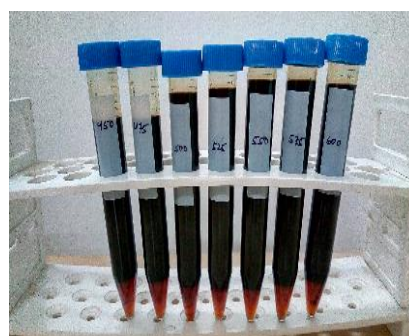


Fig. 3.10 MSPS 1:1 blend pyrolysis oil with different temperature



Fig. 3.11 Mahua seed bio-char



Fig. 3.12 MSPS bio-char

3.3.3.2 Thermal co-pyrolysis of Mahua seed: polystyrene blend

Co-pyrolysis of MS:PS was carried out in a semi-batch reactor with different operating conditions such as blending ratios (of 9:1, 3:1, 4:1 and 1:1), constant heating rate of 20 °C/min, with 525 °C temperature and nitrogen flow rate of 30mL/min for 15 min. Further the optimum blend 1:1 was carried out with the temperature range of 400-600 °C for pyrolysis experiment. The above equations 3.1, 3.2 and 3.3 which were used for thermal pyrolysis of MS and PS are also used for the co-pyrolysis of MSPS to obtain the weight percentages of liquid, solid and gaseous products.

The obtained liquid and solid products are shown in Fig 3.7, Fig 3.8, Fig 3.9 , Fig 3.10 , Fig 3.11 and Fig 3.12, respectively.

3.4 Characterization of pyrolytic oil

The characterization of the pyrolytic oil was done based on its physical and chemical properties. The physical properties such as density, calorific value, viscosity, distillation temperature, pH, Conradson carbon residue, flash point, fire point, pour point analysis and water content were determined. The chemical analysis of pyrolytic oil was done by FTIR, GC-MS and ^1H -NMR, analysis. The instruments used during the analysis of the samples and conditions are prescribed below.

3.4.1. Density

The density of the pyrolytic oil was kept in thermal bath at 15 °C as per ASTM D 4052. A small volume (approximately 0.6 ml) of pyrolytic oil samples was introduced into an oscillation U-shaped tube and the change in oscillating frequency caused by the change in the mass of the tube was used in conjunction with calibration data to determine the density of the sample.

3.4.2. Calorific value

Bomb calorimeter (Model Parr 6100 EE digital bomb calorimeter) was used to determine the calorific value of the MS, PS and MS: PS mixture pyrolytic oil. Pyrolytic oil of 0.5 ± 0.05 g was taken inside the bomb and burned in the presence of oxygen. An increment of ± 0.01 °C accuracy was used to determine the calorific value as per ASTM D 4809-95.

3.4.3. Viscosity

The viscosity of the pyrolytic oil was determined using a dynamic shear rheometer RHEOPLU/32v2.66 (Anton Paar) Cone (dia 39.018 mm and length 60 mm) and cup (internal diameter 41.97) type geometry was used to determine the viscosity, where the temperature was controlled accurately ± 0.05 °C by TC 30 temperature controller.

3.4.4 Distillation temperature

Thermogravimetric analysis was also used to detect the distillation temperature of fuels [129,130]. Thermogravimetric analyzer (NETZSCH STA 449 C) was used to detect the distillation temperature of pyrolytic oil samples. Exactly 20.046 mg of pyrolytic oil samples were heated from 25 to 500 °C in Al_2O_3 crucible at a heating rate of 10 °C/min. The evaporation study of pyrolytic oil samples was conducted under argon atmosphere at a flow rate of 30 mL/min. The weight loss data were collected with respect to temperature. The percentage evaporation of oil with

temperature was considered as percentage separation with respect to temperature (as distillation temperature).

3.4.5 Water content and pH analysis

The water content of the pyrolytic oils was estimated using Aquamax KF Oil Evaporator model 51000 as per ASTM method D6304. 5 g pyrolytic oil samples were mixed in 10 ml dried hexane and shaken well till they dissolved. 1.0 ml aliquot was injected into the base oil of the oil evaporator. The liberated moisture was transferred into the titration vessel by the carrier gas, where it was titrated colorimetrically. Each experiment was repeated three times and the average was taken into consideration. The pH of the pyrolytic oil was determined by using Eutech water proof pH 510 (pH Spear) pH meter.

3.4.6. Conradson carbon residue

Conradson carbon residue is used to measure the carbonaceous materials left in the fuel after all the volatile components are vaporized in the absence of air. According to the ASTM D 189, the carbon residue was measured by weighing a known sample quantity in the crucible and subjected to destructive distillation. The residue undergoes thermal cracking and coking reactions during a fixed period of severe heating. At the end of the specified heating period, the crucible containing the carbonaceous residue is cooled in a desiccator and weighed.

3.4.7 Flash point, fire point, pour point

Flash point of a fuel is the temperature to which the fuel must be heated to produce an ignitable vapour mixture above the liquid fuel, when exposed to an open flame. Generally, flash point is used in industry specification for fuel oil. Fire point of the fuel is the temperature when an oil in an open container gives off vapour at a sufficient rate to continue to burn after a flame is applied. Pour point is defined as the lowest temperature at which the oil will just flow under standard test conditions. The flash point, fire point and pour point of all the pyrolytic oils were determined by using the ASTM D 92 for flash point, ASTM D 92 for fire point and ASTM D 97 for pour point, respectively.

According to ASTM D3828, the test cup is filled with require amount of sample with a specific level. Temperature is rapidly increased at first and then at a slow, constant rate as the flash point is approached. At specified intervals, a small test flame is passed across the cup. The lowest temperature at which the vapours above the surface of the liquid ignite is taken as the flash point. The test is continued until the application of the test flame causes the oil to ignite and burn for at least 5 second. This temperature is called fire the point. Similarly the pour point of the oil has been determined according to ASTM D 97, in this method the oil sample is poured in the vessel and

cooled at a specified temperature and examined at 3 °C intervals for flow. The lowest temperature at which no movement of the oil is detected is recorded. The 3°C the temperature value immediately preceding the recorded temperature is defined at the pour point.

3.4.8 FTIR analysis of pyrolytic liquid

The presence of organic functional groups of different chemicals in the pyrolytic oils were determined by Fourier transform infrared spectroscopy (FTIR) using a Perkin Elmer FTIR at 8 cm⁻¹ resolution in the range of 400–4000 cm⁻¹ using Nujol mull. A small drop of the oil was mounted on KBr pellet and the infra-red spectrum of the bio-oil was taken.

3.4.9 ¹H-NMR analysis of pyrolytic oil

¹H-NMR spectra were recorded for bio-oils obtained from pyrolysis of the MS,PS and MS:PS by using a 400 MHz, BRUKER DPX-400, High performance digital FT–NMR spectrometer by using chloroform-d containing TMS (tetramethylsilane) as the internal standard.

3.4.10 GC–MS analysis of pyrolytic liquid

Gas chromatography and mass spectroscopy (GC–MS) was performed to quantitatively examine the elemental compounds in the bio-oil and aqueous phase by using Agilent 7890B Network GC system that was programmed at 70 °C for 3 min and then increased to 300 °C at 10 °C/min where the total GC run time was 25 min. The DB–5ms column of diameter 0.250 µm and 30 m length was used where 1 µL bio-oil was injected into the column with the carrier gas (Helium) at 1.5 mL/min flow rate. Chemical compounds present in bio-oil and aqueous phase were ionized at 70eV ionization energy, 230 °C ion sources temperature and were analyzed over a mass electron (m/z) range of 40–700. The chromatogram of the chemical compounds at different retention time and respective mass spectra were plotted and compared against the spectral data with the W9N11 MS library.

3.5 Characterization of bio-char

The solid product obtained from the Mahua seed and Mahua seed/Polystyrene pyrolysis was called char. The characterization of char based on physical and chemical characteristics such as calorific value, pH, bulk density, proximate analysis, ultimate analysis, SEM analysis, and BET analysis was done.

Bulk density is primarily used for powder materials that reflects the flow consistency and packing quantity of solid fuel material. It is determined according to ASTM D 1895 standard method and expressed in kg/m³. Mahua biochar sample was suspended in a 0.1N KCl (neutral salt) solution in a 1:10 (wt/wt) ratio. After 30 min of stirring in an incubator shaker at 25 °C and 127 rpm, the pH of the biochar suspension was measured using Eutech water proof pH 510 (pH Spear) pH meter.

Scanning electron microscopy (SEM) is a potential technique for studying solid fuel particles physical morphology of the precursor. SEM images are very useful to obtain accurate pore structure due to the structural vibrations in biochar particles after thermal treatments. SEM images were taken at 15 kV accelerating voltage with a JEOL-JSM-6480LV model.

The surface area of biochar was determined by nitrogen adsorption at 77 K using an automatic adsorption instrument (Quanta chrome Corporation, Autosorb 1C) and operating with the static volumetric technique. Prior to gas adsorption measurements, the biochar was vacuum degassed at 200 °C for 4 hours, to remove adsorbed moisture or other impurities bound to the surface.

Chapter 4

Thermal pyrolysis of Mahua seed, polystyrene and their mixture

4.1 Introduction

Co-pyrolysis of biomass and plastic can enhance the stability of bio-oil as a fuel since plastics can provide hydrogen that the biomass lacks. Plastics have higher hydrogen fraction than biomass and their pyrolysis produces liquid with no water content. Despite their high potential as renewable energy sources, waste plastics were discarded due to many social problems [77]. Co-pyrolysis has received much attention in recent years because it provides an alternative way to dispose of and convert waste plastics and biomass to high value feed stock and fuels. Recent investigations have shown that biomass and plastic co-pyrolysis achieved a synergetic effect with increment in liquid yield products and improvement in the overall process efficiency.

In this work, we intend to produce upgraded bio-oil with lower oxygen and higher carbon and hydrogen contents by performing co-pyrolysis of Mahua seeds with polystyrene (PS) plastics in semi-batch reactor in the presence of inert atmosphere with different blending ratios of (9:1, 3:1, 4:1 and 1:1) at constant heating rate of 20 °C/min and temperature range from 400-600 °C. The highest bio-oil yield obtained at an optimum blend was characterized using various physical and chemical properties (like FTIR, GC-MS, ¹HNMR) analysis. The obtained bio-char yield at an optimum conditions was also characterized as per its physical and chemical properties studies. The experimental conditions of co-pyrolysis need to be optimized and the suitability of individually pyrolyzed MS and co-pyrolysed MSPS product as feedstock need to be investigated for the production of alternative fuels and chemicals.

4.2 Experimental Section

The experimental section of Mahua seed, Polystyrene and Mahua seed/Polystyrene blend has explained detail in chapter 3.

4.3 Analysis of feedstock

4.3.1 Characteristics of feedstocks

Proximate and ultimate analyses are one of the primary analyses for fuel characteristics evaluation to know the potentiality of the fuel. The proximate analysis provides the detail composition of biomass and plastic such as moisture, volatile matter, fixed carbon and ash content, whereas the

ultimate analysis quantifies the carbon, hydrogen, nitrogen sulphur and oxygen content of the raw materials as shown in the Table 4.1.

Table 4.1 Proximate and ultimate analysis of raw materials

Characteristics (wt %)	Mahua seed	Polystyrene	Mahua seed: Polystyrene (1:1)
Proximate analysis			
Moisture	8.6	0.2	4.02
Volatile Matter	84	99.23	91.96
Fixed carbon	5.4	0.57	3.05
Ash	2	0	0.97
Ultimate analysis			
C	61.24	89.10	74.62
H	8.4	9.75	9.06
N	4.12	1.15	2.46
S	0.74	—	0.21
O (By difference)	25.5	—	13.65
GCV (MJ/kg)	26.7	41	33.47
Empirical formula	$\text{CH}_{1.64}\text{N}_{0.05}\text{S}_{0.004}\text{O}_{0.31}$	$\text{CH}_{1.31}\text{N}_{0.01}$	$\text{CH}_{1.45}\text{N}_{0.02}\text{S}_{0.0009}\text{O}_{0.13}$
H/C molar ratio	1.64	1.31	1.45
O/C molar ratio	0.31	0	0.13
Oil content	31	—	—

The compound which is driven-off during the heating of biomass sample is mainly considered as volatile mater. In pyrolysis both volatile matter and ash content affect the quantity and quality of pyrolysis liquid. The volatile matter of Mahua seed (MS), polystyrene (PS) and its MS: PS (1:1) blend is 84, 99.23 and 91.96 %, respectively. Furthermore, the ash content of MS is 2% and MS:PS blend is 0.97%, however there is no ash present in PS, hence these solid fuels can be favorable for the production of pyrolysis oil on large scale [94,131,132]. In addition, the moisture content of solid fuel could affect the conversion efficiency during combustion. However, it was stated that the high moisture content has a tendency to bring down resulting energy of biomass during storage [7,98]. The moisture content in biomass MS is 8.6%, whereas negligible quantity of moisture present in plastic (PS) makes the moisture to 4.02% in MS: PS blend. In our study, the

presence of moisture in biomass is considerable for thermochemical process as suggested by previous literature [98]. The amount of fixed carbon in MS, MS: PS blend and PS is 5.4%, 3.05%, 0.57% respectively. Previously, it was suggested that less fixed carbon has positive contribution to increased pyrolysis oil yield [98]. From the ultimate analysis, it is estimated that the carbon content of PS and MS/PS blend is more than that of individual biomass. The hydrogen and carbon percentage in plastic is more than that of biomass because of the origin of plastic, and makes it easier to be converted into hydrocarbon fuels. The amount of oxygen in MS is more than that of MS:PS blend, whereas there is no oxygen present in PS. Abnisa et al. reported that the presence of high oxygen content is one of the factors in decreased calorific value of fuel [19]. Thus, the presence of more oxygen in MS signifies that the obtained calorific value of MS is less than that of PS and MS: PS blend. Consequently, the mixture of plastic and biomass could make positive contribution for energy production. The average chemical composition of raw materials are $\text{CH}_{1.64}\text{N}_{0.05}\text{S}_{0.004}\text{O}_{0.31}$, $\text{CH}_{1.31}\text{N}_{0.01}$ and $\text{CH}_{1.45}\text{N}_{0.02}\text{S}_{0.0009}\text{O}_{0.13}$, respectively. Oil content of Mahua seed is 31%. These analyses provide an effective way to assess the type and quality of the fuel after which further experiments can be pursued.

4.4 Thermogravimetric analysis

4.4.1 Thermal decomposition profile of Mahua seed, polystyrene and their mixture

Thermal degradation characteristics of MS, PS and MS: PS (1:1) blends were established by performing TGA and DTG, which provides the correlation between the weight loss and temperature. TGA and DTG curves are plotted from ambient temperature to about 600 °C with 20 °C/min heating rate as shown in Fig. 4.1 and Fig. 4.2. It is evident from Fig. 4.1 that the biomass, plastic and their mixture have different thermal decomposition profiles, characteristic of their structural differences. It is illustrated in the Fig. 4.1 that PS has decomposition profile at higher temperature range of 400 to 458 °C, where 99% of the maximum decomposition occurred. However, MS consists of cellulose, hemicellulose and lignin, therefore all the three different polymers have different decomposition stages. According to weight loss temperature curve of MS, the small amount of weight loss (10%) was observed from ambient temperature to around 137 °C, which suggests that inherent water was being released within the biomass sample, and similar observation has also occurred for other biomass samples in earlier studies [133]. At the intermediate stage, a maximum 82% of the conversion took place up to 600 °C. The maximum conversion was observed between 200–400 °C, after which the decomposition rate became relatively constant. A small decomposition profile was observed from 400 to 600 °C due to the

unburned carbon with 17% of residue. In the same way, the three decomposition stages were observed for MS: PS blend. Fig. 4.1 shows that the decomposition process started early at ambient temperature up to 200 °C as the presence of moisture in biomass and the plastic makes the materials softened corresponding to that temperature, but not decomposed at that temperature, therefore they could affect the heat and mass transfer process at that stage [121]. Corresponding to the second stage decomposition started from 200 to 469 °C, where the maximum 90% decomposition occurred. According to previous literature, it was suggested that the char from biomass plays a role of thermal stabilizer for PS, due to the solid-solid and gas-solid interaction in co-pyrolysis. It increases decomposition temperature compared to individual pyrolysis of PS [27]. The charcoal and some components of heavy products from biomass thermal decomposition can act like radical donors in the initiation of the polymer chain scission. According to common interpretations, the thermal degradation proceeds as a radical chain process including the steps of radical initiation, chain propagation and radical termination [25]. Subsequently, a slow rate of decomposition was observed up to 600 °C due to the presence of some extractive material present in the biomass with 10.17% of residue. DTG peak gives the better representation of the conversion of MS, PS and its blend. From Fig. 4.2, it is seen that the maximum conversion of MS occurs in the temperature range from 150 to 340 °C, PS occurs in the range from 390 to 450 °C while for MS: PS blend it is observed in the range from 400 to 500 °C. The peak temperature of MS: PS is higher (at 441 °C) than that of MS (275 °C), and PS (436 °C) with the high decomposition intensities of -3.03, -1.53, and -8.23 (mg/min), respectively. However, the increase in intensity of MS: PS blend illustrated that there is a significant synergistic effect of Mahua seed and Polystyrene during thermal degradation. From the above discussion we observed that the maximum decomposition range for MS and MS: PS blend is 400 to 600°C, therefore the active pyrolytic zone was established in the temperature range from 450-600 °C.

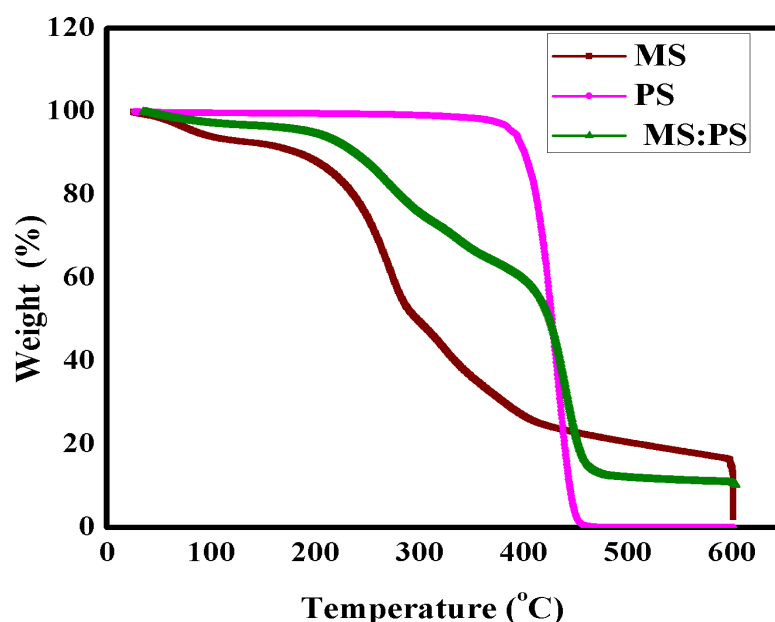


Fig. 4.1 TGA plot of MS,PS and MSPS blend

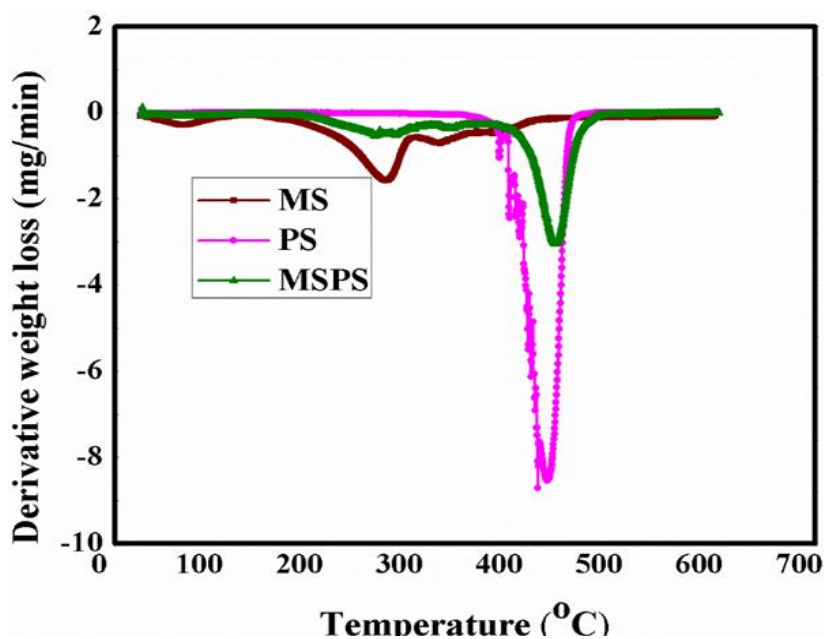


Fig. 4.2 DTG plot of MS,PS and MSPS

4.4.2.1 Influence of temperature on pyrolysis product yield of Mahua seed

Thermal pyrolysis experiments were carried out to determine the optimum temperature at which the bio-oil yield from Mahua seed was maximum. The pyrolysis yields of bio-oil, aqueous phase, bio-char and non-condensable gases of Mahua seed with 0.55–1 mm particle sizes and temperature ranging from 450 to 600 °C at 20 °C/min heating rate have been represented in Fig. 4.3. It can be seen from the graph that the bio-oil yield increased with temperature and at 525 °C, the maximum yield of 49% was obtained, after which the yield percentage continued to decrease. The maximum bio-oil yield at 525 °C can be attributed to thermal cracking, depolymerization and

recondensation of secondary reactions [134]. The bio-char yield, however, decreased from 26 % to 14 % with increasing temperature, probably because of greater primary decomposition of Mahua seed or secondary decomposition of the char residues with rising temperature. The non-condensable gas increased from 18% to 28%, with increasing temperature, mainly due to secondary decomposition of pyrolysis vapors and bio-char at higher temperatures [98].

4.4.2.2 Comparison of thermal pyrolysis product yield of Mahua seed, Polystyrene with Co-pyrolysis yield

Focusing on previous study of co-pyrolysis, it was proved that plastic like polyolefin material is one of the suitable co-feeds for improving the quality and quantity of oil [15]. In this study, Polystyrene (PS) was used as a co-feed to improve the quality and quantity of oil. Here, pyrolysis of MS, PS and MS: PS blends of (1:1, 3:1, 4:1, and 9:1) were performed in batch reactor at various temperature ranges of 450 to 600 °C with 25°C elevation temperature. Fig. 4.3, Fig. 4.4 and Fig. 4.6 show that temperature had a major influence on pyrolysis product yield of MS, PS and MS: PS (1:1) blend, respectively.

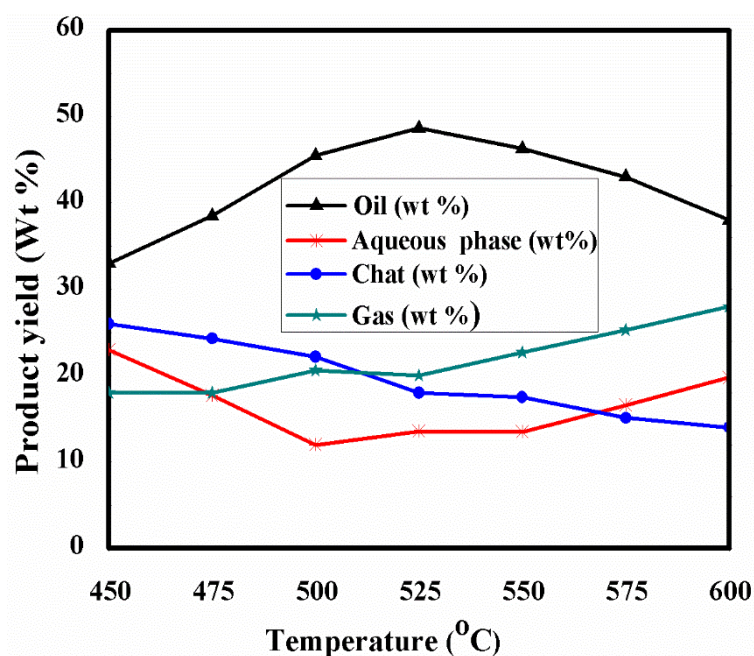


Fig. 4.3 Influence of temperature on pyrolysis product yields of Mahua seed

The volatile content of MS, PS and MS: PS (1:1) blend was quite large, therefore the liquid product obtained is more than that of other products. From the Fig. 4.3 it is illustrated that bio-oil yield of MS increased with increase in temperature. At 525 °C, the maximum yield of 49% was obtained, after which the yield percentage continued to decrease. But the oil yield was less than that of co-pyrolysis yield of MS:PS. Similarly, the maximum oil yield of 99.65 % of PS obtained at 525 °C, because PS consists of a single polymer and the highest decomposition occurred at this

particular temperature and there was no residual product obtained. According to Lee et al. [135] during thermal decomposition of polystyrene its reaction mechanism follows both end-chain and random-chain scission. Polystyrene starts to thermally decompose from the end groups, successively yielding the monomers units as well as cracking randomly into smaller molecules of one or more benzene-ring structures, yielding high fraction of monomers. The maximum 100 % conversion took place in PS, whereas 82 % conversion took place for MS with 18 % residual product. Henceforth, 525 °C is considered as the suitable temperature for co-pyrolysis of MS: PS with the different blending ratios of (1:1, 3:1, 4:1, and 9:1). From Fig. 4.5, it is seen that the maximum bio-oil was obtained with increase in the plastic ratio. Hence, the maximum bio-oil yield of 74.25% was obtained at 525 °C with 1:1 blend. This is attributed to the polyolefin materials like PS, PP, HDPE, and LDPE that are good hydrogen sources, which supports to enhance the liquid yield, while co-processing with biomass [19]. Moreover, MS is less thermally stable as compared to PS, which is one of the positive significant to the degradation of synthetic macromolecules by affecting their radical degradation mechanism. Biomass and plastic have different decomposition mechanism in the thermal pyrolysis process. However, pyrolysis of biomass involves a series of exothermic and endothermic reactions, whereas the pyrolysis of plastic alone occurs by radical mechanism (initiation, propagation, and termination). Hence, the pyrolysis of biomass mixed with polystyrene yielded about 25.25 wt % more oil than pyrolysis of biomass alone, which also resulted in a decrease in char product. The reason for decreasing of char yield is that due the presence of hydrogen in plastic partly inhibited the condensation reactions. Here we can also observe that the degree of polymerization has a strong influence on the thermal degradation of polymers. From the above discussion, it can be concluded that the addition of PS with MS has shown significant influence on enhancing the oil yield and decreasing the aqueous phase yield, and the ratio of the feed was also a significant variable affecting liquid yield production.

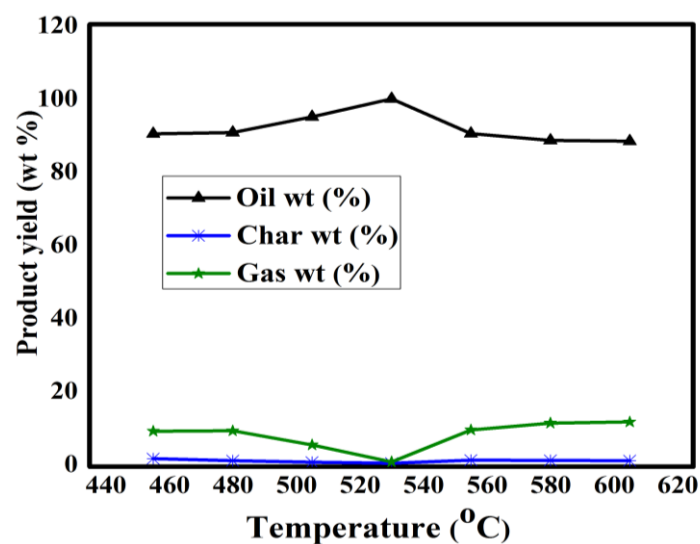


Fig. 4.4 Pyrolysis product yield of Polystyrene

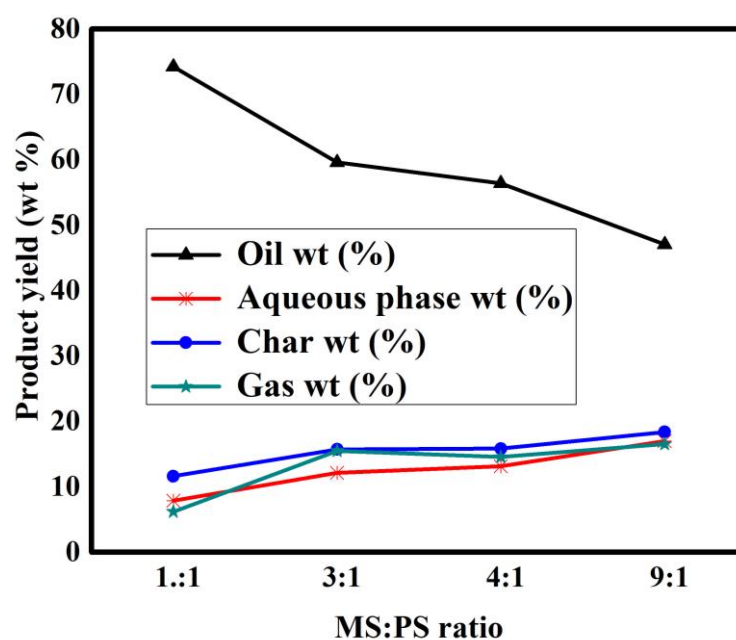


Fig. 4.5 Co-pyrolysis of different ratio of MS:PS at 525 °C

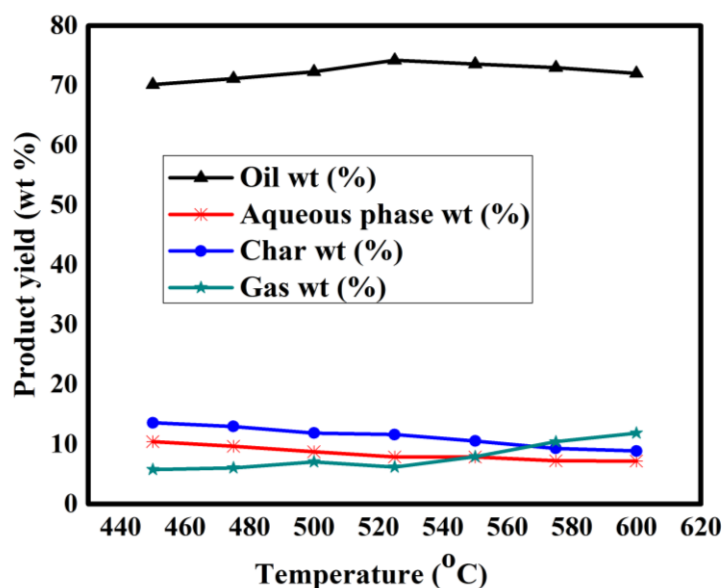


Fig. 4.6 Co-pyrolysis of 1:1 ratio of MS:PS at different temperature

4.5 Characterization of pyrolytic oil

4.5.1 Elemental analysis of Pyrolytic oils

The elemental analysis of pyrolytic oil was accomplished to reveal the effect of PS addition to biomass. The quantitative representation of carbon, hydrogen, nitrogen, sulfur and oxygen in MS, MS: PS (9:1), (4:1), (3:1), (1:1) and PS pyrolytic oils are estimated and shown in Table 4.2. Heat formation arises during the combustion of pyrolytic oil, which is commonly owing to burning of carbon and hydrogen in pyrolytic oil. Thus, to estimate the fuel potential, elemental composition of products from biomass, plastic pyrolysis is important. The presence of carbon and hydrogen in biomass is 69.32% and 9.12%, respectively, which is less than that of plastic, however the carbon and hydrogen percentage increases in all the blends of MS:PS as compared to MS, with increasing ratio of plastic (PS). After co-pyrolysis is applied, hydrogen and carbon content of oil increased to enhance the H and C content of biomass pyrolysis oil. The reason for the increment of H and C content of co-pyrolysis oil is due to the composition of plastic. The amount of nitrogen and sulphur content in the co-pyrolysis oil is also decreased. The presence of oxygen in biomass pyrolytic oil is more as compared to the co-pyrolysis and plastic pyrolysis oil. Therefore, the obtained calorific value of MS pyrolysis, plastic pyrolysis oil and co-pyrolysis are varying. Fuel classification is mostly based on the atomic ratio. In order to produce potential bio-oil, the O/C molar ratio should be decreased and H/C molar ratio.

Table 4.2 Elemental analysis of pyrolytic oils

Elemental analysis (wt%)	MS oil	PS oil	MS/PS 1:1	MS/PS 3:1	MS:PS 4:1	MS:PS 9:1
Carbon	69.32	85.68	74.07	72.65	72.48	70.53
Hydrogen	9.12	13.48	12.24	11.44	11.23	9.68
Nitrogen	2.53	0.84	0.72	1.02	1.08	1.56
Sulphur	0.89	0.00	0.18	0.31	0.33	0.53
Oxygen	18.14	0.00	12.79	14.58	14.88	17.7
(by difference)						
H/C	1.58	1.88	1.98	1.89	1.85	1.66
O/C	0.19	0.12	0.12	0.15	0.15	0.18
Calorific value (MJ/kg)	39.02	43	42.3	41.26	41.26	39.58
Empirical formula	CH _{1.58} N _{0.03} S _{0.005} O _{0.19}	CH _{1.88}	CH _{1.98} O _{0.79}	CH _{1.89} O _{0.15}	CH _{1.85} N _{0.01} O _{0.15}	CH _{1.66} N _{0.01} O _{0.18}

should be increased [40]. Our results followed the same trend for biomass pyrolysis oil as well as plastic and co-pyrolysis oil. Consequently, co-pyrolysis oil could be useful for the production of potential bio-oil. The average chemical composition of pyrolytic oils are CH_{1.58}N_{0.03}S_{0.005}O_{0.19}, CH_{1.88}, CH_{1.98}O_{0.79}, CH_{1.89}O_{0.15}, CH_{1.85}N_{0.01}O_{0.15}, and CH_{1.66}N_{0.01}O_{0.18}, respectively. From the above it was revealed that the co-pyrolysis oil of 1:1 blend represents the effective results as compared to the biomass pyrolysis oil and other co-pyrolysis oil blends.

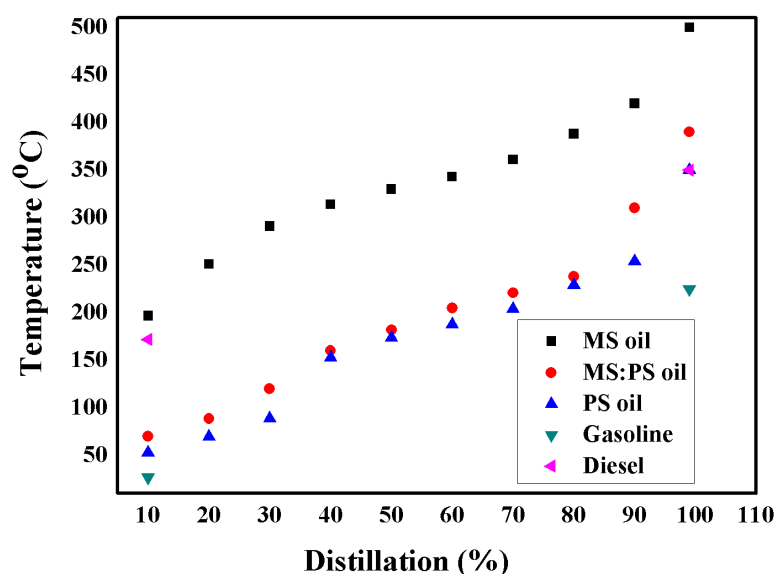
4.5.2 Physical properties of pyrolytic oil

From the above elemental analysis, it was found that co-pyrolysis oil of MS: PS 1:1 blend gives the more suitable results than that of the biomass pyrolysis oil. However, for further application in chemical industry and as a substitute of conventional fuel, the physical properties of bio-oil are very essential. The fuel properties have biggest impact on its performance when it is used for various purposes. Thus, for better understanding of the fuel characteristics, some of the physical properties are required to characterize it. The physical properties include viscosity, heating value, water content, pH value, density, distillation range, flash point, fire point, pour point and carbon

residue of the MS, PS and MS:PS 1:1 blend pyrolytic oil, which have been identified and compared with conventional petroleum fuel, which is shown in the table 4.3. The results indicated that the density of pyrolysis oil produced from the MS and mixture of MS:PS is higher than that of conventional fuel, because of the presence of a large amount of water and macromolecules such as cellulose, hemicelluloses, oligomeric and phenolic compounds [136]. Moreover, the kinematic viscosity of the MS pyrolysis oil is 23.19 cSt at 40 °C which is higher than that of co-pyrolysis oil and conventional fuel, owing to some high molecular weights of the lignin-derived chemical compounds which are responsible for the higher viscosity [137]. The pH of the Mahua pyrolysis oil is 4.8, which shows that biomass pyrolysis oil is acidic in nature, however previously it was stated that most of the biomass pyrolysis oils are acidic in nature and have the pH value ranging from 2-4. The high acidic content is due to the presence of carboxylic acid, acetic acid and formic acid in the pyrolytic oil [32]. Acidity causes corrosion of materials in the storage and also while used in Internal Combustion (IC) engine. Mahua bio-oil contains organic acids like octanoic acid, octadecenoic acid and tetradecenoic acid. Therefore the pH of Mahua bio-oil is acidic in nature, but the pH of co-pyrolysis oil slightly increases, which is due to the presence of polystyrene [138]. The oil obtained from polystyrene is not acidic in nature, having the pH of 7.2. However, the formation of these acids in bio-oils is due to the depolymerization of cellulose and hemicelluloses. High cellulose content in the biomass produces more acid in the pyrolytic oil during pyrolysis. The presence of various acids in the pyrolytic oil also reduces the thermal stability during storage [140].

Table 4.3 Physical properties of pyrolytic oil

Property	MS oil	MS/PS oil	PS oil	Gasoline	Diesel fuel
Density at 15 °C (kg/m ³)	921.3	908	810	750 at 20 °C	830 kg/m ³
Kinematic viscosity at 40 °C (cSt)	23.19	1.943	0.976	–	2.58
Flash point (°C)	84	58	44	-43	50
Fire point (°C)	118	60	47	–	56
Pour point (°C)	33	6	-18	-40	-28
Water content (Wt %)	1.1	0.50	–	0	0
pH	4.8	5	7.12	–	–
Carbon residue (Wt %)	3.08	0.813	0.02	–	0.1

**Fig. 4.7 Distillation Curve of MS, PS, MSPS pyrolysis oil with other conventional fuel**

But the addition of plastic in biomass improves and lowers the acidic nature as the pH of plastic oil is neutral. Flash point is the lowest temperature at which vapors from heated oil flash when exposed to an ignited open flame. If the heating continues, sufficient vapors are driven off to produce continuous burning for at least 5 seconds. The temperature at which this latter phenomenon occurs is called the fire point. Flash point is important because it is a measure of the volatility of the oil as well as its ignition characteristics, and indicates the maximum temperature for safe handling. Pyrolysis oil of biomass often has a reported flash point of between 50 °C and over 100 °C, reflecting a wide variation in the content of volatiles. However, above temperatures

of 70–75 °C, water vapors from the biomass pyrolysis oil start to disturb the analysis and a reproducible value is difficult to obtain [126]. The obtained flash point of Mahua bio-oil is 87 °C, the increase in flash point is due to the presence of water vapor in the bio-oil. The flash point of co-pyrolysis oil is 58 °C, which is lower than that of individual biomass pyrolysis oil. Pour point of the oil is the lowest temperature at which it flows under normal conditions. If the pour point will be higher, then it will be the disadvantages of the pyrolytic oil. However, if the oil is having a higher, pour point, then it will reduce the flow ability in winter especially in low temperature regions, due to the crystals formation, which clogs the filter and also reduces the efficiency of the combustion engines. Pyrolytic oil can be used as a transportation fuel, but due to its high pour point it may damage the engine. In the present study the obtained pour point is 33 °C, which is higher than that of conventional fuel, but it is reduced when biomass is co-pyrolysed with plastic. The presence of moisture content in biomass feed stock makes the water formation during pyrolysis. Moreover, during pyrolysis of biomass, dehydration reaction takes place and it produces water with the pyrolysis oil yield. The high water content of the pyrolysis liquid is responsible for low energy density, thus hindering its proper utilization as a fuel and hence making water content an undesirable property. The water content of Mahua bio-oil is 1%, whereas the co-pyrolysis mixture was found to be decreasing the water content of the pyrolysis liquid by approximately 0.5%. This decrease also contributed to the high calorific value of the co-pyrolysis liquid. The carbon residue of bio-oil is the amount of carbonaceous residue left over after the evaporation and pyrolysis of the oil under controlled condition. When an oil is evaporated, free carbon remains either because it was originally present, or because it was formed by cracking during the evaporation process. Higher carbon residue may cause clogging in the injector nozzles and coke formation in the combustion chamber [38]. The carbon residue of Mahua bio-oil is 3.08%, which is comparatively higher than that of conventional fuel; after the addition of polystyrene in Mahua seeds it reduces the carbon residue by 0.813%. This indicates that the plastic addition to biomass pyrolysis gives the synergetic effect on production of bio-oil. Distillation unit temperature operational limits are based on the temperatures at which the feedstock will decompose. The units are operated below temperatures at which the feedstock would undergo significant cracking, to minimize fouling in the unit. The volatility of the bio-oil was characterized with distillation temperature for combustion characteristics of the diesel engine. Fig 4.7 represents the distillation curve of MS, PS and MSPS pyrolysis oil with other conventional fuel. Mahua bio-oil chemical composition is a mixture of various valuable chemicals and shows a wide range of boiling temperatures. The initial and final boiling point of Mahua bio-oil is 197 °C and 500 °C, respectively. The slow heating of bio-oil during distillation causes polymerization, however the

distillation in co-pyrolysis oil gives good results which is near about that of conventional fuel. From the above physical properties study, it shows that the influence of plastic in biomass pyrolysis provides effective result and improves the quality of bio-oil as compared to the individual biomass pyrolysis oil.

4.5.3 Chemical properties analysis

4.5.3.1 Functional group analysis

Determining the chemical composition of bio-oil is also one of the important fuel characteristics similar to physical properties analysis. Chemical composition analyses such as FTIR, GC-MS and $^1\text{H-NMR}$ are the major analyses to determine the chemical compounds present in the liquid fuel. FTIR spectroscopy is also known as a non-destructive method of analysis, which is generally based on the absorption of the functional groups present in liquid fuel in infrared region. On interaction of infrared light with oil, chemical bonds will stretch, contract, and absorb infrared radiation in specific wavelength range, regardless of structure of the rest of the molecules [139]. The decomposition of cellulose, hemicellulose and lignin present in the biomass material and the interaction of these molecules with styrene during co-pyrolysis distinguishes the complex molecules through FTIR. Further, these were confirmed by GC-MS and $^1\text{H-NMR}$. The FTIR spectra of liquid fuel obtained at 525 °C for MS, PS and MSPS (1:1) were shown in the Fig 4.8 (A), Fig 4.8 (B) Fig 4.8 (C). Several peak with strong, and medium intensities were established with various bond types of C=O, O–H, C=C, and C–O in bio-oil fraction.

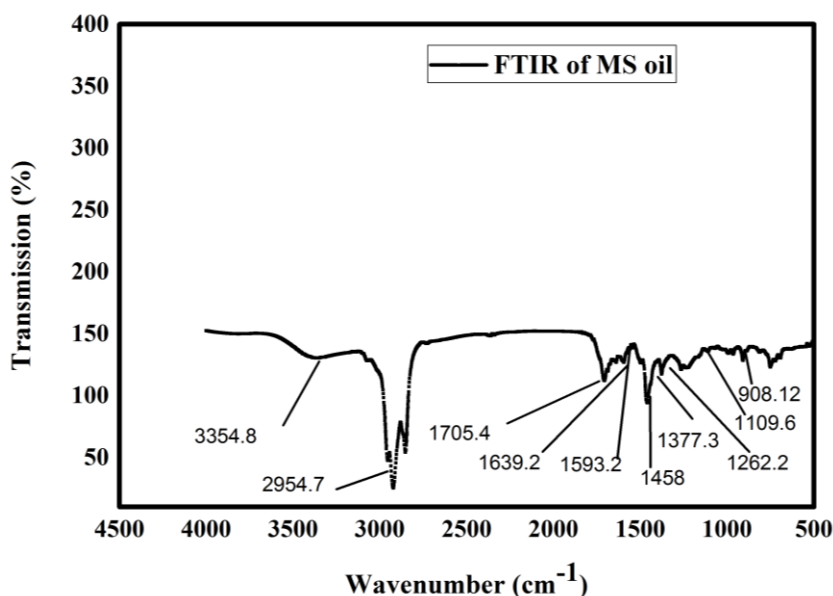


Fig. 4.8 (A) FTIR analysis of MS pyrolysis oil

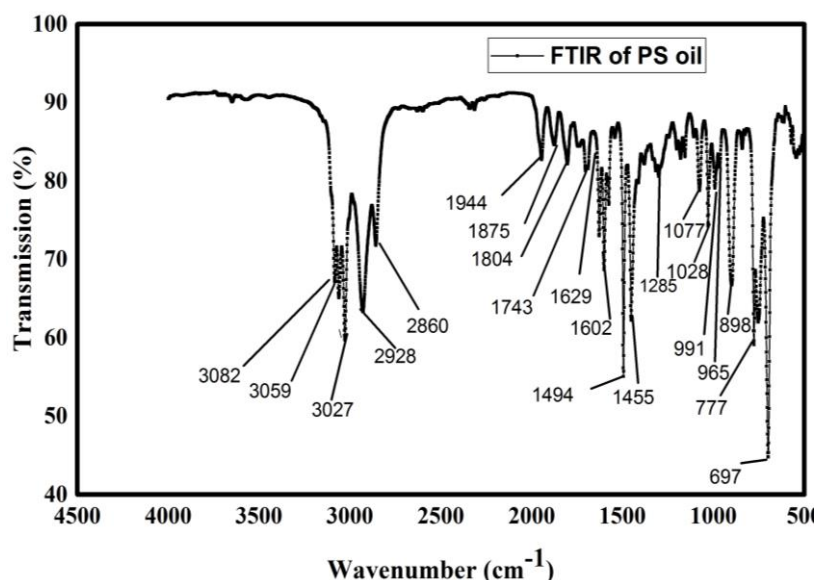


Fig. 4.8 (B) FTIR analysis of PS pyrolysis oil

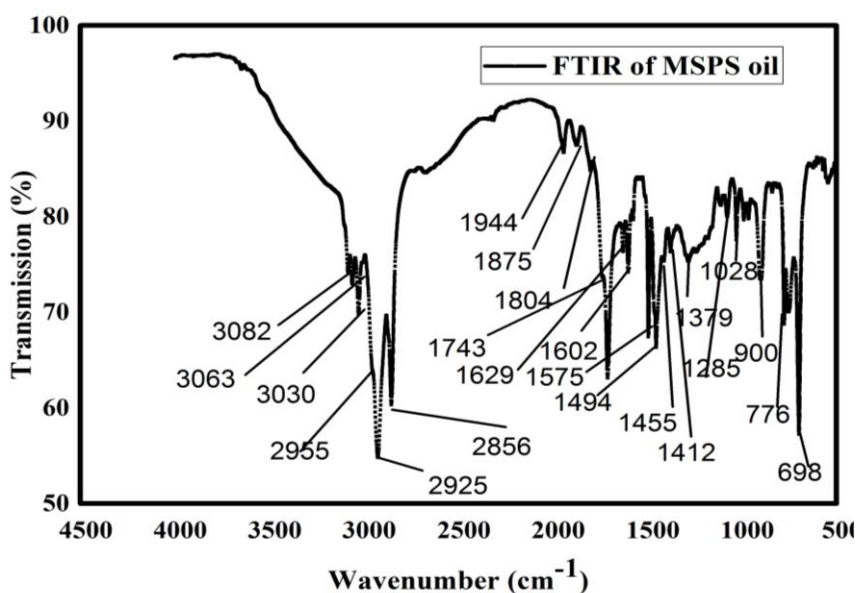


Fig. 4.8 (C) FTIR analysis of MSPS pyrolysis oil

Table 4.4 Table 4.5 and Table 4.6 represent the several functional groups corresponding to the wavelength range present in MS, PS and MSPS pyrolytic oil. O-H stretching vibration observed in 3354 cm⁻¹ represents the presence of phenol, carboxylic acid and water impurities in MS oil, however these functional groups are diminishing in the spectra of pyrolytic oil obtained from MSPS mixture. C=C Stretching vibration between 2000-1800 cm⁻¹ shows the presence of aromatic ring (aryl) group, aromatic combination bond in both MSPS and PS pyrolysis oil, but this is not observed in MS pyrolysis oil. This alteration of MSPS pyrolysis oil occurred because of the addition of polystyrene. C=O Stretching vibration between 1740-1700 cm⁻¹ and 1735-1750 cm⁻¹

indicates the presence of ketone and ester. The C=C stretching vibration with absorbance between 1650-1580 cm^{-1} indicates the presence of alkenes, aromatics. The C-C=C asymmetric stretching vibration between 1500-1400 cm^{-1} indicates the presence of benzene in MSPS and PS pyrolysis oil, which is not observed in MS pyrolysis oil. C \equiv C stretching vibration between 1470-1350 cm^{-1} indicates the presence of alkyne in all the pyrolysis oil. The C-O stretching vibration between 1300-950 cm^{-1} indicates the presence of ester and ether in all the pyrolysis oil. O-H bending vibration between the wavelength ranges of 1000–650 cm^{-1} indicates the presence of mono and polycyclic substituted aromatics groups in MS, PS and MSPS pyrolysis oil, but more aromatic compounds are there in both the MSPS and PS pyrolysis oil. From the spectra of co-pyrolysis oil, it was found that there is a significant decrease of phenolic, acidic compound, however most of the functional groups present in co-pyrolysis oil are aromatic compounds. The possible reason might be that the presence of aromatic polymers in polystyrene. Besides that, polystyrene acts as a hydrogen medium during co-pyrolysis of biomass and plastic this is also in agreement with previous literature [19,140,141]. The FTIR spectrum of the oil obtained from the co-pyrolysis closely resembles that of PS pyrolysis oil rather than that of MS pyrolysis oil.

Table 4.4 FTIR analysis of MS pyrolytic oil

Wave length range (cm^{-1})	Frequency (cm^{-1})	Functional group	Type of vibration
3500-3300	3354.8	Phenol, Carboxylic acid, Water impurities	O-H Stretching
2960-2850	2954.7	Alkane	C-H Stretching
1740-1700	1705.4	Ketone	C=O Stretching
1650-1580	1639.2, 1593.2	Alkenes, Aromatics	C=C stretching
1470-1350	1458, 1377.3	Alkyne	C \equiv C stretching
1300-950	1262.2, 1109.6	Esters and ethers	C-O stretching
1000–650	908.12	Mono and polycyclic substituted aromatics groups	O-H bending

Table 4.5 FTIR analysis of PS pyrolysis oil

Wave length range (cm ⁻¹)	Frequency (cm ⁻¹)	Functional group	Type of vibration
3010-3100	3082, 3059,3027	Alkene	=C-H Stretching
2960-2853	2928,2860	Alkane	C-H Stretching
2000-1800	1944,1875,1804	Aromatic ring (aryl) group, aromatic combination bond	C=C stretching
1735-1750	1743	Ester	C=O Stretching
1650-1580	1629,1602,1575	Alkene, Aromatics	C=C stretching
1500-1400	1494	Benzene	C-C=C Asymmetric Stretching
1470-1350	1455	Alkyne	C≡C stretching
1300-950	1285, 1077, 1028	Ester, Ether	C-O Stretching
1000-650	991,965,898,777,697	Mono and polycyclic substituted aromatics groups	O-H Bending

Table 4.6 FTIR analysis of MSPS pyrolysis oil

Wave length range (cm ⁻¹)	Frequency (cm ⁻¹)	Functional group	Type of vibration
3010-3100	3082, 3063,3030	Alkene	=C-H Stretching
2960-2853	2955,2925,2856	Alkane	C-H Stretching
2000-1800	1944,1875,1804	Aromatic ring (aryl) group, aromatic combination bond	C=C stretching
1735-1750	1743	Ester	C=O Stretching
1650-1580	1629,1602,1575	Alkene, Aromatics	C=C stretching
1500-1400	1494	Benzene	C-C=C Asymmetric Stretch
1470-1350	1455,1412,1379	Alkyne	C≡C stretching
1300-950	1285,1028,900	Ester, Ether	C-O Stretching
1000-650	900,776,698	Mono and polycyclic substituted aromatics groups	O-H bending

4.5.3.2 Comparison study on GCMS analysis of MSPS co-pyrolysis oil with MS and PS pyrolysis oils

GC–MS analysis provides the information regarding diversity of components present in pyrolysis oil. In this study, the detected compounds were identified, by searching the W9N11 MS library database. More than 100 compounds were identified which are present in MS, PS and MSPS pyrolysis oil by GC-MS analysis. The chromatogram is shown in Fig. 4.9, Fig. 4.10 and Fig 4.11. From the chromatograms, the peaks with high degree of probability ($\geq 80\%$) and peak areas around or greater than 0.1% are listed in Table 4.7, Table 4.8 and Table 4.9, respectively. The compounds, which were identified in MS pyrolysis oil were instigated in consequence of the thermal cracking of cellulose, hemicellulose and lignin in the biomass. Bio-oil (Biomass pyrolysis oil) consists of more than 300 different organic compounds because of its complex nature [33]. Hence, they were branched into six major classes such as monoaromatics, polyaromatics, aliphatic, hetrocyclic, oxygenates and nitogenates, which had been previously demonstrated by Nanda et al. [142]. The various prominent organic products such as acid, alcohols, ketones, aldehydes, esters, amines, ethers, and nitriles are found in most of the bio-oils. Mahua pyrolytic oil consisted of various chemical groups such as alkanes, alkenes, branched hydrocarbon, saturated fatty acids and their derivatives, i.e., esters, amides and nitriles, which were typically the primary products. The most significant compounds in bio-oil are acids tetradecanoic acid, hexadecanoic acid, octadecenoic acid, etc. which had the combined relative composition of 37.36%. Out of these, hexadecanoic acid is used to produce soap/cosmetics agent and as a non-drying oil for surface coating [102]. The IUPAC name of stearic acid is known as n-Octadecanoic acid, which is mainly used as emulsifying agent and solubilizing agent in aerosol product. But the purification of these fatty acids is limiting the application in laundry soaps or detergents. On the other hand, it has been considered that the presence of acid is an important issue for subsequent bio-oil treatment, since it is responsible for corrosion of the manifolds and potential chemical instability of bio-oil during the storage conditions [143]. However, this problem has been reduced by the addition of plastic in Mahua seed. From the table 4.9, it can be observed that the acid and its derivatives were reduced as compared to Mahua pyrolysis oil. The presence of acid in MSPS pyrolysis oil is 16.24%, whereas its derivatives like esters and nitrile are 2.77% and 9.04%, respectively. Some other aliphatic compounds, such as alkanes and alkenes were found in MS pyrolysis oil, with relative composition of 17.6% and 6.3%, respectively. Benzene and its derivatives constituted about 4.9%. As a consequence, the presence of benzene derivatives in MSPS pyrolysis oil is more (44.04%) as compared to MS pyrolysis oil. The addition of plastic in Mahua pyrolysis oil influences the chemical composition of pyrolysis oil

and also increases the oil yield percentage. The presence of some aliphatic compounds like alkane and alkene in co-pyrolysis oil is 8.93% and 5.8%. Both aliphatic compound were reduced while MS was co-pyrolyzed with the addition of aromatic PS polymer. The aromatic polymer PS influences to increase the aromatic compound in MSPS pyrolysis oil. However, from the table 4.8 it is evident that the higher aromatic and heterocyclic compounds in PS pyrolysis oil are present.

Table 4.7 GC-MS analysis of MS pyrolysis oil

Identified compound	Chemical formula	Area % of MS
<i>Alkanes</i>		
4-Decane	C ₁₀ H ₂₀	0.14
n-Undecane	C ₁₁ H ₂₄	0.82
n-Dodecane	C ₁₂ H ₂₆	0.66
n-Tetradecane	C ₁₄ H ₃₀	2.24
Pentadecane	C ₁₅ H ₃₂	3.84
Hexadecane	C ₁₆ H ₃₄	3.41
n-Heptadecane	C ₁₇ H ₃₆	5.16
n-Octadecane	C ₁₈ H ₃₈	1.38
<i>Alkenes</i>		
D-Limonene	C ₁₀ H ₁₆	0.24
5-Undecene	C ₁₁ H ₂₂	0.46
Cyclooctene	C ₈ H ₁₄	0.18
1-Dodecene	C ₁₂ H ₂₄	0.44
1-Cyclopentene	C ₇ H ₁₂	0.37
n-tridecene	C ₁₃ H ₂₆	0.67
Cyano-8-pentadecene	C ₁₉ H ₂₉ N	3.96
<i>Ketones</i>		
2-4-methylphenylcyclopentanone	C ₁₂ H ₁₄ O	1.03
<i>Phenols</i>		
o-Cresol	C ₇ H ₈ O	0.48
<i>Benzene and its derivatives</i>		
1,1'3',1'-Terphenyl, 5'-phenyl- (benzene)	C ₂₄ H ₁₈	2.72
Benzenemethanol	C ₇ H ₈ O	0.68
1-Hydroxy-2-ethylbenzene	C ₈ H ₁₀ O	0.13
n-Pentyl benzene	C ₁₁ H ₁₆	0.88

Hexylbenzene	$C_{12}H_{18}$	0.51
<i>Acids</i>		
Octanoic acid	$C_8H_{16}O_2$	0.35
Tetradecanoic acid	$C_{14}H_{22}O_2$	0.98
Hexadecanoic acid	$C_{16}H_{32}O_2$	11.79
6-Octadecenoic acid	$C_{18}H_{34}O_2$	12.58
n-Octadecanoic acid	$C_{18}H_{36}O_2$	10.67
9-Tetradecenoic acid	$C_{14}H_{26}O_2$	0.99
<i>Ester</i>		
1,2,4-Benzenetricarboxylic acid, 4-dodecyl dimethyl ester	$C_{23}H_{34}O_6$	0.64
Succinic acid, nonyl tetradec-11-enyl ester	$C_{27}H_{50}O_4$	0.31
Octadecanoic acid, methyl ester	$C_{19}H_{35}O_2$	1.14
<i>Amide</i>		
Tetradecanamide	$C_{14}H_{29}NO$	1.20
9-Octadecenamide	$C_{18}H_{35}NO$	1.09
n-methyloctadecanamide	$C_{14}H_{29}NO$	1.20
<i>Amines</i>		
N-Acetyldioctylamine	$C_{18}H_{37}NO$	0.68
<i>Heterocyclic compound</i>		
Cyclopentane, 1,1'-[3-(2-cyclopentylethyl)-1,5-pentanediy]bis-	$C_{22}H_{40}$	1.08
pyrrolo[3,2-c]dibenzofuran	$C_{14}H_{13}NO$	0.63
<i>Nitrile</i>		
Pentadecanenitrile	$C_{15}H_{29}N$	2.37
Heptadecanenitrile	$C_{17}H_{33}N$	3.37

The presence of benzene derivatives is 61.88% and heterocyclic compound is 34.58%, very few other acids (6.11%), ketones (5.35%) and amines (1.55%) were present. From the result it can be noticed that most of the compounds present in MSPS pyrolysis oil are similar to those of PS pyrolysis oil. The presence of more aromatic compounds in MSPS pyrolysis oil is due to the chemical structure of PS. PS contains a lot of benzene rings, which can be converted to aromatics and even polyaromatics. Other study has also identified the major contribution of the aromatic compounds in co-pyrolysis oil due to the presence of aromatic polymers [30]. The chemical

composition of MS, MSPS and PS pyrolysis oil was ascertained to be that of straight-chain carbon in the range of C_7 – C_{27} for MS pyrolysis oil, C_9 – C_{24} , for MSPS pyrolysis oil and C_6 – C_{18} for PS pyrolysis oil. Because of the existence of such various compounds in the co-pyrolysis oil, it can be used as an alternative fuel and a chemical source.

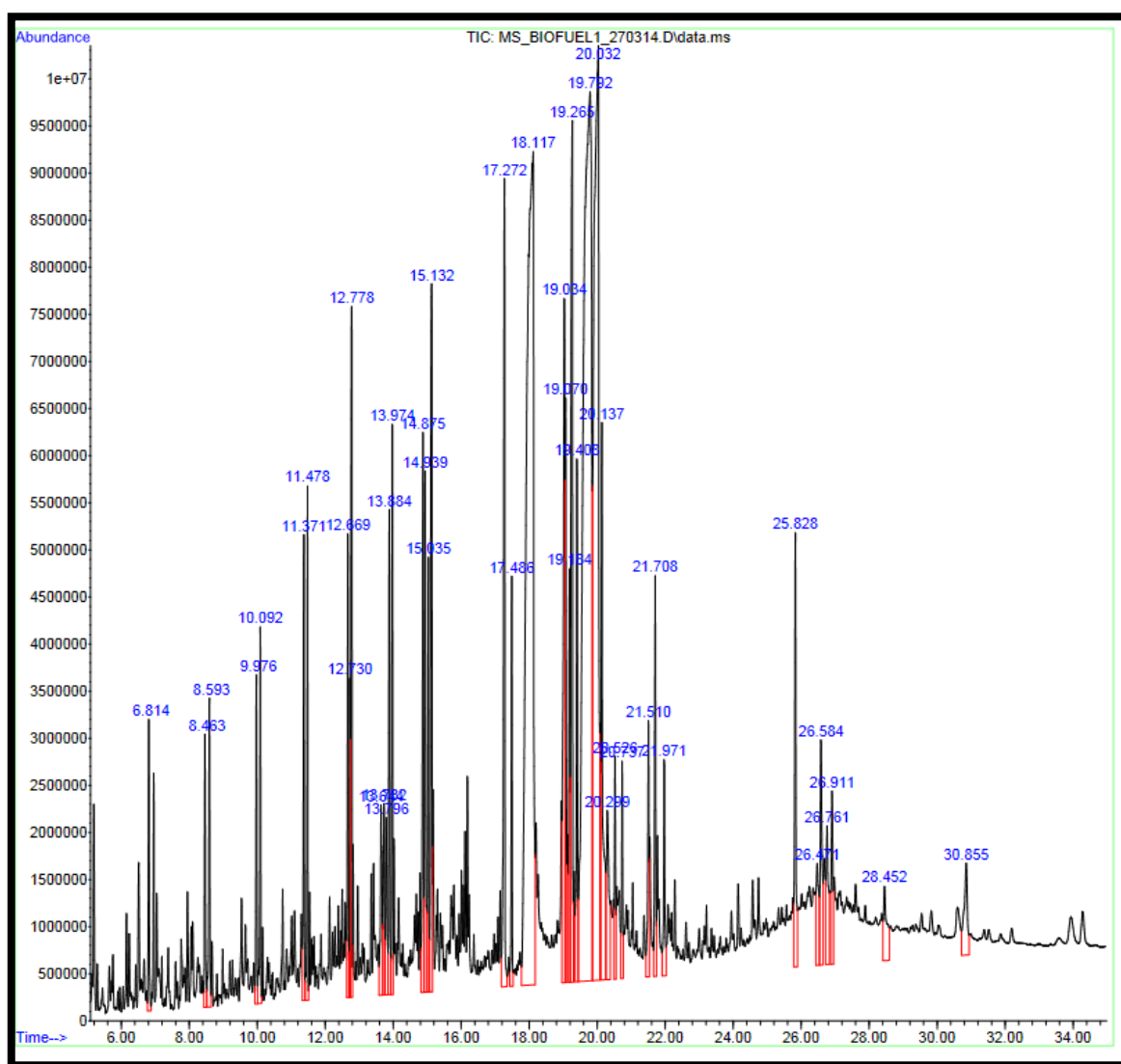


Fig. 4.9. GC-MS chromatogram of MS pyrolysis oil

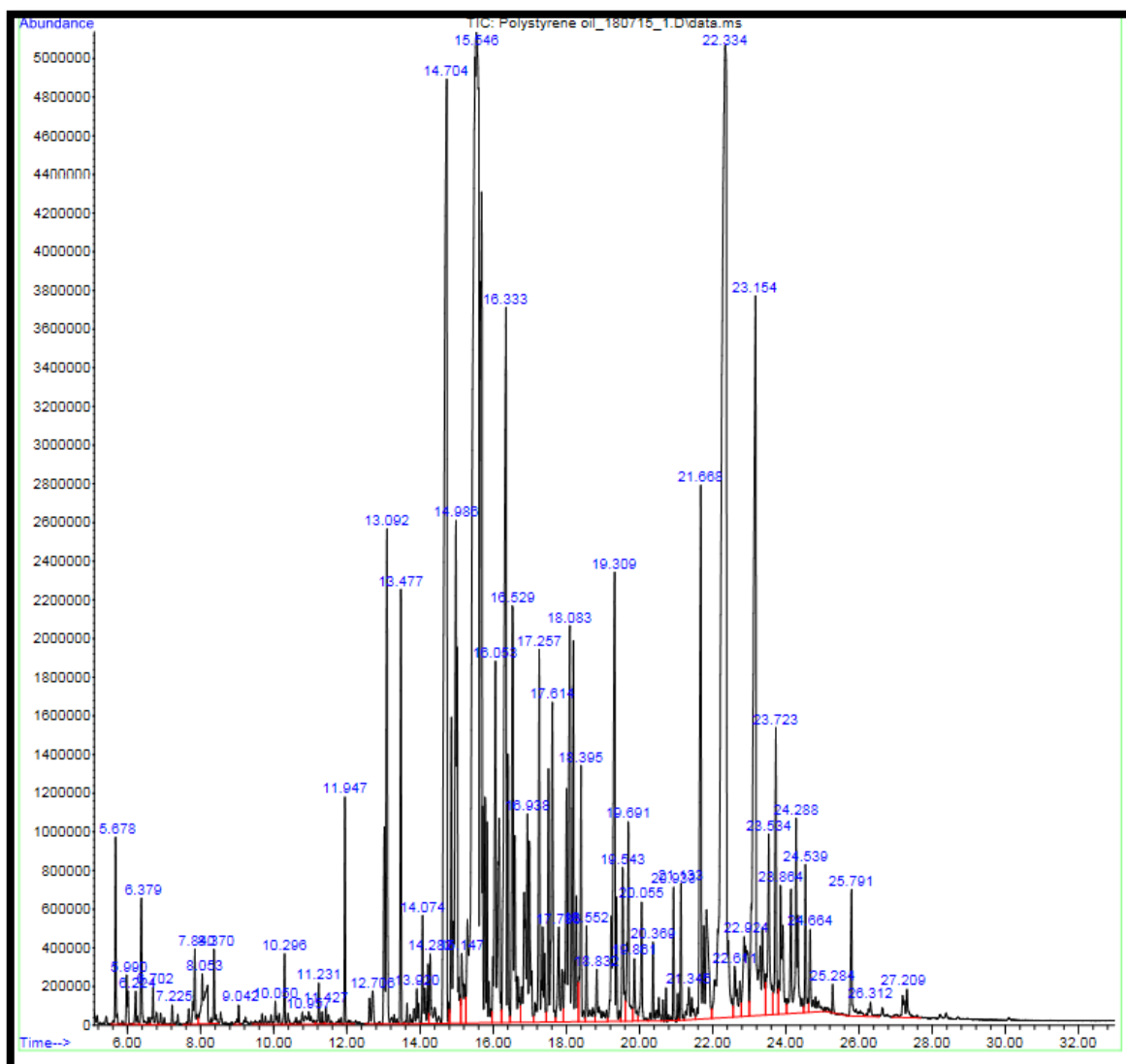


Fig. 4.10. GC-MS chromatogram of PS pyrolysis oil

Table 4.8 GC-MS analysis of PS pyrolysis oil

Identified compound	Chemical formula	Area % of PS
<i>Ketone</i>		
2-Phenylisoindolin-1-one	C ₁₄ H ₁₁ NO	3.16
methyl 2-cyanomethylphenyl ketone	C ₁₀ H ₉ NO	1.73
1,3-dihydro-3-methyl-2H-indol-2-one	C ₉ H ₉ NO	0.46
<i>Benzene and its derivatives</i>		
Phenyldodecane	C ₁₈ H ₃₀	0.20
4-Ethylbenzaldehyde	C ₉ H ₁₀ O	0.12
2',2'-dideuteroethenylbenzene	C ₈ H ₆ D ₂	0.36
(Z)-3-Phenyl-2-propenal	C ₉ H ₈ O	0.56
Benzene, 2,5-cyclohexadien-1-yl-	C ₁₂ H ₁₂	0.14
2',2'-dideuteroethenylbenzene	C ₈ H ₆ D ₂	0.27
3-(1-methylpyrrol-2-yl)indole	C ₁₃ H ₁₂ N ₂	0.55
(Z)-3-Phenyl-2-propenal	C ₉ H ₈ O	0.56
4-Bromo-2-methylbenzonitrile	C ₈ H ₆ BrN	4.05
Undecane, 3-phenethyl-1-phenyl	C ₅ H ₃₆	21.96
8-Aminoquinoline	C ₉ H ₈ N ₂	0.21
Benzeneacetonitrile, 4-bromo	C ₈ H ₆ BrN	2.35
methyl 2-cyanomethylphenyl keton	C ₁₀ H ₉ NO	1.73
Benzenebutanoic acid	C ₁₀ H ₁₂ O ₂	2.03
1-Methyl-4-[2-(4-methylphenyl)ethynyl]benzene	C ₁₆ H ₁₄	4.15
1-methoxy-4-(phenylethyl Benzene)	C ₁₅ H ₁₂ O ₂	0.37
Undecylbenzene	C ₁₇ H ₂₈	0.53
Benzene, dodecyl-	C ₁₈ H ₃₀	13.10
Benzene, undecyl-	C ₁₇ H ₂₈	0.98
Benzaldehyde, (phenylmethylene	C ₁₄ H ₁₂ O	1.09
1,3-dihydro-3-methyl-2H-indol-2-one	C ₉ H ₉ NO	0.46
Benzene, nonyl-	C ₁₅ H ₂₄	0.11
3-Methyl-2-nitrobenzyl alcohol	C ₈ H ₉ NO ₃	0.43
Benzene, 1,1'-(1,3-propanediyl)bis-	C ₁₅ H ₁₆	0.32
P,P'-dideuterodiphenylmethane	C ₁₃ H ₁₀ D ₂	0.57
bis(o-Tolyl)acetylene	C ₁₆ H ₁₄	2.11
Benzamide, 2,4,6-trinitro-N,N-dimethyl-	C ₉ H ₈ N ₄ O ₇	0.67
4-Amino-dl-phenylalanine	C ₉ H ₁₂ N ₂ O ₂	0.33
N,N-dimethyl-2-methoxy-5-nitroaniline	C ₉ H ₁₂ N ₂ O ₃	0.48

Benzene, undecyl-	C ₁₇ H ₂₈	0.98
Benzene, nonyl-	C ₁₅ H ₂₄	0.11
<i>Heterocyclic compound</i>		
1H-Indole, 2,3-dihydro		
1H-Benzimidazole, 3-oxide	C ₆ H ₇ N ₂ O	0.10
1H-Indole, 2,3-dihydro	C ₈ H ₉ N	0.49
8-Aminoquinoline	C ₉ H ₈ N ₂	0.21
3-Pyridinecarboxamide	C ₆ H ₆ N ₂ O	0.21
3,3'-Dimethyl-2,2'-bipyridine	C ₁₂ H ₁₂ N ₂	0.22
1,2-Bis(4-pyridyl)ethane	C ₁₂ H ₁₂ N ₂	2.30
1H,6H-pyrrolo(2,3-b)pyrrole	C ₆ H ₆ N ₂	1.14
3-(1-methylpyrrol-2-yl)indole	C ₁₃ H ₁₂ N ₂	0.55
N-Phenyl-4-pyridinecarboxamide	C ₁₂ H ₁₀ N ₂ O	6.71
1,2,3,4-Tetrahydroacridine	C ₁₃ H ₁₃ N	0.45
Acetonitrile, 2-[4-(cyanomethyl)-1H-3-pyrrolyl]	C ₈ H ₇ N ₃	0.84
3-(5-Methylpyridin-2-yl)quinoline	C ₁₅ H ₁₂ N ₂	2.55
2,3,10-Trimethylphenanthrene	C ₁₇ H ₁₆	0.66
6-Methyl-11H-indolo[3,2-c]quinoline	C ₁₆ H ₁₂ N ₂	0.86
2-Formyl-9-methylcarbazole	C ₁₄ H ₁₁ NO	5.79
2-p-Tolylpyridine	C ₁₂ H ₁₁ N	0.37
4-(Dimethylamino)-5-(methylthio)pyridazine	C ₇ H ₁₁ N ₃ S	0.28
Pyridine, 3-butyl	C ₉ H ₁₃ N	0.93
2-(2'-Aminophenyl)indole	C ₁₄ H ₁₂ N ₂	0.90
7-Methyl-2-phenylquinoline	C ₁₆ H ₁₃ N	0.10
3-Dimethylamino-6-nitro-4-phenylquinolin-2-ol	C ₁₇ H ₁₅ N ₃ O ₃	0.55
<i>Acids</i>		
Cyclopentanecarboxylic acid	C ₆ H ₁₀ O	0.35
Nicotinic acid hydrazide	C ₆ H ₇ N ₃ O	0.45
3-Pyridinecarboxylic acid	C ₆ H ₅ NO ₂	0.16
Indoleacetic acid	C ₁₀ H ₉ NO ₂	0.22
Cyclopentanecarboxylic acid	C ₆ H ₁₀ O	0.35
1R-cyclopropanecarboxylic acid	C ₄ H ₆ O ₂	4.58
<i>Homocyclic</i>		
bicyclo[4.2.1]nona-2,4,7-triene	C ₁₆ H ₁₄	4.15
	C ₉ H ₁₀	2.44
<i>Amines</i>		
2-Amino-1,1,3-tricyanopropene	C ₆ H ₄ N ₄	1.55

Table 4.9 GC-MS analysis of MSPS pyrolysis oil

Identified compound	Chemical formula	Area % of MSPS
<i>Alkanes</i>		
Hendecane	C ₁₁ H ₂₄	0.67
Dodecane	C ₁₂ H ₂₆	0.80
Tridecane	C ₁₃ H ₂₈	0.77
Pentadecane	C ₁₅ H ₃₂	3.03
Hexadecane	C ₁₆ H ₃₄	3.66
<i>Alkene</i>		
1H-Indene	C ₉ H ₈	0.57
1-Undecene	C ₁₁ H ₂₂	0.61
1-Dodecene	C ₁₂ H ₂₄	1.30
1-Tridecene	C ₁₃ H ₂₆	0.99
1-Tetradecene	C ₁₄ H ₂₈	2.33
<i>Alcohol</i>		
(2S*,5S*,7S*)-7,11-Dimethylbicyclo[5.4.0]undec-1(11)ene-2,5-diol	C ₁₃ H ₂₂ O ₂	0.19
<i>Ketone</i>		
5,7-Dimethoxy-4-(3-methoxyphenyl)-2H-1-benzopyran-2-one	C ₁₈ H ₁₆ O ₅	0.48
2-(4Methylphenyl)cyclopentanone	C ₁₂ H ₁₄ O	1.49
10-Allyl-3,3,6,6,9-pentamethyl-1,2,3,4,5,6,7,8,9,10-decahydroacridine-1,8-dione	C ₂₁ H ₂₉ NO ₂	0.32
1,2,3,4-Tetrahydro-6-hydroxy-7-nitro-5H-2-benzazepin-1-one	C ₁₀ H ₁₀ N ₂ O ₄	1.0
<i>Benzene and its derivatives</i>		
trans-1-Phenyl-1-pentene	C ₁₁ H ₁₄	0.42
1-Bromo-1-phenylpropane	C ₉ H ₁₁ Br	0.60
1,2-Diphenylcyclopropane	C ₁₅ H ₁₄	2.22
2,4-Diphenyl-1-butene	C ₁₆ H ₁₆	9.24

1,5-Diphenyl-1,5-hexadiene	C ₁₈ H ₁₈	0.37
1,3,5-Triphenylhexane	C ₂₄ H ₂₆	1.08
2,4,6-Triphenyl-1-hexene	C ₂₄ H ₂₄	3.59
1-Propene, 3-(2-cyclopentenyl)-2-methyl-1,1-diphenyl-	C ₂₁ H ₂₂	0.71
1,1':3',1''-Terphenyl, 5'-phenyl-	C ₂₄ H ₁₈	0.98
Benzene, 1,2-diethyl-	C ₁₀ H ₁₄	0.11
Propenylbenzene	C ₉ H ₁₀	1.26
s-Diphenylethane	C ₁₄ H ₁₄	1.89
Diphenylmethane	C ₁₃ H ₁₂	1.74
Alpha.-Dimethylstyrene	C ₁₀ H ₁₂	0.84
Benzenemethanol	C ₇ H ₈ O	0.58
Benzene, 2-butenyl-	C ₁₀ H ₁₂	0.34
Benzene, (2-methylcyclopropyl)-	C ₁₀ H ₁₂	0.28
(1-Propylvinyl)benzene	C ₁₁ H ₁₄	0.70
n-Amylbenzene	C ₁₁ H ₁₆	1.24
Benzene, (1-methylenepentyl)-	C ₁₂ H ₂₆	0.59
Benzene, hexyl-	C ₁₂ H ₁₈	0.66
Benzene, 1,1'-(1-methyl-1,2-ethanediyl)bis-	C ₁₅ H ₁₆	1.38
Benzene, 1,1'-(1,3-propanediyl)bis	C ₁₅ H ₁₆	5.55
Benzene, 1,1'-(1-methyl-1,3-propanediyl)bis-	C ₁₆ H ₁₈	4.62
Benzene, 1,1'-(1,4-butanediyl)bis-	C ₁₆ H ₁₈	0.79
Benzene, 1,1'-(3-methyl-1-propene-1,3-diyl)bis-	C ₁₆ H ₁₆	1.67
Benzoxazole, 2-[2-(4-morpholyl)ethyl]thio-	C ₁₃ H ₁₆ N ₂ O ₂ S	0.32
2-(Benzyloxy)-4-bromo-1,3-butanediol	C ₁₁ H ₁₅ BrO ₃	0.27
<i>Acids</i>		
n-Hexadecanoic acid	C ₁₆ H ₃₂ O ₂	7.04
9-Octadecenoic acid (Z)	C ₁₈ H ₃₄ O ₂	4.50

Octadecanoic acid	$C_{18}H_{36}O_2$	5.15
-------------------	-------------------	------

Esters

Hexadecanoic acid, methyl ester	$C_{17}H_{34}O_2$	1.18
---------------------------------	-------------------	------

Thiocarbamic acid, N,N-dimethyl, S-1,3-diphenyl-2-butenyl ester	$C_{19}H_{21}NOS$	0.13
--	-------------------	------

1,2,4-Benzenetricarboxylic acid, 4-dodecyl dimethyl ester	$C_{23}H_{34}O_6$	0.20
--	-------------------	------

Methyl stearate	$C_{19}H_{38}O_2$	1.26
-----------------	-------------------	------

Nitrile

Pentadecanenitrile	$C_{15}H_{29}N$	2.31
--------------------	-----------------	------

Oleanitrile	$C_{18}H_{33}N$	3.09
-------------	-----------------	------

Octadecanenitrile	$C_{18}H_{35}N$	3.64
-------------------	-----------------	------

Naphthalene

Naphthalene, 2-methyl-	$C_{11}H_{10}$	0.49
------------------------	----------------	------

Naphthalene, 2,6-dimethyl-	$C_{12}H_{12}$	0.47
----------------------------	----------------	------

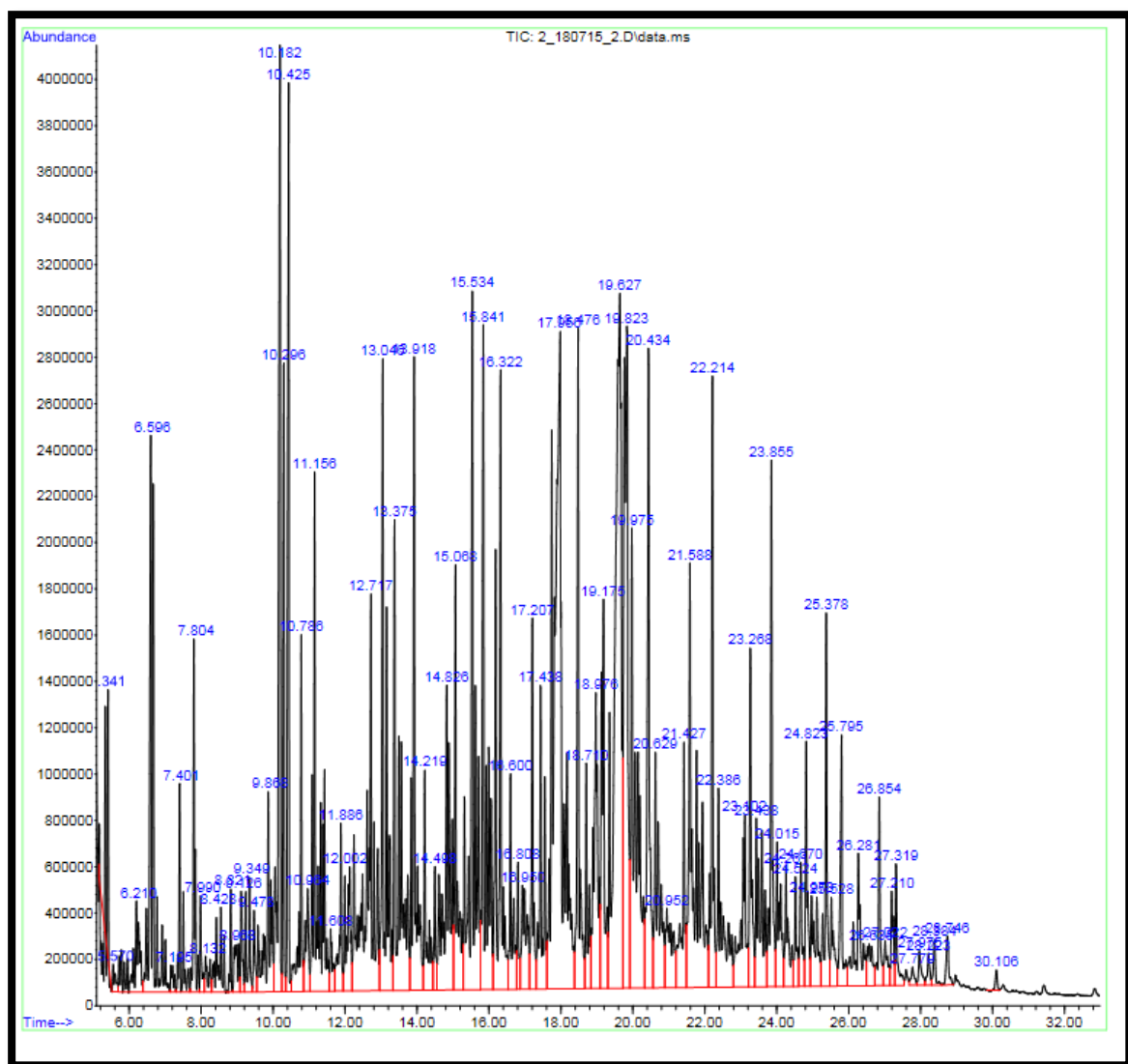


Fig. 4.11 GC-MS chromatogram of MSPS pyrolysis oil

4.5.3.3. GCMS analysis of MS and MSPS aqueous phase

Fig 4.12 , Fig 4.13 shows the chromatogram of MS and MSPS aqueous phase, the compound present in both MS and MSPS aqueous phase are summarized in table 4.10 and table 4.11. The compound present in MS aqueous phases are amine, ester, acid, alcohol, heterocyclic compound, ketone, phenol and benzene. The similar compound also present MSPS aqueous phase.

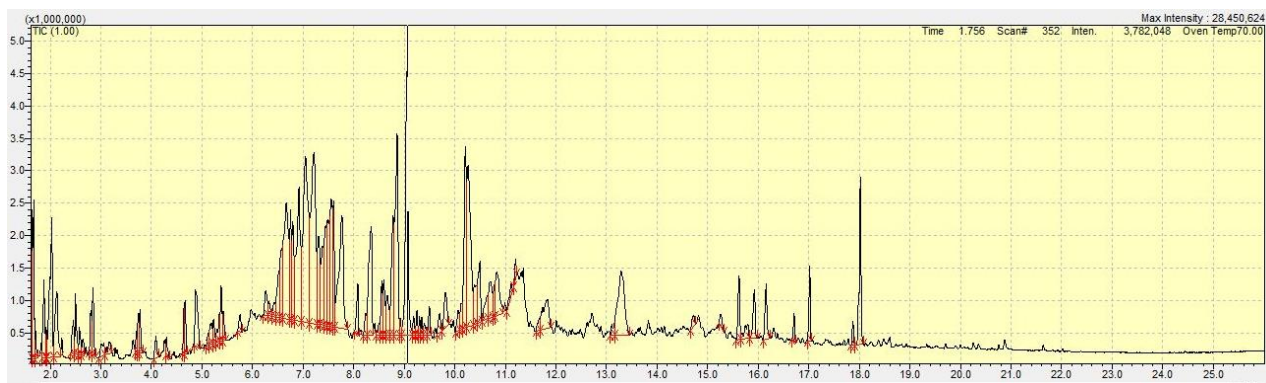


Fig. 4. 12 GC-MS chromatogram of MS aqueous phase

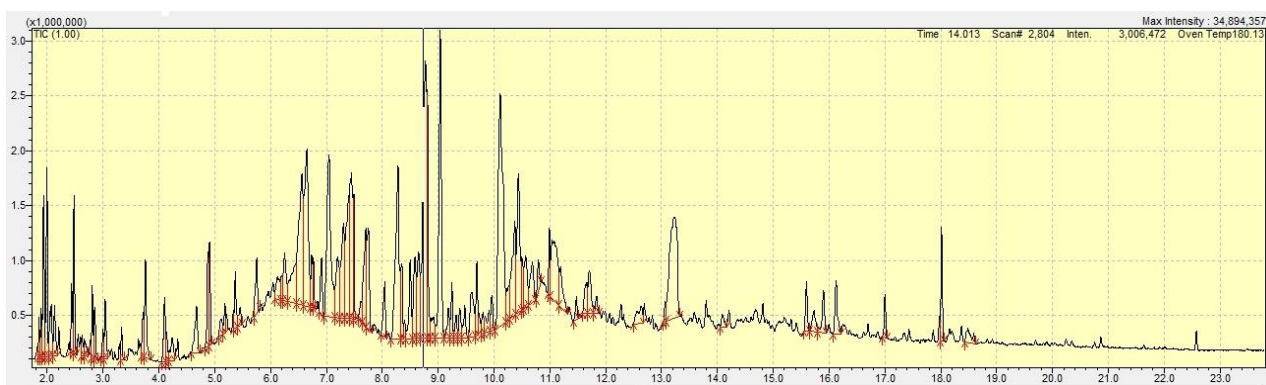


Fig. 4. 13 GC-MS chromatogram of MSPS aqueous phase

Table 4.10 GCMS analysis of MS aqueous phase

Identified compound	Chemical formula	Area % of MS aqueous phase
<i>Amine</i>		
2-Amino-1,3-Propanediol	$C_3H_9NO_2$	8.26
Valine	$C_5H_{11}NO_2$	1.77
D-Valine	$C_5H_{11}NO_2$	1.11
Guanidine	CH_5N_3	1.79
<i>Ester</i>		
Ammonium acetate	$C_2H_7NO_2$	7.62
<i>Acid</i>		
Butanoic acid	$C_4H_8O_2$	0.98
3-Heptenoic acid	$C_7H_{12}O_2$	0.81
Octanoic acid	$C_8H_{16}O_2$	0.96
<i>Alcohol</i>		
Phenol	C_6H_6O	0.75
Furaneol	$C_6H_8O_3$	0.92
1,6-Heptadien-4-ol, 4-propyl-	$C_{10}H_{18}O$	2.79
3-Pyridinol, 6-methyl-	C_5H_5NO	1.39
Maltol	$C_6H_6O_3$	1.1
Catechol	$C_6H_6O_2$	2.81
2,4-Dimethylphenol-D3	$C_8H_7D_3O$	2.41
1,2,3-Propanetriol	$C_8H_7D_3O$	4.11

<i>Hetero cycle compound</i>		
5,10-Diethoxy-2,3,7,8-tetrahydro-1H,6H-dipyrrolo[1,2-a:1',2'-d]pyrazine	C ₁₄ H ₂₂ N ₂ O ₂	1.43
1H-Imidazole1,5-dimethyl-Ketone	C ₅ H ₈ N ₂	1.47
Cyclopentanone, 2-Cyclopentylidene-	C ₁₀ H ₁₄ O	0.83
2,5-Pyrrolidinedione 1-Methyl-Benzene	C ₄ H ₅ NO ₂	2.67
4-Ethoxy Benzaldehyde	C ₉ H ₁₀ O ₂	0.62
Benzo-1,4-Quinone	C ₄ H ₄ O ₂	2.8
Methane, Tert-Butoxymethoxy-	C ₆ H ₁₄ O ₂	4.39

Table 4.11 GCMS analysis of MSPS aqueous phase

Identified compound	Chemical formula	Area % of MSPS aqueous phase
<i>Amine</i>		
Methanamine N,N-Dimethyl	C ₃ H ₉ N	0.19
<i>Ester</i>		
Ammonium Acetate	C ₂ H ₇ NO ₂	10.33
1-Butan-2,2-D2-Ol, Acetate	C ₆ H ₁₀ D ₂ O ₂	0.16
Hexanoic acid, 2-ethylcyclohexyl ester	C ₁₄ H ₂₆ O ₂	3.74
Butanedioic Acid, Methylene-, Dimethyl Ester	C ₇ H ₁₀ O ₄	0.8
1-Propanol, 2,2-Dimethyl-, Acetate	C ₇ H ₁₄ O ₂	0.34
2-Hydroxy-gamma-butyrolactone	C ₄ H ₆ O ₃	0.16
Hexanoic acid, 2-ethylcyclohexyl ester	C ₁₄ H ₂₆ O ₂	3.74
Methyl 2-methoxypropenoate	C ₅ H ₈ O ₃	0.33
Butanedioic Acid, Methylene-, Dimethyl Ester	C ₇ H ₁₀ O ₄	0.8
Hexanoic acid, 2-ethylcyclohexyl ester	C ₁₄ H ₂₆ O ₂	3.74
<i>Acid</i>		
2-Propenoic Acid	C ₃ H ₄ O ₂	2.15
Butyric Acid	C ₄ H ₈ O ₂	0.44
<i>Heterocyclic compound</i>		
Pyridine	C ₅ H ₅ N	0.19
Pyrrolidine,1-Methyl-	C ₅ H ₁₁ N	0.14
Pyridine-4-Methyl-	C ₆ H ₇ N	0.96
Pyridine,3-Methyl-	C ₆ H ₇ N	0.49
2,6-Lutidine	C ₇ H ₉ N	0.14
Pyridine, 2,4-dimethyl-	C ₇ H ₉ N	0.4
Pyridine, 2,4,6-Trimethyl-	C ₈ H ₁₁ N	0.18
Isosorbide heterocyclic	C ₆ H ₁₀ O ₄	1.25

1H-Imidazole, 2,4,5-trimethyl	C ₆ H ₁₀ N ₂	3.08
<i>Alcohol</i>		
2-Furanmethanol	C ₅ H ₆ O ₂	0.28
1,2,3-Propanetriol	C ₃ H ₈ O ₃	0.19
2-Nitro-1-Phenyl-3-(Tetrahydro-2h-Pyran-2-Yloxy)-1-Propanol	C ₁₄ H ₁₉ NO ₅	2.14
2,5-Dimethylcyclohexan-1-Ol	C ₈ H ₁₆ O	0.35
3-Pyridinol	C ₅ H ₅ NO	0.48
Catechol	C ₆ H ₆ O ₂	1.29
3-Pyridinol, 6-Methyl	C ₆ H ₇ NO	2.26
3-Pyridinol, 2,6-dimethyl-	C ₇ H ₉ NO	.65
<i>Ketone</i>		
5-(Hydroxymethyl)Dihydro-2(3h)-Furanone	C ₅ H ₈ O ₃	0.84
2,5-Pyrrolidinedione, 1-Methyl-	C ₅ H ₇ NO ₂	0.38
2,5-Pyrrolidinedione	C ₄ H ₅ NO ₂	0.83
2-Pyrrolidinone	C ₄ H ₇ NO	0.16
2-Cyclopenten-1-one	C ₅ H ₆ O	0.13
1,2-Cyclopentanedione, 3-methyl-	C ₆ H ₈ O ₂	0.41
4h-Pyran-4-One, 3-Hydroxy-2-Methyl	C ₆ H ₆ O ₃	1.16
<i>Phenol</i>		
2-Methoxy-4-Vinylphenol	C ₉ H ₁₀ O ₂	0.37
Phenol	C ₆ H ₆ O	1.06
1,2-Ethanediol, 1-Phenyl-	C ₈ H ₁₀ O ₂	1.44
Phenol, 3-amino-	C ₆ H ₇ NO	1
Phenol, 2-Methyl-	C ₇ H ₈ O	0.46
<i>Benzene</i>		
5-Methyl-1,3-Benzenediol	C ₇ H ₈ O ₂	1.42
Benzoic acid	C ₇ H ₆ O ₂	0.49

4.5.3.4 ¹H-NMR analysis of MS, PS and MSPS pyrolytic oil

Hydrogen percentage was computed on the basis of chemical shift values from the ¹H-NMR spectra, which is summarized in Table 4.12. Fig. 4.14 (A), Fig. 4.14 (B) and Fig. 4.14 (C) shows the ¹H-NMR spectrum of all pyrolytic oils which provide detailed information on aromatic, olefinic and aliphatic compounds based on the proton type. Most of the highest single ring aromatics protons are present in the chemical shift range of 8.5-6.5 ppm in both MSPS and PS pyrolysis oil i.e. mainly the presence of benzene and benzene derivatives compounds in these pyrolysis oil. However, this is also confirmed through GCMS analysis, from the GCMS analysis the obtained aromatic compound of MSPS is higher than that of MS pyrolysis oil. Table 4.10 shows that the presence of proton in MSPS pyrolysis is as similar to the proton present in PS pyrolysis oil. On the other hand maximum protons attached to β-CH₃, CH₂ and CH γ to an

aromatic ring accounted for 66.86% in the chemical shift region of 1.6-1.0 ppm for MS pyrolysis oil. The presence of higher amount of protons attached to the aromatic ring is due to the presence of acid, ester, amide and amines. 2.05% of olefinic proton was observed in the region of 6.5-5.0 ppm whereas the presence of olefinic proton for MSPS and PS pyrolysis oil is 9.83% and 10.67%, respectively. The 10.87% and 11.98% of proton attached to CH_3CH_2 and CH to an aromatic ring lied in the chemical shift region of 3.3-2.0 ppm for MS and MSPS pyrolysis oil, whereas 20.94% proton attached to CH_3CH_2 and CH to an aromatic ring for PS pyrolysis oil. From the above, it is evident that the proton present in the MSPS pyrolysis is more similar to the PS pyrolysis oil, which is due to the influence of plastic in biomass pyrolysis. This is also confirmed through various literatures [30,143,144].

Table 4.10 ^1H -NMR integration of MS MSPS and PS pyrolytic oil

Types of hydrogen	Chemical shift (ppm)	Hydrogen content (integrated area % of all hydrogens)		
		MS pyrolysis oil	PS pyrolysis oil	MSPS pyrolysis oil
Aromatic	8.5-6.5	3.25	65.11	40.98
Phenolic (OH) or olefinic proton	6.5-5.0	2.05	10.67	9.83
CH_3 CH_2 and CH to an aromatic ring	3.3-2.0	10.87	20.94	11.98
CH_2 and CH_β to an aromatic ring (naphthenic)	2.0-1.6	5.76	3.16	3.47
β - CH_3 , CH_2 and CH γ to an aromatic ring	1.6-1.0	66.86	—	34.42
CH_3 γ or further from an aromatic ring	1-0.5	11.19	—	—

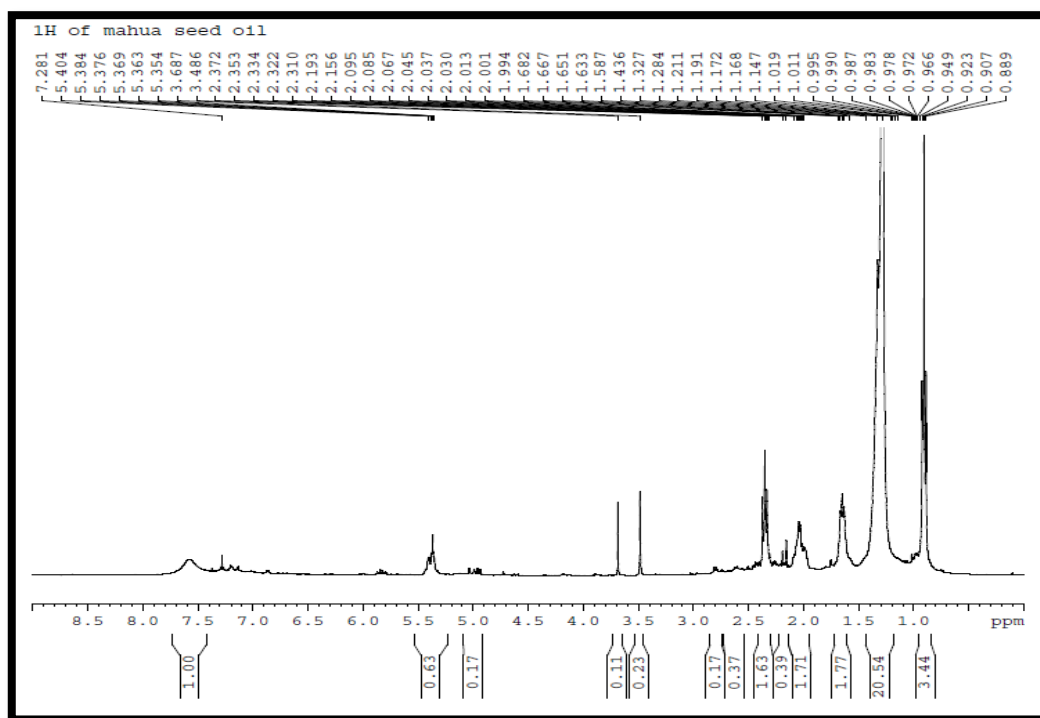


Fig. 4.14 (A) ^1H -NMR analysis of MS pyrolysis oil

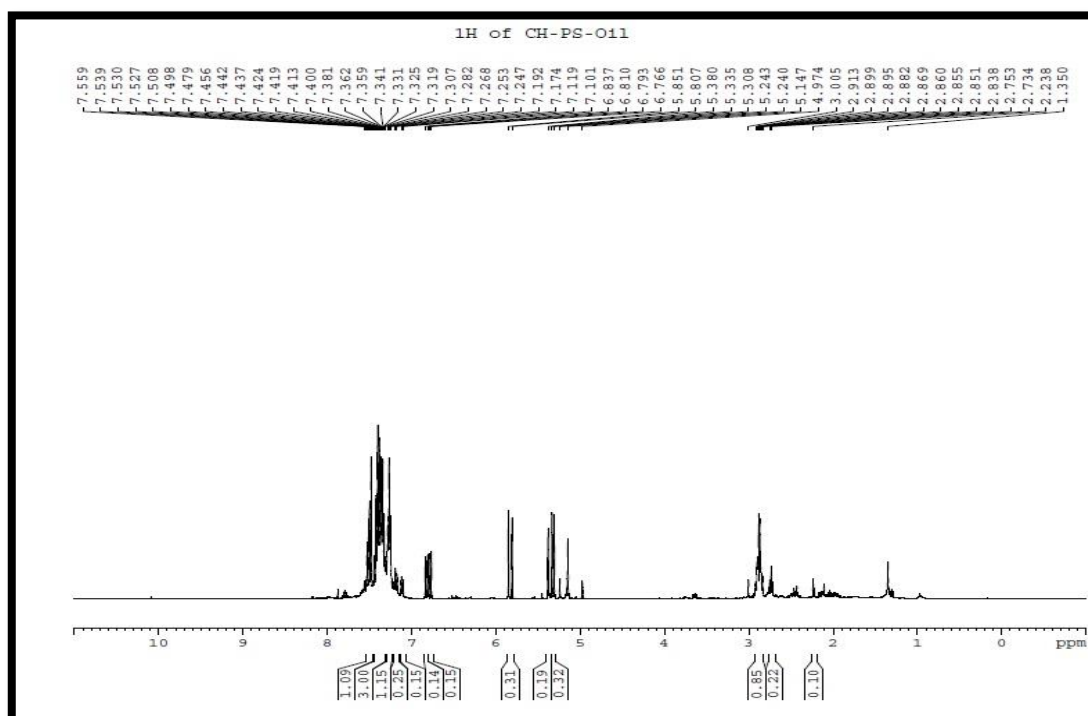


Fig. 4.14 (B) ^1H -NMR analysis of PS pyrolysis oil

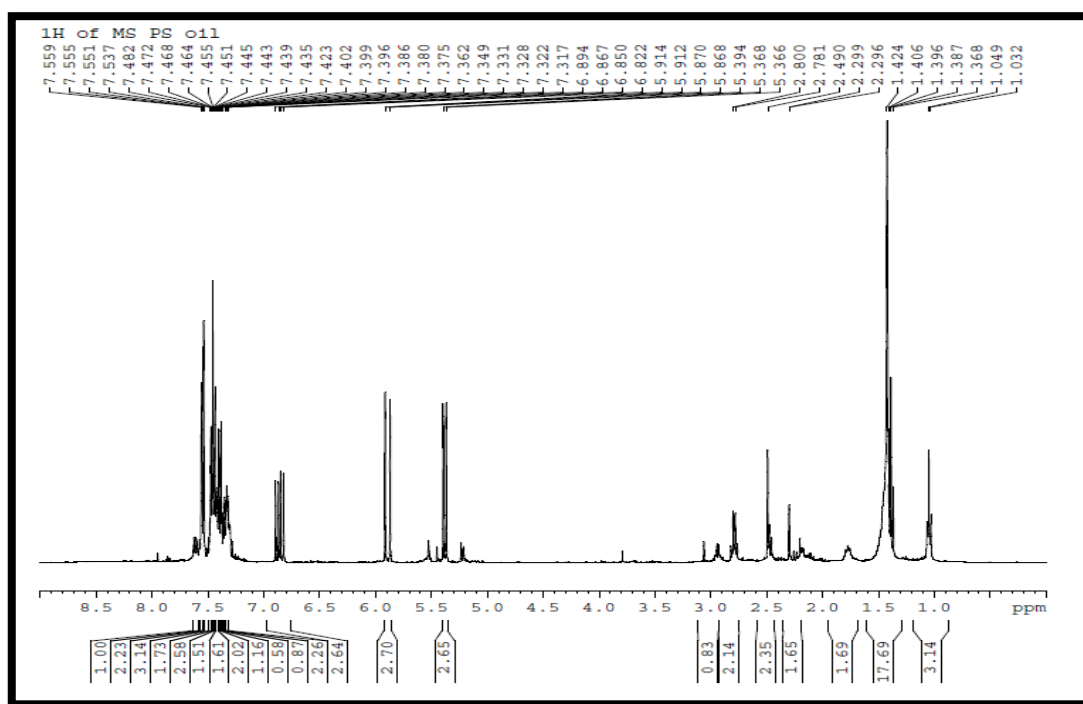


Fig. 4.14 (C) ^1H -NMR analysis of PS pyrolysis oil

4.6 Characterization of bio-char

The principle of bio-char yield is due to slow pyrolysis of lignocellulosic materials. It can be used as cheap absorbent, carbon coating, solid fuel, and for soil amendment [145]. Bio-char having high calorific value with low sulfur content is a carbon-rich fuel that is suitable for direct fuel and household briquette production. The growing interest of bio-char is due to its potential in carbon sequestration, and improvement in soil nutrient, retention capacity, and water holding capacity of soil, reduced total fertilizer requirements and environmental deteriorations associated with fertilizers. Thus, due to the above physical and biological changes with the addition of biochar in agricultural soil is receiving considerable interest in the current decades [146–149]. Moreover, characterization of bio-char was done to understand its potential for use as a solid fuel.

4.6.1 Physical characterizations of bio-char

4.6.1.1 Proximate and ultimate analyses of bio-char

To study the solid fuel potentiality of bio-char, proximate and ultimate analyses is required. Table 4.13 shows the solid fuel characteristics of Mahua seed bio-char and Mahua seed: Polystyrene 1:1 blend bio-char obtained at 525°C. From the proximate analysis, it was observed that the moisture content of MS biochar is 5.14%, which is more than that of MSPS. This might be due to the decomposition reaction of biomass, and the evolved moisture occurred due to the natural convection [150]. The volatile content of the MS biochar is 10.02%, more than that of the MSPS

biochar. This is attributed to the presence of lignin in MS that was not fully pyrolysed at this temperature. Whereas the maximum decomposition of lignin is taking place around 850 °C [151], while in the decomposition of MSPS, the char acts as a thermal stabilizer to enhance the liquid yield. The presence of plastic polymer make stronger effect to the conversion of volatile product during the pyrolysis reaction. The fixed carbon percentage of the MSPS biochar is more than that of MS biochar. The higher fixed carbon content reveals the presence of PS residue, while pyrolysed with MS increases the fixed carbon percentage. Ash content of MS and MSPS biochar were 8.66% and 5.44%, respectively, higher ash percentage indicates the presence of more alkali earth metals in MS biochar as compared to the MSPS bio-char. Ultimate analysis was used to compute the different elements present in bio-char. In this study, the carbon and hydrogen percentage of MSPS is more than that of the MS bio-char, whereas, nitrogen and sulphur are quite varying. The low level of nitrogen and sulphur found in bio-char is indicating for attractive use in incineration and low level of NO_x emissions during the combustion process [152]. The presence of higher oxygen in MS bio-char reduces the heating value. However, the heating value of MSPS bio-char is more due to the presence of higher carbon and less oxygen, the carbon and oxygen are participating for estimating the heating value. It was interesting for calculating the empirical formula, H/C and O/C molar ratio of bio-char sample from ultimate analysis. Moreover, H/C and O/C ratios are one of the most important characteristics to classify the fuel. These ratios are based on the hydrogen, oxygen and carbon content of the fuel [40]. On the other hand, these ratios are also used to determine the degree of aromaticity and maturation, for instance it is often described in Van Krevelen diagrams [153]. The H/C ratio of MSPS bio-char is more than that of MS bio-char, whereas the O/C molar ratio of MSPS is less than that of MS bio-char. On the other hand, both the MS and MSPS bio-char lie within the range coal and anthracite [40]. The existing empirical formulas for both MS and MSPS are $\text{CH}_{0.63}\text{N}_{0.03}\text{O}_{0.14}$ and $\text{CH}_{0.87}\text{N}_{0.02}\text{O}_{0.07}$, respectively. The obtained calorific value of MSPS bio-char is more than that of MS bio-char, however both are more than that Indian standard coal. Hence, it can be used as a fuel in boiler (either alone or as a mixture with biomass). These bio-chars can also be used as a good source of solid fuel for cooking and heating.

Table 4.11 Proximate and ultimate analysis of bio-char

Characteristic	MS bio-char	MSPS bio-char
Proximate analysis (wt %.)		
Moisture content	5.14	0.34
Volatile content	36.17	26.15
Fixed carbon	50.03	68.07
Ash content	8.66	5.44
Ultimate analysis (wt %)		
Carbon	78.12	83.21
Hydrogen	4.07	6.08
Nitrogen	2.81	2.59
Sulfur	0.16	0.11
Oxygen	14.84	8.01
H/C molar ratio	0.63	0.87
O/C molar ratio	0.14	0.07
Empirical formula	$\text{CH}_{0.63}\text{N}_{0.03}\text{O}_{0.14}$	$\text{CH}_{0.87}\text{N}_{0.02}\text{O}_{0.07}$
Gross heating value (MJ/kg)	26.053	33.08

4.6.1.2 Bulk density and pH of bio-char

Bulk density of bio-char reflects the flow consistency and packing quantity of solid fuels. The obtained bulk densities of MS and MSPS bio-char were 0.83 and 0.96 g/cc, respectively, whereas the bulk density of coal is in the range of about 0.60 to 0.80 g/cc [35,154].

The pH of bio-char is an important property to be determined as this changes the soil pH, depending on the quantity of bio-char added. KCl was used to enhance the properties of bio-char because it could release the exchangeable protons from bio-char into the solution due to its ionic nature. The solution pH of bio-char was more alkaline as it was produced from pyrolysis with long residence time. The pH of MS and MSPS bio-char were 11.9 and 12.5, respectively which is probably good for acidic soils. The soil pH of around 6.3–6.8 is the optimum range in terms of nutrient availability for most plants and is preferred by most beneficial soil bacteria[155]. Moreover, alkalinity can be influenced by three factors: organic functional groups, carbonates and inorganic in order to meet with the requirement of soil pH [156].

4.6.1.3 SEM and BET analysis of bio-char (morphological characteristics)

Scanning electron microscopy (SEM) is a potential technique for determining the morphology of solid fuel particles. SEM analysis has been especially used to evaluate the structure vibration in biochar properties after different thermal treatments, and this analysis is also useful to obtain the detail accuracy about pore structure of bio-char [157]. Bio-char's porous structural examination as observed under scanning electron microscopy with different magnifications are presented in Fig 4.15, Fig 4.16, Fig 4.17 and Fig 4.18. Volatile matters, which escape during pyrolysis of biomass and biomass: plastic mixture, have left pores behind the surface of the bio-char. These pores can be represented by the SEM images which shows the heterogeneous distribution of macropores and a rough texture. SEM image of MSPS bio-char possesses well oriented pore structure. However, for MS bio-char, surface is rough with not so well organized pores. Moreover, we can observe that MSPS bio-char is more porous than MS biochar. The structure characteristics of bio-char determines its potential to act as an adsorbent. Highly porous bio-chars have more adsorption sites for ions and provide spaces for nutrients and water retention [160–162]. These findings were consistent with BET analysis for surface area measurement. Whereas the surface area of MS and MSPS bio-char is important like other physicochemical characteristics, the average surface areas were found to be 13.2 m²/g. and 35 m²/g. However, with further activation of the bio-char with acid, and alkali, its quality can be improved to use it for adsorption process. It may strongly affect the reactivity and combustion behavior of char.

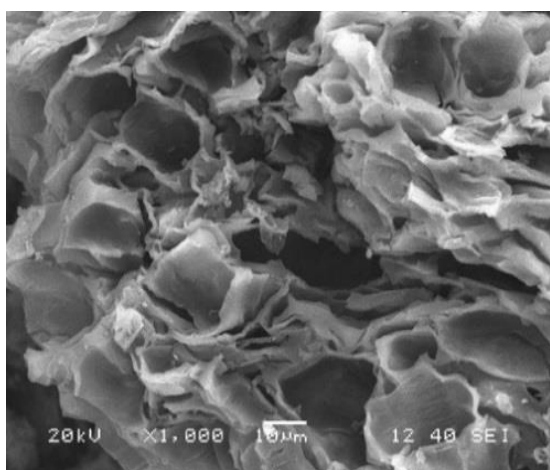


Fig. 4.15 SEM image of MS bio-char at 1000x 500x

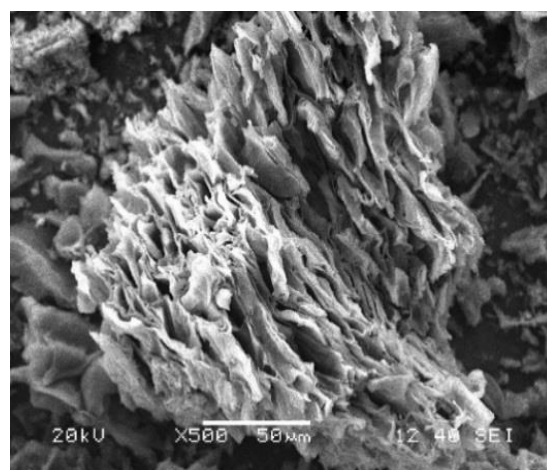


Fig. 4.16 SEM image of MS bio-char at 500x

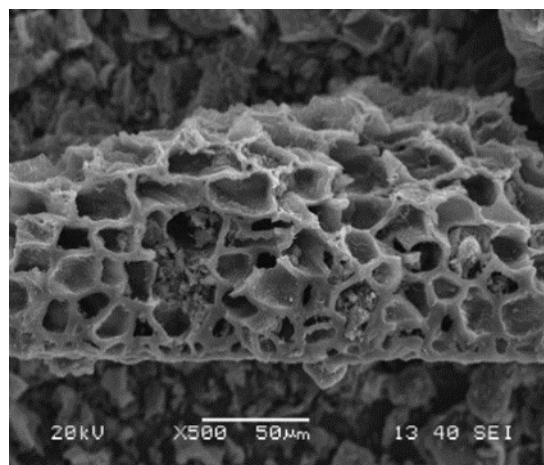
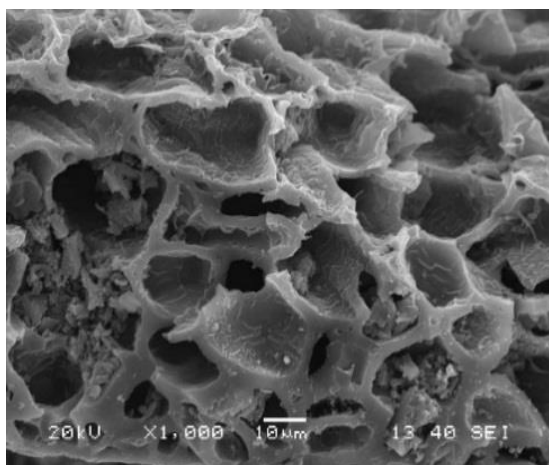


Fig. 4. 17 SEM images of MSPS bio-char at 1000x Fig .4.1 8 SEM image of MSPS bio-char at 500x

Since the obtained bio-char from MS and MSPS pyrolysis is mainly macroporous with low surface area , it could be used for the production of activated carbon after chemical and physical activation [158].

4.5 Conclusion

From this study it is seen that the pyrolysis of Mahua seed mixed with Polystyrene waste is a potentially suitable method for the production of upgraded pyrolysis oil. The maximum co-pyrolysis oil yield of 74.25% was obtained at a temperature of 525 °C with 1:1 blend and a constant heating rate of 20 °C/min and with nitrogen flow rate of 30 mL/min. The co-pyrolysis of biomass mixed with polystyrene produced 25 wt. % more oil than the pyrolysis of individual biomass. The heating value of the co-pyrolysis oil is somewhat more than that of biomass pyrolysis oil. The oxygen content of the co-pyrolysis oil is reducing with increasing the ratio of polystyrene. From the physical properties studies, it was found that the viscosity of the co-pyrolysis oil is less than that of MS pyrolysis oil and it is near about conventional fuel. The obtained flash point of MSPS pyrolysis oil is also more effective than that of MS pyrolysis oil. The distillation range of co-pyrolysis oil is near about conventional fuel and the range is also less than that of biomass pyrolysis oil. From the physical analysis studies, it was concluded that, with the addition of plastic, the quality of oil is improved. From the chemical analysis studies such as FTIR, NMR and GCMS, it was observed that the compounds present in co-pyrolysis oil are similar to polystyrene oil and most of the compounds are aromatic in nature, whereas the oxygenated and phenolic compounds are reduced with the addition of plastic. The by-product, bio-char obtained from MS and MSPS pyrolysis is also characterized for its further application like a solid fuel. From the physical characterization of bio-char it was concluded that both the bio-chars can be used as solid fuel. From the physical characterization studies, it was observed that the

calorific value of MSPS bio-char is more than that of MS bio-char. However, both the calorific values are more than that of coal. The obtained bulk density of MS and MSPS bio-chars are 0.83 and 0.96 g/cc. From SEM and BET analysis studies, it was found that the MSPS bio-char is more porous than that of MS bio-char. The surface area of MSPS bio-char is also more than MS bio-char. From the present study it has been proved that the co-pyrolysis products like bio-oil and bio-char give better results than MS pyrolysis products. Thus, we can conclude from the present study that the co-pyrolysis of MS and PS could be an environmental friendly process for the production of valuable chemicals and fuels.

Chapter 5

Thermal kinetics of Mahua seed, Polystyrene and their mixtures

5.1 Introduction

Thermal decomposition or devolatilisation occurring during pyrolysis process of the biomass-plastic mixture is very important as kinetics is intrinsically related with the decomposition mechanism [159]. Hence, thermogravimetric analysis (TGA) is a very powerful technique used in this study to investigate the solid-phase thermal degradation and also the determination of kinetic triplets, namely pre-exponential factor (A), activation energy (E_A), and order of reaction model (n) from the kinetic analysis of solid raw materials such as coal, biomass and plastic [160,161]. This gives the knowledge of the chemical composition, pyrolytic characteristics, and kinetic analysis of the main pyrolysis process and also gives the effective design and operation of thermochemical conversion units. Kinetic study of co-pyrolysis is useful in order to understand the degradation mechanism, to know the rate of reaction and reaction parameters. Kinetic modelling of co-pyrolysis of biomass and plastic waste is extremely important for the selection, design and operation of the reactors for industrial application. Study of the synergistic effect between biomass and polymer is important in order to predict the interaction between the two species during co-pyrolysis and the nature of products obtained. Specific studies related to the thermal degradation and determination of kinetic parameters of the mixtures of polymer and lignocellulose biomass during the pyrolysis process had been carried out by other researchers.

Suriapparao et al. studied the kinetic analysis of co-pyrolysis of cellulose and polypropylene of different mixture compositions at different heating rates from 5 to 180 K min⁻¹, and stated that the activation energies of thermal decomposition of the mixtures clearly indicated the presence of interaction between cellulose and PP [162]. The presence of cellulose in the mixture decreased the apparent activation energy of PP decomposition from 210 to 120 kJ mol⁻¹, while the presence of PP did not affect the apparent activation energy of cellulose decomposition $E_A = 158 \pm 3$ kJ mol⁻¹. Chin et al. studied the thermal decomposition behaviour of rubber seed shell and high density polyethylene (0.2:0.8 weight ratio) using thermogravimetric analyzer, with the main components of biomass such as hemicellulose, cellulose, and lignin also analyzed, and compared the pyrolysis behavior with RSS. He found that the activation energies (E_A) for RSS, HDPE, and HDPE/RSS mixtures are 46.94–63.21, 242.13–278.14, and 49.14–83.11 kJ mol⁻¹, respectively [163].

Previously many researchers worked on biomass and plastic mixture with different blends and different plastics with biomass mixture. However, there is no work related to co-pyrolysis kinetic analysis on Mahua seed and polystyrene studied before. Therefore, a systematic study on the co-pyrolysis behaviors and kinetics of Mahua seed and Polystyrene using the uniform kinetics parameters calculation method in identical experimental conditions is highly significant for analysis and comparison. In this study, in order to compare the thermal and kinetic behaviors of individual raw materials with the mixtures, biomass-plastic materials were blended in definite ratio (1:1, w/w) and pyrolyzed with different heating rates of 5, 10, 20 and 50 °C/min from room temperature to 600 °C in the presence of N₂ atmosphere with a flow rate of 100 mL/min in thermogravimetric analyser. The kinetics parameters were obtained using TG data at different heating rates, and the activation energy and pre-exponential factors were evaluated by Kissinger method, Flynn-Wall-Ozawa method and Kissinger-Akahira-Sunose method. The results of the analysis have suggested that the co-pyrolysis characteristics of the blends are quite different to the combination of the individual materials and therefore, the possible synergistic effect points to the existence of chemical interaction during co-pyrolysis between the plastic and biomass fractions of the blends. This study aims to investigate the feasibility and advantages of plastics and biomass co-pyrolysis for solid waste disposal and to gather useful data in the solid waste treatment.

5.2 Experimental and materials

5.2.1 Feed stock preparation

The raw materials used in this study are Mahua seed (MS) and Polystyrene (PS), the samples were collected from NIT, Rourkela campus. Prior to use in experiment, the collected Mahua seeds were sun dried for one day and kept in oven for 24 hours at 50 °C. Waste polystyrene was kept in hot air oven for two hours with 100 °C to reduce its volume and easy to brittle for powder form. Both MS and PS samples were made into powder by using mixture grinder and after that sieved into an average particle size (of < 1 mm). Before performing co-pyrolysis of MS with PS, the powdered sample of (MS: PS) (1:1) was blended by tumbling for 30 min in order to achieve homogeneity.

5.2.2 Equipment and procedure detail

Mahua seed (MS), Polystyrene (PS) and their mixtures (MS: PS) (1:1) blend samples were subjected to thermogravimetric analysis (TGA) in an inert atmosphere of nitrogen. (SHIMADZU model DTG-60/60H TGA instrument). TGA analyser was used to measure and record the sample mass change with temperature over the course of pyrolysis reaction. Thermogravimetric curves were obtained at four different heating rates (5, 10, 20 and 50 °C/min) from ambient temperatures to 600 °C. Nitrogen gas was used as an inert purge gas to displace air in the pyrolysis zone, thus

avoiding unwanted oxidation of the sample. A flow rate of around 100 mL/min was fed to the system. The balance can hold a maximum of 20 mg, therefore, all sample amounts used in this study averaged approximately 12 mg.

5.3 Results and discussion

5.3.1 Thermal decomposition characteristics of raw materials and their mixture

5.3.1.1 Thermal decomposition characteristic of Mahua seed

TGA curves of MS with different heating rates (of 5, 10, 20 and 50 °C/min), under nitrogen atmosphere, are shown in Fig. 5.1. It is obviously seen that the weight loss (%) decreases with increasing pyrolysis temperature of the MS. It is generally followed that biomass pyrolysis proceeds in two main stages, evaporation of moisture, main degradation of more unstable polymers, and continuous slight devolatilisation. From the plot it can be seen that a minor mass loss associated with ambient temperature to about 150 °C occurs due to the removal of moisture and external water bound by surface tension as suggested by previous literature [164]. The main decomposition of MS starts from 200 °C which extends up to 400 - 430 °C. During this time period the main pyrolysis reaction takes place, where 60-75 % of weight loss occurs. Further, a constant loss of mass occurs until 600 °C, after which there is essentially no further loss of mass. TGA curve has laterally shifted to higher temperature with increasing heating rate due to the combined effect of heat transfer at different heating rate.

Fig. 5.2 shows the differential mass loss (DTG) thermograms of thermal decomposition of MS pyrolysis, with four heating rates (of 5, 10, 20 and 50 °C/min). DTG peaks clearly indicate the maximum rate of conversion with the corresponding temperature. DTG plot includes two overlapping peaks, as the heating rate was increased the two peaks become progressively merged and are also indicated in the Fig. 5.2. The maximum value of the pyrolysis rate increases in response to increasing heating rates. Each peak corresponds to the maximum degradation of one subcomponent of the biomass. The lower temperature shoulder represents the decomposition of hemicellulose present in the biomass and the higher temperature peak corresponds to the decomposition of cellulose. The flat tailing section of the conversion rate curves at higher temperatures corresponds to lignin, which is known to decompose slowly [165]. DTG curves shifted towards a higher temperature zone, as well as the temperatures corresponding to the maximum loss of mass peaks also shifted towards higher values with increasing heating rate. At low heating rates, there may be some resistances to mass or heat transfer in the complex matrix of biomass, causing low conversion. However, an increase in heating rate may overcome these

resistances by means of strengthened driving forces of mass and heat transfer inside the particles of biomass and lead to a higher conversion rate shifting the DTG curves to higher temperature zone [4].

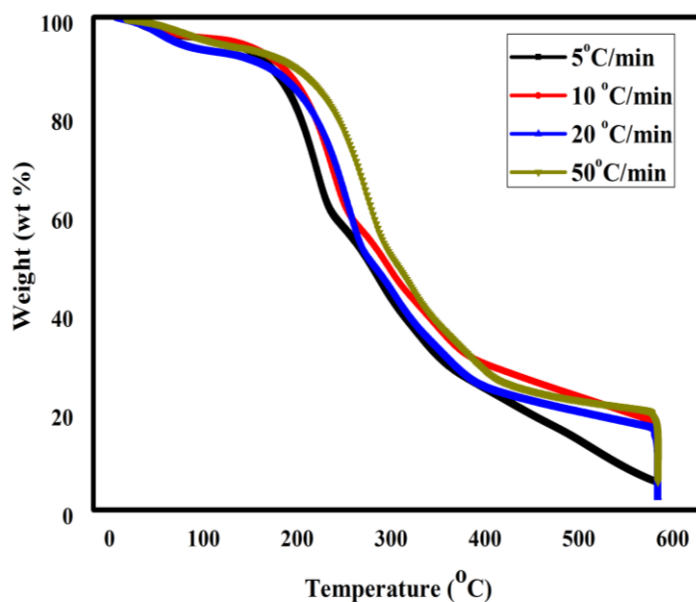


Fig. 5.1 TGA plot of Mahua seed at different heating rate

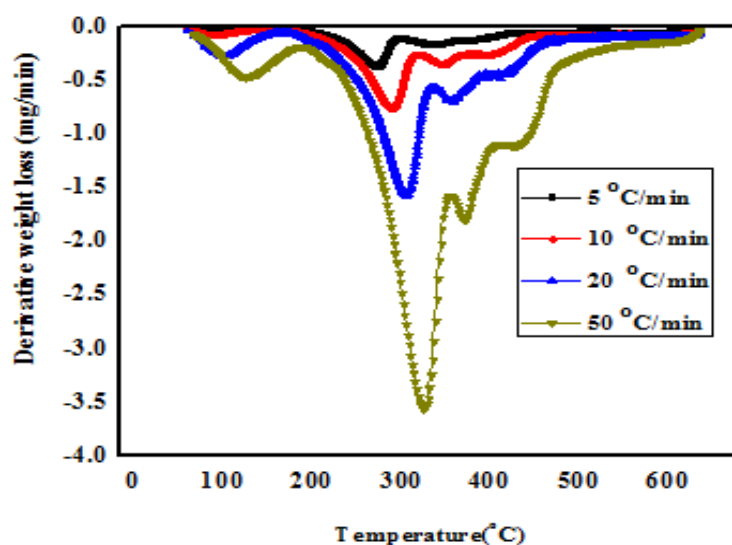


Fig. 5.2 DTG plot of Mahua seed at different heating rate

5.3.2 Thermal decomposition characteristic of Polystyrene

Fig. 5.3 and Fig. 5.4 shows the thermal decomposition of TG and DTG characteristic curves of PS with different heating rate, they show weight loss of plastic as a function of temperature, where a one-step decomposition curve occurred for PS as previously mentioned that plastic does not have complicated structure as compared to biomass. The main decomposition of plastic occurred at higher temperature compared to the biomass and completed in short time period. Increase in temperature led to increased weight loss of plastic. Also, it was previously mentioned that the thermal stability of plastic is more than that of biomass. The main decomposition of PS started from 350 °C and corresponding to that the complete decomposition was accrued at 400 °C. From the DTG curve, it is seen that as the heating rate increases, there is a lateral shift of curve to higher temperature. The rate of weight loss also reflects the lateral shift with an increase in the rate as the heating rate is increased from 5, 10, 20 and 50 °C/min. Williams and Nasir [166] suggested that the shift to higher temperatures of degradation represented differences in the rate of heat transfer to the sample as the heating rate is varied.

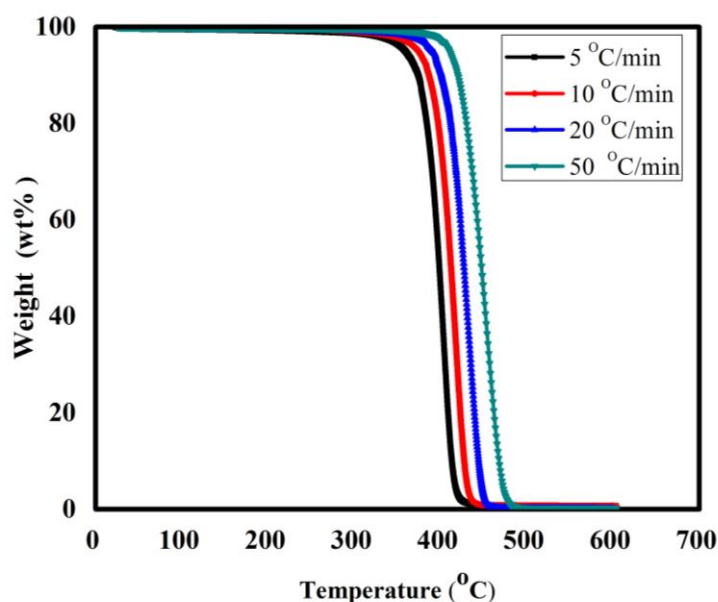


Fig. 5.3 TGA plot of Polystyrene at different heating rate

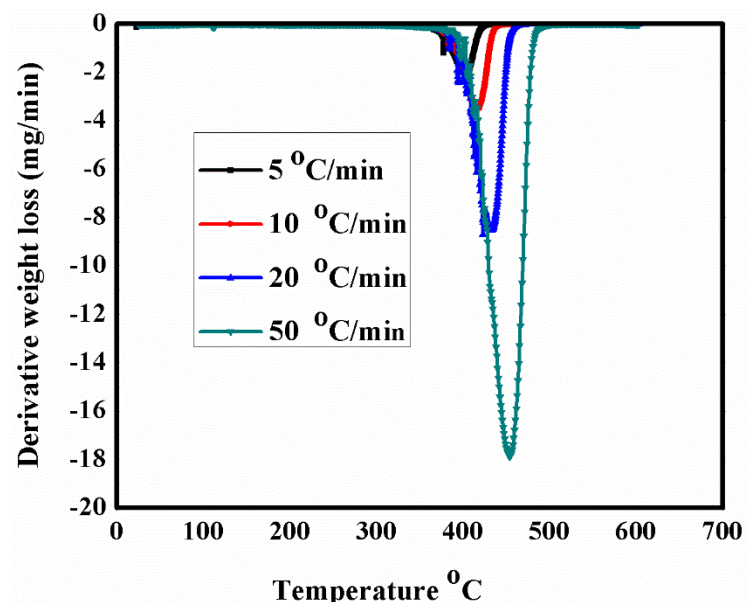


Fig. 5.4 DTG plot of Polystyrene at different heating rate

5.3.3 Thermal decomposition characteristics of biomass/ plastic mixture

The TG/DTG curves of the mixture of MS:PS at heating rate of 5, 10, 20, and 50 °C/min are depicted in Fig. 5.5 and Fig 5.6. In general, we can note that the domains of degradation are well differentiated. Thermal decomposition of MS has started earlier as compared to plastic in the mixture due to the structural difference between biomass and plastic, which directly affects their thermal decomposition behaviour. It was noticed that the temperature range for the mixture changed in comparison with those for each component. When plastic and biomass are mixed together, the pyrolysis is characterized by three decomposition stages unlike one decomposition stage for PS and two decomposition stages for MS which are observed when they are pyrolyzed alone. Plastic in a mixture degrades at lower temperatures than plastic alone, while biomass in a mixture degrade at the same temperature, similar to the decomposition of biomass alone. A significant interaction is observed in the third stage of degradation at 370 °C to 450 °C, while the first and second stage degradation is less affected. The significant interaction in the third stage is probably due to the products formed during biomass residue degradation which may influence on plastic degradation processes.

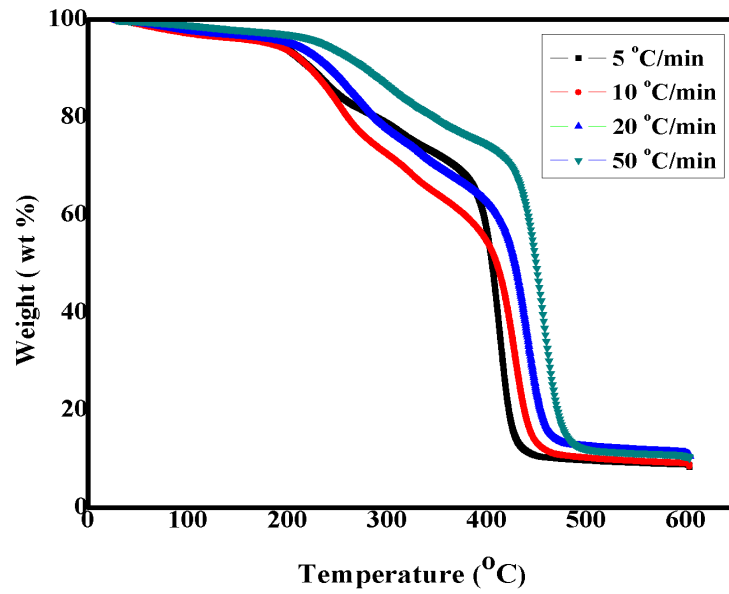


Fig. 5.5 TGA plot of MS:PS 1:1 blend at different heating rate

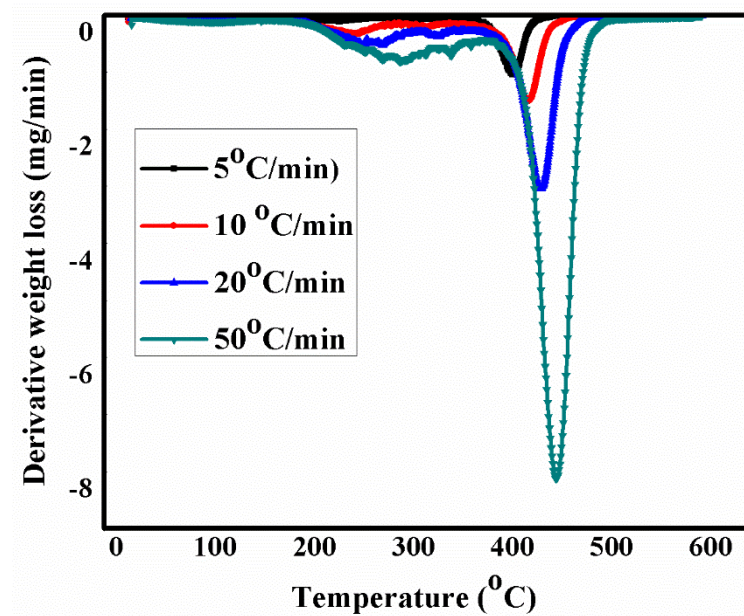


Fig 5.6 DTG plot of MS:PS (1:1) blend at different heating rate

5.4 Kinetic modelling

The decomposition and the reaction of solid fuel can be represented by a differential equation which is function of temperature and conversion. The conversion, x , is normalized form of weight loss data of decomposed sample and is defined by the expression

$$x = \frac{m_i - m_t}{m_i - m_f} \dots\dots\dots(1)$$

where, x is the conversion, m_i = Initial mass of the sample, m_t = Sample mass at time t, m_f = Final mass of the sample.

The rate of reaction kinetics is described by the following equation,

$$\frac{dx}{dt} = kf(x) \dots\dots\dots(2)$$

where x is degree of conversion, f(x) is a function of which depends on the reaction mechanism, the temperature dependence of the rate constant k is usually described by Arrhenius equation as

$$k = A \exp\left(-\frac{E_a}{RT}\right) \dots\dots\dots(3)$$

where A is pre-exponential (frequency) factor. E_A is the activation energy, R is the universal gas constant and T is the absolute temperature.

f(x) can be defined as

$$f(x) = (1-x)^n \dots\dots\dots(4)$$

where n is the order of reaction. Now substituting the above equation (3) and (4) in equation (1), and rearranging it gives

$$\frac{dx}{dt} = A \exp\left(-\frac{E_a}{RT}\right) (1-x)^n \dots\dots\dots(5)$$

In non-isothermal TGA experiments, the linear heating rate (β) is usually expressed by

$$T = T_0 + (\beta t) \dots\dots\dots(6)$$

$$\frac{dT}{dt} = T - T_0$$

where T_0 , is the initial temperature, β is the linear heating rate and T is the absolute temperature at time t.

For non-isothermal measurements with a linear heating rate $\beta = \frac{dT}{dt}$, the above equation (6) can be written as,

$$\frac{dx}{dT} = \frac{dx}{dt} \times \frac{1}{\beta} \dots\dots\dots(7)$$

Substituting equation (7) in equation (5) and the following expression can be obtained,

$$\frac{dx}{(1-x)^n} = \frac{A}{\beta} \exp\left(-\frac{E_a}{RT}\right) dT \dots\dots\dots(8)$$

This equation expresses the fraction of material consumed in the given time. In this work, the activation energy and pre-exponential factors were obtained from non-isothermal TGA experiments. Kinetic parameters were obtained from non-isothermal rate laws by both model-fitting and model free method [167].

5.5 Model-free methods

5.5.1 Kissinger method

Kissinger developed a non-isothermal model-free method, where the solid state reaction can be determined without knowing the reaction mechanism. Kinetic parameter like E_A for each conversion is not required to establish [115,168]. However, this method allows us to obtain the value of activation energy from the plot $\ln \frac{\beta}{T_m^2}$ versus $\frac{1000}{T_m}$ for a series of experiments at different heating rates (β), where the T_m is the temperature peak of the DTG curve of MS, PS and MS: PS blend. The Kissinger equation is shown below

$$\ln \frac{\beta}{T_m^2} = \ln \left(\frac{AR}{E} \right) - \frac{E}{RT_m} \dots\dots\dots(9)$$

where, $-\frac{E}{R}$ is the slope of the plot from which the activation energy can be calculated.

5.5.2 Flynn-Wall-Ozawa method

The Flynn-Wall-Ozawa [115,169,170] method is a model-free method that involves measuring the temperature corresponding to fixed values of α from experiments at different heating rates, β and plotting $\ln(\alpha)$ against $1/T$, and the slopes of such plots give $\frac{-E_A}{R}$.

We know that, the non-isothermal rate law is given as

$$g(\alpha) = \frac{AE}{\beta R} p(x)$$

where, $g(\alpha)$ is constant at a given value of conversion, $p(x)$ is the exponential integral.

Taking logarithm on both side, we get

$$\log g(\alpha) = \log \frac{AE}{\beta R} + \log p(x) \dots \dots \dots (10)$$

From Doyle's approximation, which shows that $\log p(x)$ is linear with respect to x over a short range of x .

$$\log p(x) \approx -A - Bx$$

where, $28 < x < 50$

By interpolation, $A=5.3305$ and $B=1.052$

$$\log p(x) \approx -5.3305 - 1.052x \dots \dots \dots (11)$$

Substituting equation (11) Doyle's approximation in equation (10), we will get

$$\log g(\alpha) = \log \frac{AE}{\beta R} - 5.3305 - 1.052x \dots \dots \dots (12)$$

Putting E/RT in place of x , we get

$$\log g(\alpha) = \log \frac{AE}{\beta R} - 5.3305 - 1.052 \frac{E}{RT} \dots \dots \dots (13)$$

Now, rearranging the above equation we get,

$$\log \beta = \log \frac{AE}{g(\alpha)R} - 5.3305 - 1.052 \frac{E}{RT} \dots \dots \dots (14)$$

The above equation is the desired equation. A plot of $\log(\beta)$ versus $1/T$ at each α yields activation energy (E_A) from the slope regardless of the model.

5.5.3 Kissinger-Akahira-Sunose Method

In this method [115,171–174] the overall rate of reaction is given by

$$\frac{d\alpha}{dt} = k(T) f(\alpha) \dots \dots \dots (15)$$

where $\frac{d\alpha}{dt}$ is the reaction rate, α is the conversion degree, $k(T)$ is the rate constant, t is the time, T is the temperature, and $f(\alpha)$ is the reaction model.

The rate constant $k(T)$ is described by the Arrhenius law

$$k(T) = A e^{\frac{-E_A}{RT}} \dots \dots \dots (16)$$

where E_A is the activation energy, A is the pre-exponential factor or frequency factor and R is the gas constant.

We know that the linear heating rate $\beta = \frac{dT}{dt}$

Therefore, equation (15) can be written as

$$\frac{d\alpha}{dT} = \frac{k(T) f(\infty)}{\beta} \dots\dots\dots(17)$$

or

$$\frac{d\alpha}{dt} = \frac{A}{\beta} e^{-\frac{E}{RT}} f(\alpha) \dots\dots\dots(18)$$

which is the differential non-isothermal rate law.

Integrating both sides we get,

$$g(\infty) = \frac{A}{\beta} \int_0^T e^{-\frac{E}{RT}} dT \dots\dots\dots(19)$$

This equation does not have any analytical solution. So it can be written as

$$g(\alpha) = \frac{AE}{BR} \int_x^\infty \frac{e^{(-x)}}{x^2} dx \dots\dots\dots(20)$$

$$\text{Put } \int_x^\infty \frac{e^{-x}}{x^2} dx = p(x)$$

$$\therefore g(\alpha) = \frac{AE}{BR} p(x) \dots\dots\dots(21)$$

From the approximation used by Murray and White, [175].

$$p(x) \cong \frac{e^{-x}}{x^2}$$

which is valid for $20 < x < 50$

where $x = E/RT$

Putting the value of $p(x)$ and x in equation (20), we get

$$g(\infty) = \frac{AE}{BR} \frac{e^{-\frac{E}{RT}}}{\left(\frac{E}{RT}\right)^2} \dots\dots\dots(22)$$

Rearranging, we get:

$$\frac{\beta}{T^2} = \frac{AR}{Eg(\infty)} e^{-\frac{E}{RT}} \dots\dots\dots(23)$$

Taking logarithm on both sides, we get

$$\ln\left(\frac{\beta}{T^2}\right) = \ln\left(\frac{AR}{E}\right) - \ln g(\infty) - \frac{E}{RT} \dots\dots\dots(24)$$

For a constant conversion value, we can write the above equation as

$$\ln\left(\frac{\beta_i}{T_{\alpha i}^2}\right) = \ln\left(\frac{A_\alpha R}{E_A}\right) - \ln g(\alpha) - \frac{E_\alpha}{RT_{\alpha i}} \dots\dots\dots(25)$$

The activation energy can be evaluated from the above equation by plotting the left hand side of the equation against $\frac{1}{T_{\alpha i}}$ at constant conversion for the *i*th heating rate.

5.6 Kinetic analysis

The purpose to study kinetics was to solve the dynamics of three factors: activation energy, E_A , pre-exponential A and the reaction model $f(\alpha)$, which could describe the reaction equations. Activation energy refers to the threshold by reaching which a chemical reaction takes place, which reflect the difficulty of chemical reaction. In the present study, we consider the iso-conversion method to analyse the pyrolysis dynamics, which could eliminate the influence of the mechanism function of uncertainty on activation energy. Kissinger method, Flynn-Wall-Ozawa (FWO) method and Kissinger- Akahira-Sunose method (KAS) were used to determine the activation energies of MS, MS: PS 1:1 blend in the research at four different heating rates (5, 10, 20 and 50 °C/min). The results obtained from TGA analysis were elaborated according to model-free methods to calculate the above kinetics parameters. In the Kissinger method the activation energy and pre-exponential factor were calculated from equation (9), where T_m is the temperature, which corresponds to the maximum weight loss. The peak temperatures for MS, PS and MS: PS (1:1) were obtained from Fig. 5.2, Fig. 5.4 and Fig 5.6. Kissinger plot of $\ln(\beta/T_m^2)$ versus $1000/T \text{ K}^{-1}$ of decomposition process for MS, PS and MS: PS (1:1) are shown in the Fig. 5.7, Fig. 5.8 and Fig. 5.9. The activation energy (E_A) and pre-exponential factor (A) for MS, PS and MS: PS (1:1) were derived from the slope and intercept of plotting regression line, respectively. The results obtained from Kissinger methods are presented in Table 5.1 from the Table it is found that the obtained activation energy and pre- exponential factor for MS, PS and MS:PS (1:1) are 82.12 kJ/mol, 165.23 kJ/mol, 235.57 kJ/mol, 5.20×10^7 , 1.32×10^{12} and $2.22 \times 10^{17} \text{ min}^{-1}$ respectively. We can observe that there is a synergistic effect between MS: PS kinetics, however the value of activation

energy increase for the MS: PS blend which is higher than that of pure biomass and plastic. Similarly, the other kinetic models such as FWO and KAS were used for MS, PS and MS: PS (1:1) blend to determine the activation energy and pre-exponential factor using equation (14) and (25) which and summarised in the Table 5.1. These methods are used to study the relation between activation energy and conversion, where the selected conversion values of α are (0.1 to 0.7). From the table it is observed that the R^2 of all curves are within the narrow interval of 0.936 to 0.999, which means that the points have fitted well for most of the E_A values for MS and PS but it was slightly varying for MS: PS blend. Thus, it can be expected that the results are acceptable. The average activation energy and pre-exponential factor for MS, PS and MS: PS, blends are 239.83, 181.58, and 165.02 kJ/mol, 8.70×10^{31} , 2.80×10^{13} and 4.15×10^{15} , respectively. Whereas from the KAS method the obtained activation energy and pre-exponential factors are 214.01 KJ/mol, 179.54 KJ/mol and 161.80 KJ/mol and 7.90×10^{30} , 1.92×10^{13} , and 5.7×10^{15} respectively. The apparent activation energy for MS and MS:PS blend of FWO and KAS method from the conversion of 0.1 to 0.7 is shown in the Fig. 5.10 and Fig. 5.12, which is not similar for all the conversion and a large variation occurs in both biomass and biomass/ plastic blend due to the influence of composition of biomass species on the thermal behaviors and influence of heating rate on biomass [172]. As stated by Bartocci et al, that the biomass involves a complex, multistep mechanism which occurs in the solid state [115] also he stated that reaction mechanism is not similar for the whole decomposition process and the activation energy depend on the conversion. The model-free isoconversion methods allow to estimate activation energy as a function of conversion without previous assumption on the reaction model and allows nearly unmistakably detecting multi-step kinetics as a dependence of activation energy on conversion in contradiction to Kissinger method which produces a single value of the E_A for the whole process and complexity may not be revealed. Moreover, there is a small variation of activation energy observed for PS in Fig. 5.11 which is due to its origin and it decomposes solely. The large difference of activation energy in Kissinger method as compared to the FWO and KAS methods for all the samples is due to different model equations and biomass complexity.

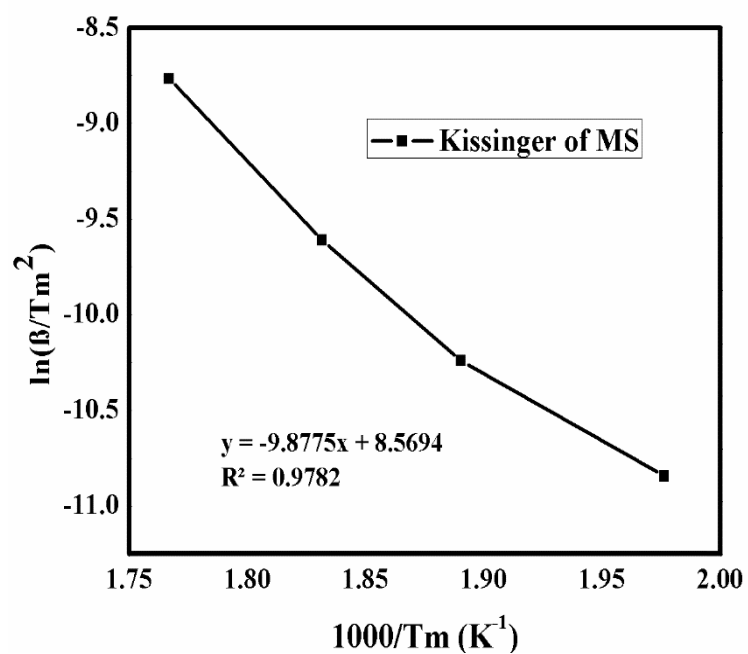


Fig. 5.7 Kissinger plot of MS

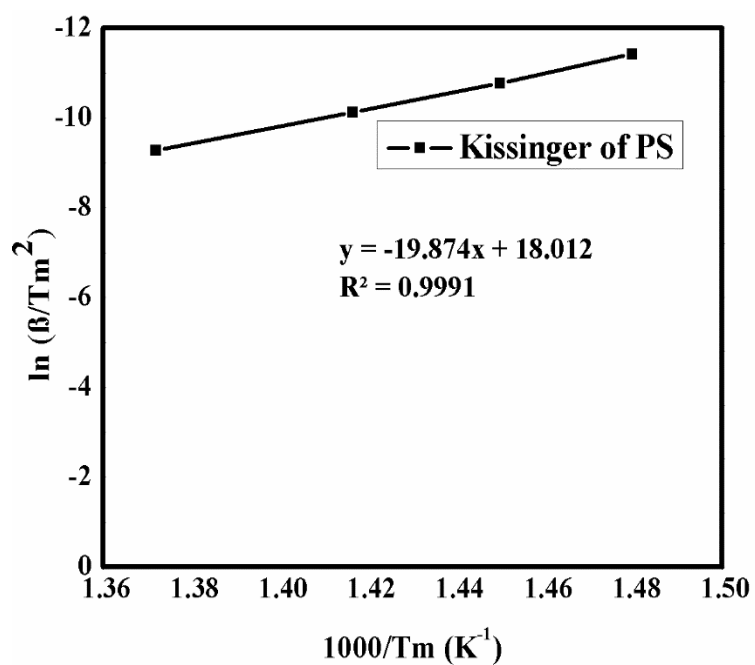


Fig. 5.8 Kissinger plot of PS

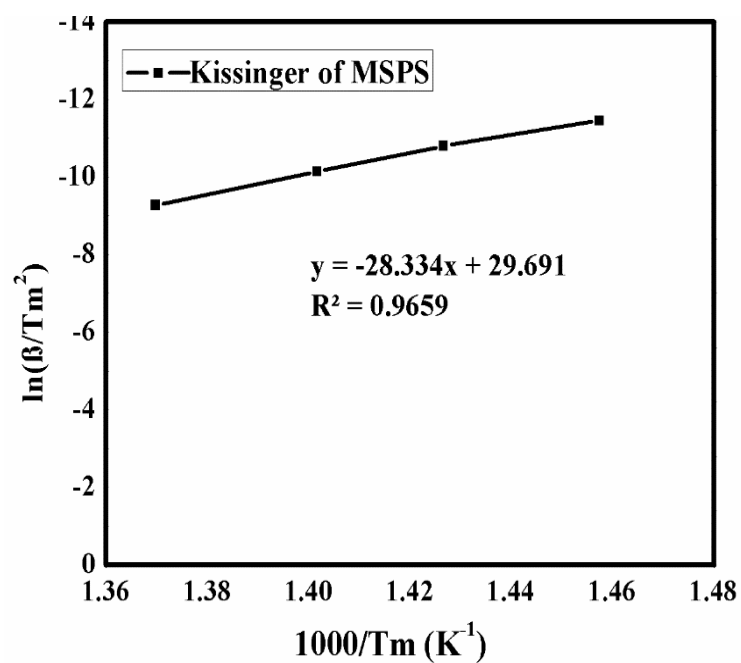


Fig. 5.9 Kissinger plot of MS:PS

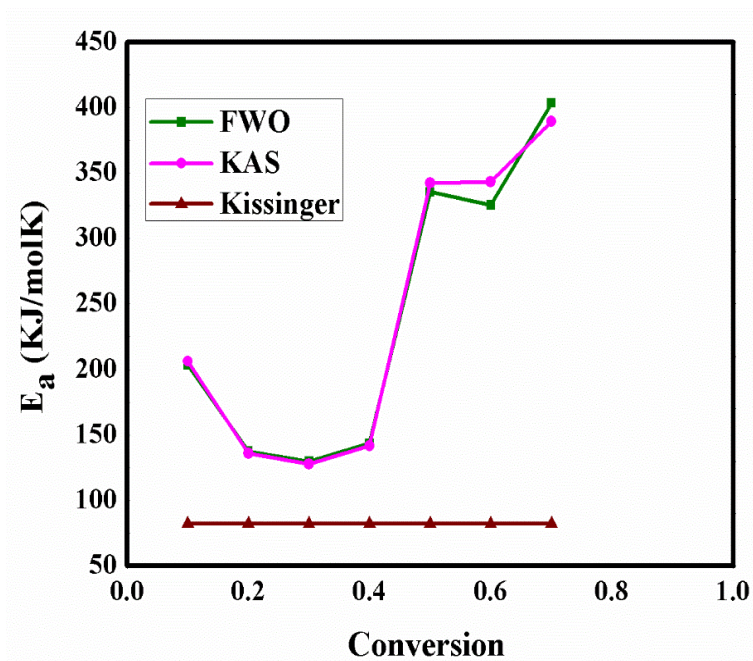


Fig. 5.10 Activation energy as a function of conversion for MS

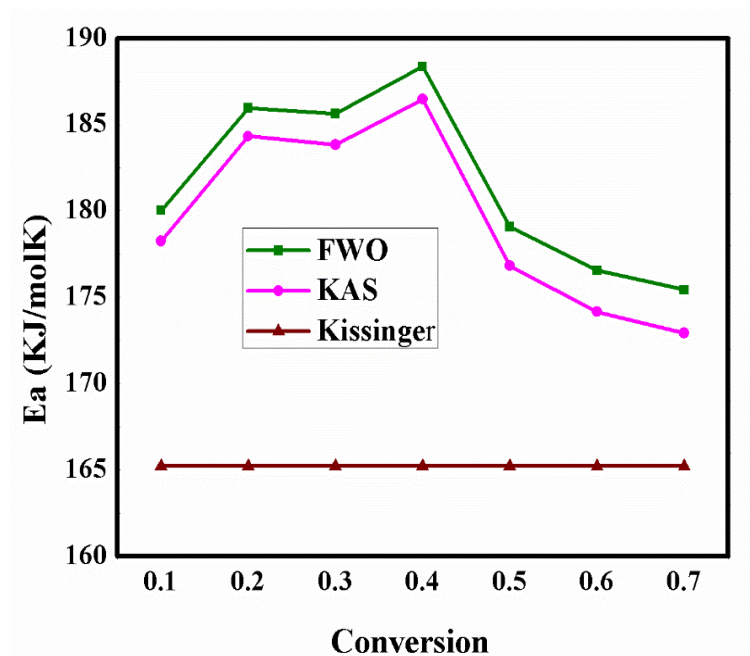


Fig. 5.11 Activation energy as a function of conversion for PS

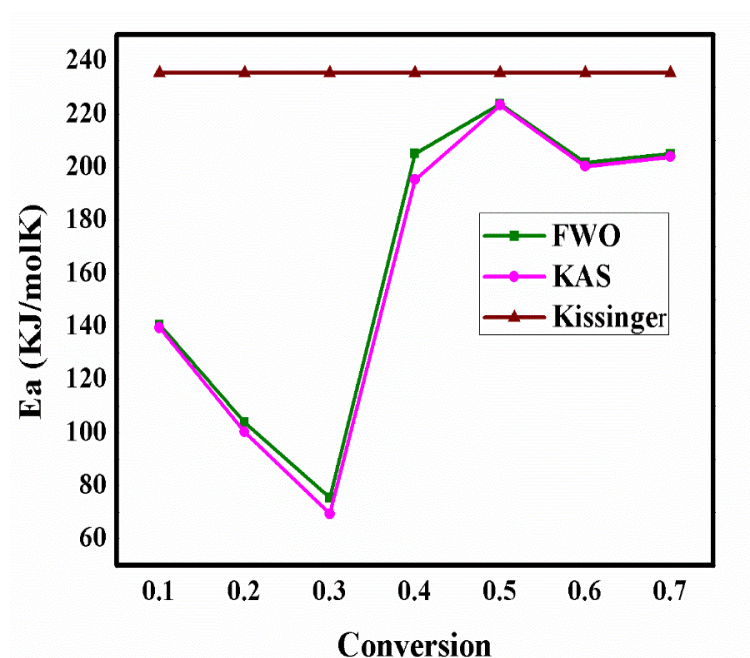


Fig. 5.12 Activation energy as a function of conversion for MSPS

Table 5.1 The kinetic parameters activation energy (E_A) and pre-exponential factor (A) obtained by Kissinger, FWO and KAS methods for MS, PS and MS: PS (1:1) blend.

		FWO			KAS		
Sample	α	E_a (kJ/mol)	A (min^{-1})	R^2	$E_a(\text{kJ/mol})$	A (min^{-1})	R^2
MS	0.1	203.61	8.84×10^{21}	0.940	206.35	1.59×10^{22}	0.936
	0.2	137.38	2.92×10^{13}	0.966	136.01	1.99×10^{13}	0.962
	0.3	129.87	2.39×10^{13}	0.986	127.78	1.33×10^{12}	0.984
	0.4	143.50	2.83×10^{13}	0.984	141.83	1.82×10^{13}	0.982
	0.5	335.48	6.30×10^{30}	0.971	342.28	3.47×10^{29}	0.988
	0.6	325.60	1.70×10^{28}	0.938	343.28	2.75×10^{31}	0.969
	0.7	403.34	6.02×10^{32}	0.979	389.51	2.75×10^{31}	0.982
	Average	239.83	8.70×10^{31}	0.966	241.01	7.90×10^{30}	0.971
Kissinger		82.12	5.20×10^7	0.978			
PS	0.1	180.03	1.01×10^{13}	0.999	178.25	6.83×10^{12}	0.999
	0.2	185.95	3.6×10^{13}	0.999	184.32	2.56×10^{13}	0.999
	0.3	185.64	4.02×10^{13}	1	183.82	2.77×10^{13}	1
	0.4	188.36	7.29×10^{13}	1	186.48	5.2×10^{13}	0.999
	0.5	179.08	1.54×10^{13}	0.999	176.83	9.5×10^{12}	0.999
	0.6	176.55	1.09×10^{13}	0.999	174.17	6.49×10^{12}	0.999
	0.7	175.44	9.95×10^{12}	0.999	172.93	5.79×10^{12}	0.999
	Average	181.58	2.80×10^{13}	0.999	179.54	1.92×10^{13}	0.999
Kissinger		165.23	1.32×10^{12}	0.999			
MS/PS (1:1)	0.1	140.67	7.95×10^{21}	0.916	139.59	4.07×10^{13}	0.865
	0.2	103.92	1.5×10^9	0.959	100.26	5.0×10^8	0.952
	0.3	75.47	1.1×10^6	0.946	69.33	1.4×10^5	0.929
	0.4	205.08	4.16×10^{15}	0.962	195.33	7.75×10^{14}	0.958
	0.5	223.84	2.52×10^{16}	0.994	223.39	3.78×10^{16}	0.993
	0.6	201.68	8.17×10^{14}	0.987	200.36	6.33×10^{14}	0.985
	0.7	205.00	1.38×10^{15}	0.998	203.94	1.11×10^{15}	0.997
	Average	165.02	4.15×10^{15}	0.966	161.80	5.7×10^{15}	0.954
Kissinger		235.57	2.22×10^{17}	0.996			

5.7 Conclusion

In this study, we have examined the thermogravimetric and kinetics study of the biomass, plastic and co-pyrolysis of biomass and plastic blends. The results show that the thermal decomposition of the MS and PS materials can be characterized by two and one single reaction stages respectively, while that of the blends can be characterized by three decomposition reaction stages. The results of the analysis suggested that the co-pyrolysis characteristics of the blends are quite different to the combination of the individual materials and therefore, it can be concluded that there exists interaction and significant synergistic effects between plastic and biomass co-pyrolysis. The values of E_A and A are higher for mixtures than for individual components in the Kissinger method, whereas the activation energy and pre-exponential factors obtained for FWO and KAS methods are lower than those of individual ones. However, quantitatively, they are not vary significant. The activation energy and pre-exponential factor obtained from Kissinger method for MS, PS and MS: PS blends are 82.12, 165.23 and 235.57 kJ/mol, and pre-exponential factors are 5.20×10^7 , 1.32×10^{12} and $2.22 \times 10^{17} \text{ min}^{-1}$, whereas in case of FWO method the activation energies are 239.83 181.58 and 165.02 KJ/mol, and pre-exponential factors are 8.70×10^{31} , 2.80×10^{13} and 4.15×10^{15} respectively. From the KAS method the obtained activation energy and pre-exponential factors are 214.01, 179.54 and 161.80 kJ/mol and 7.90×10^{30} , 1.92×10^{13} , and 5.7×10^{15} , respectively. Kinetic parameters obtained from three different methods were in good agreement, but KAS and FWO methods are more efficient in the description of the degradation mechanism of solid-state reactions.

Chapter 6

Mahua seed pyrolysis oil blends as an alternative fuel for light-duty diesel engines

6.1 Introduction

The demand for energy and fuel cost have been increasing unpredictably in the last four decades, as a result of increasing population. The continuous degradation of the environment is probably due to increased pollutants in the air, water, soil, climate, temperature, and light. The main source of hazardous emissions is originated from the combustion of fossil fuels. Hence, the research on potential alternative fuels has been growing to meet the energy demand. The conversion of biomass to energy has been recently focused to substitute or replace the existing fossil fuel utilization [41]. In the last three decades, the interest on utilization of biodiesel in the diesel engines has grown enormously [176], but hindrances such as less production in comparison with the availability of crude oil, NO_x emission [177], lower oxidation stability [178] and poor cold flow properties [179] have been identified as the barriers to a maximum utilization of biodiesel. Introducing diversified technologies in harnessing energy from biomass is of great interest today. Energy conversion techniques such as pyrolysis, hydrolysis, and catalytic cracking are popular for converting waste biomass materials into useful liquid fuels. Pyrolysis, a type of thermochemical conversion which is believed to play an important role in the near future to produce potential liquid fuels from high volatile biomass materials. Pyrolysis of biomass is an attractive option and has drawn renewed interest due to the abundant availability of feedstock, easy pre-treatment methods and eco-friendliness [180]. The pyrolysis oil obtained from biomass, commonly referred to as “bio-oil”, is considered to be a renewable fuel. Various research works have been encouraged for the utilization of bio-oil derived from different edible and non-edible seeds e.g. tamarind (*Tamarindus indica*), pomegranate (*Punica granatum*), cherry (*Prunus avium*), rape (*Brassica napus*), karanja (*Millettia pinnata*), sal (*Shorea robusta*), cotton (*Gossypium*), tobacco (*Nicotiana tabacum*) and Mahua seed (*Madhuca indica*) [94,98–100,104,107,145,181,182].

The bio-oil contains various hydrocarbon compounds, moisture and acidic in nature. Most of the bio-oils are denser than diesel fuels but have low heating values. Also, the bio-oil requires a necessary pre-treatment to remove water content and neutralization before using it as an alternative fuel in compression ignition (CI) engine [41,176].

Many experiments have already been conducted to determine the performance and emission of a diesel engine run on bio-oil [124,183]. For instance, Vikranth et al. used the mustard cake pyrolytic oil blends in a diesel engine and found that 30% blend gave 4.7% higher brake thermal efficiency and lower exhaust emissions compared to diesel [125]. The utilization of bio-oil derived from pyrolysis of waste wood was investigated by Prakash et al. in a diesel engine for replacement of petroleum fuel [184]. The emulsions of coffee bean residue pyrolysis oil were tested in a diesel engine, and it was reported that the combustion efficiency and the NO_x emission with a penalty of smoke emissions were reduced [185]. Many research works have been performed on minimizing the problems associated with the use of bio-oils in the CI engines. The continuous search for potential liquid alternative fuels for diesel engines has been carried out using various biomass feed stocks. In the year 2013-14, a total of 28.051 million hectares of land in India was occupied by the oilseed crops as per Indian Institute of Oilseeds Research [93]. Among the oil seed crops, Mahua seed (*Madhuca indica*) is a plant originated from India which has a tremendous therapeutic potential. It is grown in the indo-Pakistan subcontinental area, Malaysia, and Bangladesh. In India, large numbers of Mahua trees are found in the states of Uttar Pradesh, Madhya Pradesh, Odisha, Chhattisgarh, Jharkhand, Gujarat, Andhra Pradesh, Maharashtra, Bihar, West Bengal and Karnataka [31]. As per Food Safety and Standards Authority of India (FSSAI) recommendation, the presence of free fatty acid (FFA) in an edible diet must be in the range of 0.5-0.2%. But Mahua seed, crude oil contains 19% FFA [186,187] and hence Mahua oil is not considered for edible purpose. The presence of saponins are responsible for the toxicity of Mahua species in animal feed. The cake is used mainly as a fertilizer and to a limited extent as feed for cattle because of its protein content [188]. Madhuca products are not consumed by humans. Therefore, human dietary exposure to Mahua saponin through the consumption of animal products is very unlikely. In Mahua, the most important saturated fatty acids are palmitic acid and stearic acid. The saturated fatty acids gives more stability to the fat, but they are considered harmful to the heart and blood vessels especially palmitic acid, while stearic acid has little or no effect [189].

Numerous research articles are available on the bio-diesel production from Mahua oil and its application in industries [190,191]. However, very few literature is available on the utilization of bio-oil obtained from the Mahua seed. Some investigations on bio-oil revealed that the quantity and quality of bio-oil were influenced by the quality of the feedstock, type of reactor and method of pyrolysis, temperature and conditions at which pyrolysis has been carried out [8,183,192]. Mohanty et al. [96] studied the properties of thermal and catalytic bio-oil obtained from the pyrolysis of Mahua seed. They used 2:1 feed to catalyst (CaO) ratio to improve the quality of bio-oil. Vikranth et al. [193] pyrolyzed Mahua deoiled-cake to produce bio-oil and concluded that the

maximum yield of 41% bio-oil was obtained at 550 °C. However, the Mahua bio-oil was not tested in a diesel engine for determining its performance and emissions. Hence, the current research is aimed to test the Mahua seed bio-oil as an alternative fuel in the CI engine. In this investigation, the Mahua pyrolytic oil (MPO) obtained by the pyrolysis process was pretreated for reducing its acidity and then blended with diesel at four different percentages from 10–40% on a volume basis in steps of 10% in the blend, and used as fuels in a single cylinder, four stroke, air-cooled direct injection (DI) diesel engine. The blends were denoted as MPO10, MPO20, MPO30 and MPO40, where the numeric value indicates the percentage of MPO in the blend. The performance and emission parameters of the engine run on the four different MPO-diesel blends were evaluated, compared with the diesel fuel operation, and presented.

6.2 Materials and Methods

6.2.1 Characterization of raw material

The detail characterization of raw materials (Mahua seed), experimental setup and experimental procedure has been explained in chapter 3, Experimental section.

6.2.2 Characterization of MPO

The characterization of the Mahua bio-oil such as physical properties and chemical properties studies are explained in chapter 3, Experimental section.

6.2.3 Engine experimental setup

For the experimentation, a single cylinder, four stroke, air cooled, direct injection (DI), diesel engine (make: Kirloskar, model: TAF 1) developing the power of 4.4 kW at 1500 rpm, was coupled to an alternator. Fig. 6.1 shows the schematic diagram of the experimental setup. The specification of the test engine is given in Table 6.1. A Kistler (model: 5395) piezoelectric pressure transducer with a charge amplifier and crank angle encoder was used in the data-acquisition system for pressure measurement. An automatic solenoid controlled burette was used to measure fuel consumption, whereas a differential pressure sensor was fitted to the air box to measure the air consumption. For speed measurement, a non-contact type sensor was fixed near the engine flywheel. The exhaust emissions such as nitric oxide (NO), carbon monoxide (CO), and unburnt hydrocarbons (HC) were measured using the AVL 444 DiGas analyzer. The smoke opacity was measured using an AVL 437C smoke opacity meter situated in the exhaust manifold. Initially, the engine was operated with neat diesel for obtaining the reference data. Further, the engine was tested with the MPO diesel blends. The combustion, performance, and emission

parameters were evaluated, and the results were compared with reference to neat diesel. All the experiments were carried out at a constant speed of 1500 rpm by varying the load conditions.

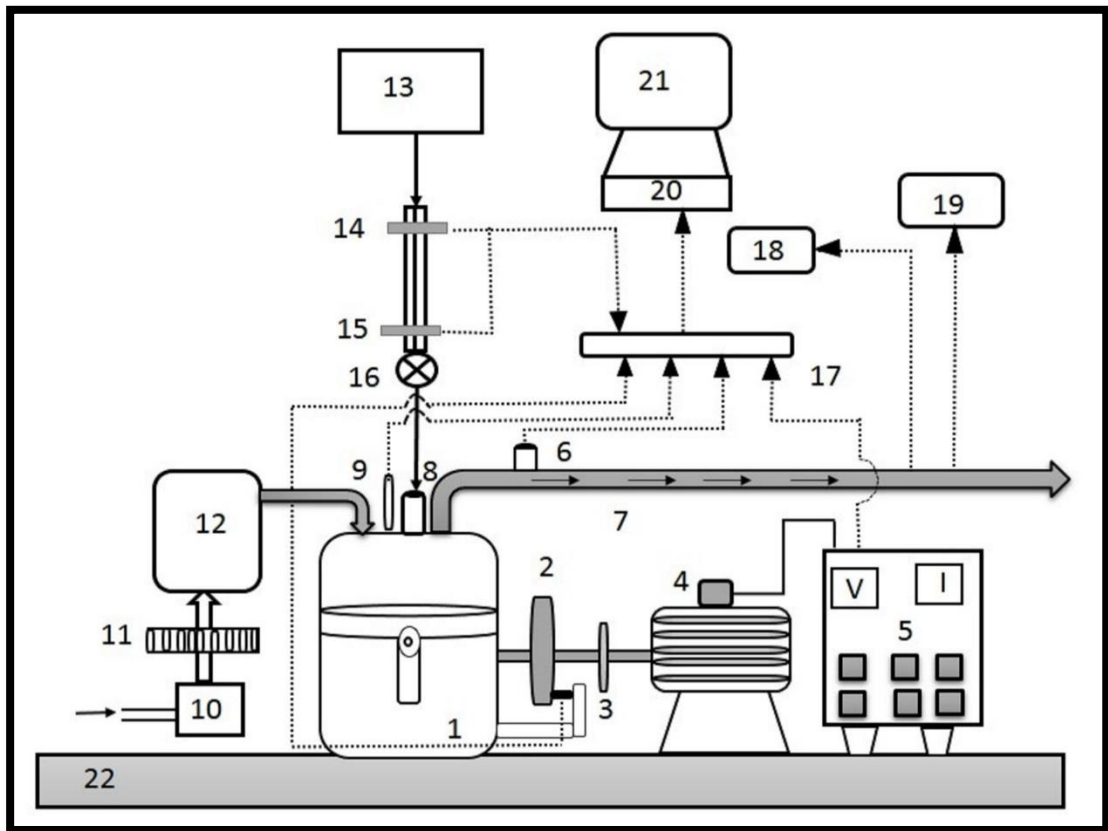


Fig. 6.1 Engine experimental setup

- | | | |
|------------------------|------------------------------------|-----------------------------|
| 1. Engine | 9. Pressure transducer | 17. Control panel |
| 2. Fly wheel | 10. Air filter | 18. Exhaust gas analyzer |
| 3. Speed sensor | 11. Air flow sensor | 19. Smoke meter |
| 4. AC dynamometer | 12. Air box | 20. Data acquisition system |
| 5. Resistive load cell | 13. Fuel tank | 21. Monitor |
| 6. EGT sensor | 14. High fuel level optical sensor | 22. Engine base |
| 7. Exhaust manifold | 15. Low fuel level optical sensor | |
| 8. Fuel injector | 16. Fuel pump | |

Table 6.1 Test engine specifications

Engine parameter	
Rated power and speed	4.4 kW at 1500 rpm
Bore x stroke	87.5 mm x 110 mm
Piston type	Bowl-in-piston
Compression ratio	17.5:1
Nozzle opening pressure (bar)	200
Injection timing (CA)	23 bTDC
Nozzle type	Multi hole (3)
Intake valve opening/closing	4.5° bTDC/35.5° aBDC
Exhaust valve opening/closing	35.5° bBDC/4.5° aTDC

6.2.4 Uncertainty analysis

An uncertainty analysis is essential to ensure the reliability of the readings obtained from different instruments during experimentation. In any experimental investigation, knowledge of the details of instruments to be used is essential. The details of instruments, their range, and accuracy and percentage uncertainties are listed in Table 6.2. Further evaluating the uncertainty analysis the following equation can be used [195].

$$\frac{U_y}{y} = \left[\sum_{i=1}^n \left(\frac{1}{Y} \frac{\partial y}{\partial x_i} U_{xi} \right)^2 \right]^{\frac{1}{2}} \quad (1)$$

where, Y is the physical parameter that is dependent on the parameter x_i , x_i = measured variable, n = number of variables, U_y = uncertainty in Y, \bar{x} = mean, $U_{x_i} = (\bar{x} - x_i)$.

Total uncertainty of the experiment = Square root of $\{(\text{uncertainty of TFC})^2 + (\text{uncertainty of brake power})^2 + (\text{uncertainty of BTE})^2 + (\text{uncertainty of CO})^2 + (\text{uncertainty of NO})^2 + (\text{uncertainty of HC})^2 + (\text{uncertainty of smoke})^2 + (\text{uncertainty of pressure transducer})^2\}$

$$= \sqrt{(1.5)^2 + (0.2)^2 + (1)^2 + (1)^2 + (0.2)^2 + (0.5)^2 + (1)^2 + (0.1)^2}$$

$$= \pm 2.36\%$$

As a result, the maximum uncertainty of the experiment was ± 2.36 with 95% confidence level.

Table 6.2 Details of instrumentation used in the study

S.No.	Instrument	Range	Accuracy	Percentage uncertainties
1	Gas analyzer	CO-0-10 %	±0.03%	±1
		NO-0-5000 ppm	±50 ppm	±0.2
		HC-0-20000 ppm	±10 ppm	±0.5
2	Smoke level measuring instrument	BSN 0-10	±0.2%	±1.0
3	EGT indicator	0-900 °C	±1°C	±0.15
4	Speed measuring unit	0-10000 rpm	±10 rpm	±1.0
5	Load indicator	0-100 kg	±0.1 kg	±0.2
6	Burette	—	±0.2 cc	±1.5
7	Manometer	—	±1 mm	±1.0
8	Pressure pick up	0–110 bar	±1 bar	±0.1
9	Crank angle encoder	—	±1°	±0.2

6.3 Results and Discussion

6.3.1 Pyrolysis of Mahua seed

6.3.1.1 Characterization of Mahua seed

The Mahua seed characterization is important to check its suitability for thermochemical conversion. The information on moisture content, volatile matter, fixed carbon and ash content of Mahua seed are estimated from the proximate analysis. The elemental composition such as carbon, hydrogen, nitrogen, sulfur and oxygen percentages of Mahua seed are estimated from the ultimate analysis. Table 6.3 gives the proximate and ultimate analyses of the Mahua seed in comparison to other biomass seeds. Mahua seed contains 84% volatile matter which is higher compared to Rape seed and karanja seed. The presence of high volatile matter in Mahua seed is suitable for the thermochemical conversion process. The estimated chemical composition of Mahua seed from ultimate analyses was $\text{CH}_{1.64}\text{N}_{0.05}\text{S}_{0.004}\text{O}_{0.31}$. The presence of 61.24% carbon content in the Mahua seed mainly causes 26.69 MJ/kg gross calorific value.

6.3.2 Production of Mahua bio-oil

The pyrolysis reactor was maintained at different temperatures ranging from 450–600 °C for the determination of optimum temperature at which the maximum bio-oil yield from Mahua seed was obtained. Fig 4.3 provides the details of pyrolysis products obtained from Mahua seed pyrolysis at different temperatures. It is evident from the table that the maximum bio-oil yield of 49% was obtained from Mahua seed at 525 °C. The maximum bio-oil yield at 525 °C can be attributed to thermal cracking, depolymerization, and recondensation of secondary reactions [134]. It should be noticed that the bio-oil obtained for Mahua deoiled cake is 41%, which is less than that of MPO [193].

Table 6.3 Proximate and ultimate analysis of different biomass seed

Characteristics	Mahua seed	Rape seed [100]	Karanja seed [107]
<i>Proximate analysis</i>			
Moisture (wt %)	8.6	4.9	15.2
Volatile matter (wt %)	84	81.7	73.8
Fixed carbon (wt %)	5.4	7.9	7.1
Ash (wt %)	2	5.5	3.9
<i>Ultimate analysis</i>			
Carbon (wt %)	61.24	62.1	52.79
Hydrogen (wt %)	8.4	9.1	6.26
Nitrogen (wt %)	4.12	3.9	3.88
Oxygen (wt %)	25.5	24.9	37.01
Sulphur (wt %)	0.74	n/d	0.06
Empirical formula	CH _{1.64} N _{0.05} S _{0.004} O _{0.31}	CH _{1.76} N _{0.05} O _{0.30}	C _{23.47} H _{33.39} N _{1.48} S _{0.01} O _{12.34}
H/C molar ratio	1.64	1.76	1.42
O/C molar ratio	0.31	0.30	0.52
Calorific value (MJ/kg)	26.69	26.7	22.39

6.3.3 Characterization of Mahua bio-oil

The MPO is a dark brown organic oil comprising different molecular weight compounds in it. The important physical properties of this bio-oil in comparison with diesel are listed in Table 6.4. The distillation of the fuel indicates that the volume percentage evaporation with temperature is an important combustion characteristic of the engine. The variation of the distillation temperatures of diesel and the MPO are shown in Fig. 6.2. It was found that 10% and 50% of distillation was possible at 197 °C and 330 °C, respectively, while 90% distillation occurred at 420 °C. At 500 °C, a maximum of 99.58% bio-oil was evaporated and it was found Mahua bio-oil blends are suitable for diesel engines. The pH of Mahua bio-oil is low (4.8). The total acid number (TAN) is the amount of KOH required in mg to neutralize the acid present in 1 g of fuel sample. The TAN of bio-oil was 11.2 (mg of KOH/g) as per ASTM D 974. The heating value of MPO is 39.02MJ/kg, whereas the heating value of MPO10, MPO20, MPO30 and MPO40 blends are 43.6, 43.4, 43.2 and 43 MJ/kg, respectively. Fig. 6.3. depicts the variation of viscosity, flash and fire point temperatures for various blend proportions. The viscosity of blends increases with increase in the blend ratio. The viscosity is found to be the lowest for diesel 2.7 cSt, whereas these for the MPO10, MPO20, MPO30 and MPO40 blends are about 4.75, 6.79, 8.85 and 10.89 cSt respectively. The flash point temperature increases with increase in the blend ratio.

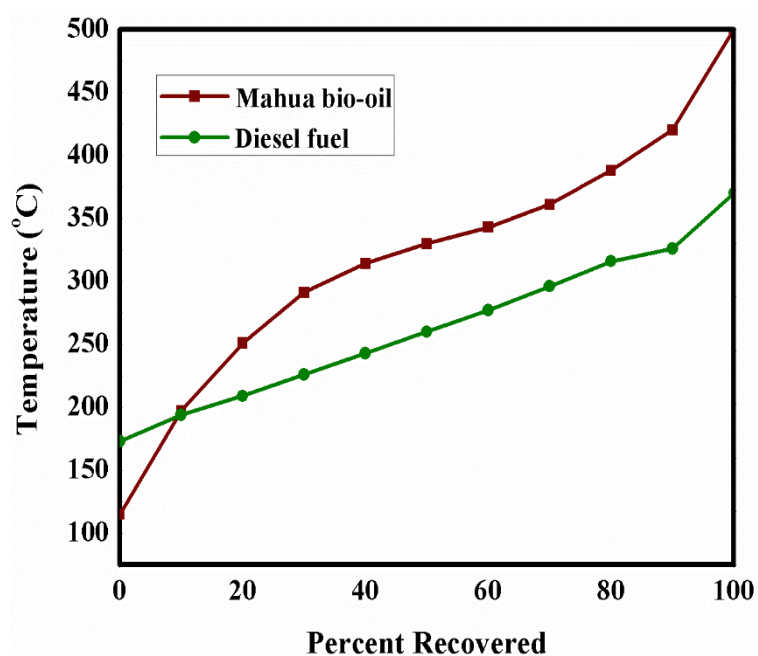


Fig. 6.2 Distillation curves of diesel and Mahua bio-oil

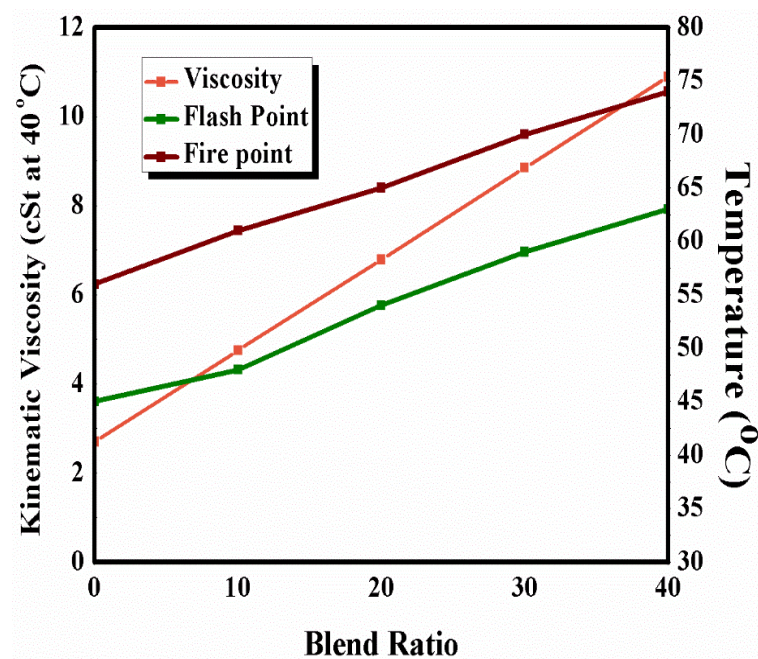


Fig. 6.3 Variation of viscosity, flash and fire point temperatures with MPO blend ratio

Table 6.4 Physical properties of MPO in comparison with diesel

Property	ASTM method	Diesel [19]	MPO
Density at 40 °C (kg/m ³)	ASTM D 1298	833	921.3
Kinematic Viscosity at 40 °C (cSt)	ASTM D 445	2.58	23.19
Calorific value (MJ/kg)	ASTM D 4809-95	43.8	39.02
Flash Point (°C)	ASTM D 3828	50	84
Fire point (°C)	ASTM D 92	56	118
Pour point (°C)	ASTM D 3828	-6	11
Cetane number	ASTM D 976	50	37.7

Table 4.4 in Chapter 4 shows the different functional group compounds of MPO obtained at 525 °C. It is clear from the table that significant amount of aliphatic compounds along with a few aromatic functional groups were observed. The GC-MS analysis provides the information regarding the diversity of components present in the bio-oil. The compounds which were identified in MPO instigated in consequence of the thermal cracking of cellulose, hemicellulose, and lignin in the biomass. MPO mostly contains aliphatic hydrocarbons (alkanes and alkenes) with carbon number C₈–C₁₉, which are summarized in Table 4.7 Chapter 4

6.4 Performance Parameters

6.4.1 Brake thermal efficiency (BTE)

The variation of brake thermal efficiency with brake power for diesel and different MPO-diesel blends is shown in Fig. 6.4. The BTE increases steadily with engine load for all the tested fuels. As the engine load increases, brake power and fuel flow rates increase. The rate at which brake power increases with the load is greater than the fuel flow rate. It can be observed that the brake thermal efficiencies are closer to each other except for the MPO40 blend. A maximum of 31.4% BTE is found for diesel at full load. For the MPO10, MPO20, MPO30 and MPO40 blends, it is 30.7%, 29.8%, 29.2% and 28.3% respectively, at full load. The rate of fuel consumption is higher for the blends, and it is found maximum for the MPO40 blend. The high viscosity and density of blends may cause higher fuel consumption. BTE is the ratio of brake power to the input energy of the fuel, which is the product of fuel flow rate and calorific value. The calorific value of the blends decreases with the percentage increase of bio-oil in the blend. High fuel flow rate is observed for

the blends compared to that of diesel operation from no load to full load. Hence, lower BTE of the engine is observed for the bio-oil blends than that of diesel.

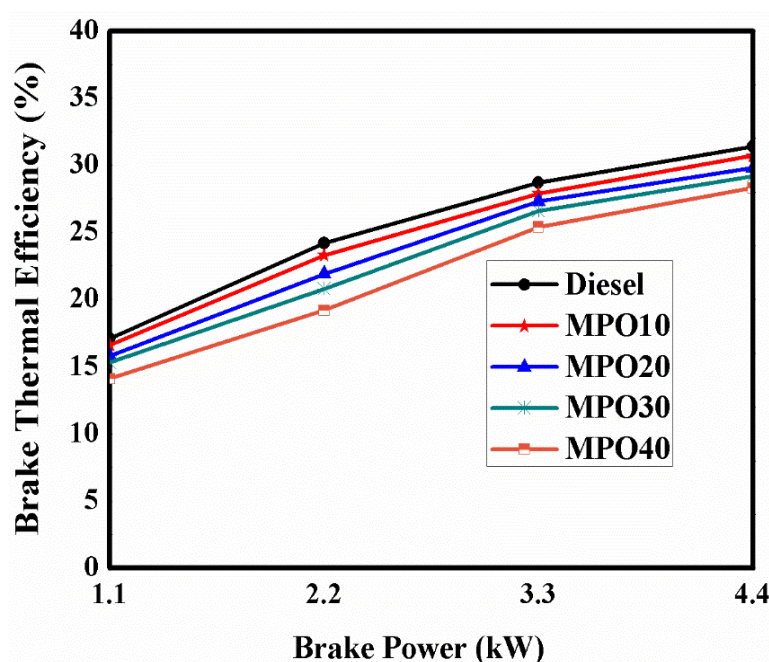


Fig. 6.4 Brake thermal efficiency with brake power for diesel and the MPO-diesel blends

6.4.2 Brake specific energy consumption (BSEC)

Fuels with different calorific value and density are not comparable with brake specific fuel consumption (BSFC). Hence, BSEC is used which is the product of BSFC and calorific value. Fig. 6.5. shows the variation of BSEC with brake power for various test fuels in this study. The BSEC was found to be 11.2 MJ/kWh for diesel at full load. For the MPO10, MPO20, MPO30 and MPO40 blends, it is 11.5, 12.2, 12.8 and 13.6 MJ/kWh, respectively. BSEC decreases with the increase in the brake power for all the test fuels as expected. The BSEC increases for the MPO-diesel blends compared to that of diesel for all loads due to the lower calorific value of the blends. For the same output power, the amount of fuel injection is more for the blends than for diesel, MPO40 shows the highest BSEC, which may be due to its lower calorific value.

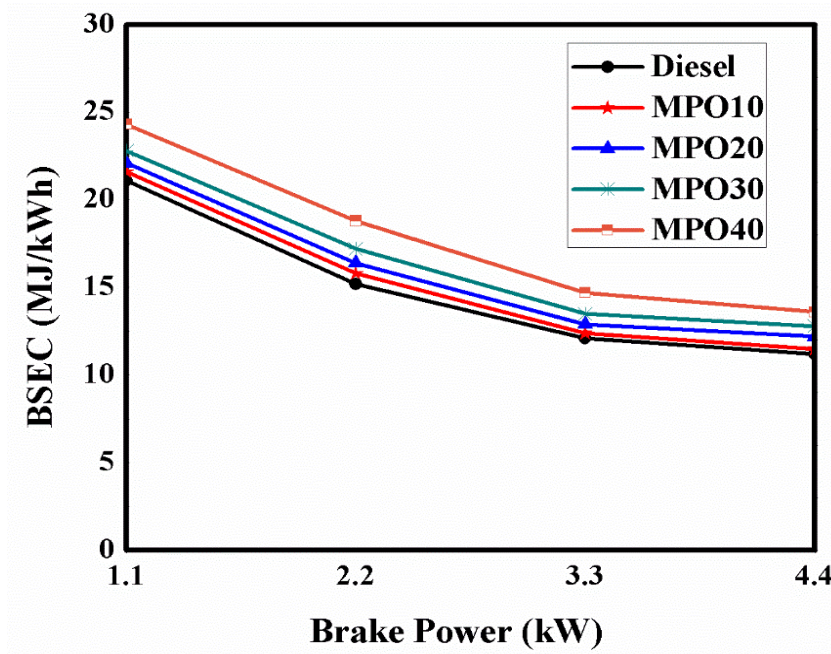


Fig. 6.5 Brake specific energy consumption with brake power for diesel and the MPO-diesel blends

6.5 Emission parameters

6.5.1 Carbon monoxide (CO) emission

Fig. 6.6 shows the variation of CO emission with brake power for diesel and the MPO blends. The intermediate product of combustion is CO, formed mainly due to the incomplete oxidation of the fuel during combustion. If the combustion is complete, then CO is converted to CO₂. In general, the CO emission is less in CI engines than in SI engines, which is due to the lean operation of air/fuel mixture in CI engines. A decreasing trend of the CO emissions in g/kWh with increasing brake power is observed for all the fuels tested in this investigation. The emission of CO is higher in the case of MPO-diesel blends compared to that of diesel operation at full load, which is due to poor mixing of fuel with air resulting in incomplete oxidation. The higher viscosity of the MPO-diesel blends might result in long spray penetration, large fuel droplets and poor atomization which results in higher CO emissions. The CO emission for diesel, MPO10, MPO20, MPO30 and MPO40 are 2.3, 2.4, 2.6, 2.9 and 3.4 g/kWh, respectively, at full load.

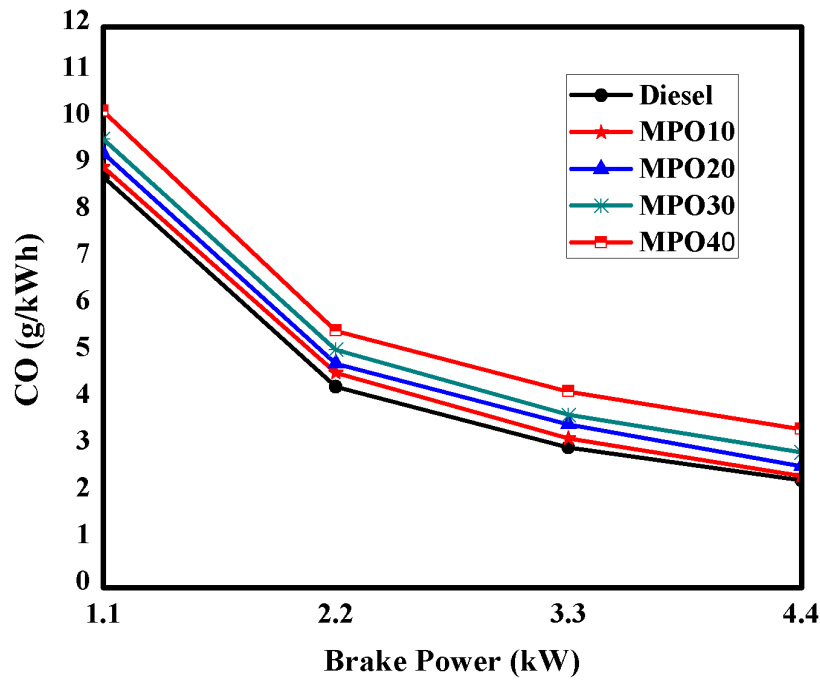


Fig. 6.6 Carbon monoxide emission with brake power for diesel and the MPO-diesel blends

6.5.2 Hydrocarbon (HC) emission

Incomplete combustion of the fuel results in hydrocarbon (HC) emission. In IC engine, the HC emissions are formed due to poor fuel volatility, improper atomization of the fuel, the high viscosity of the fuel and flame quenching at walls of the combustion chamber [196]. Fig. 6.7 shows the variation of HC emission with brake power for diesel and the MPO-diesel blends. In this study, the HC emission in g/kWh decreases with the increase in brake power for all the test fuels. The HC emission is higher for the MPO-diesel blends compared to that of diesel for all the engine operation. The increase in the bio-oil percentage results in a higher HC emission, which is due to incomplete combustion caused by poor atomization of the fuel. The HC emissions for diesel, MPO10, MPO20, MPO30 and MPO40 are 0.06, 0.07, 0.1, 0.13 and 0.17 g/kWh, respectively, at full load. A higher HC emission is noticed for the MPO-diesel blends than for diesel, which may be due to improper spray caused by higher viscosity, and the presence of unsaturated hydrocarbons in the Mahua oil, which are unbreakable during the combustion process [197].

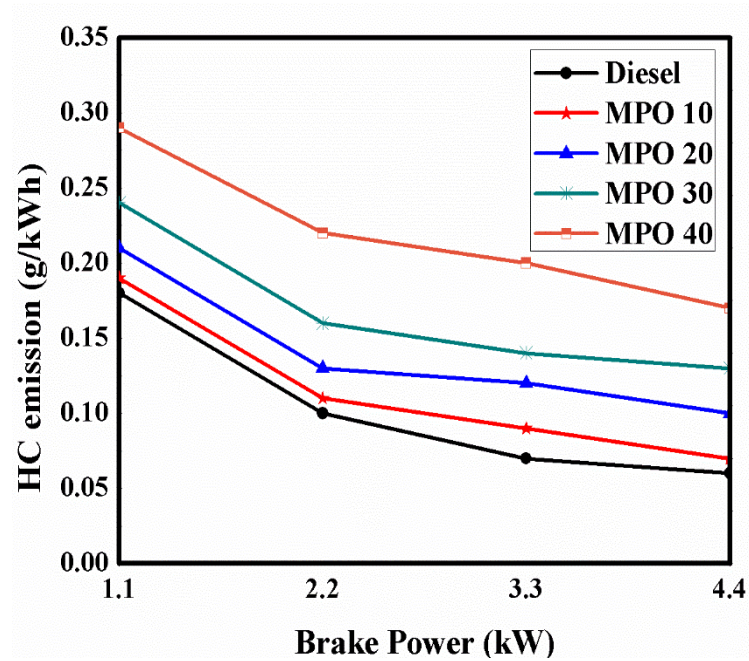


Fig. 6.7 HC emission with brake power for diesel and the MPO-diesel blends

6.5.3 Nitric oxide (NO) emission

The nitric oxide (NO) emission is a strong function of temperature, pressure and total oxygen concentration in the combustion chamber. The increase in the gas temperature with brake power results in higher NO emission for all the tested fuels. The variations of the NO emission with brake power for diesel and the MPO-diesel blends are shown in Fig. 6.8. The NO emission for diesel, MPO10, MPO20, MPO30 and MPO40 are 3.3, 3.2, 2.9, 2.8, and 2.4 g/kWh, respectively, at full load. The lower values of the NO emission for the bio-oil blends than those of diesel may be due to the lower heat release rate (HRR). The larger ignition delay causes the hot gases from combustion have a larger exchange surface with the cylinder and thus a lower temperature [198]. As mentioned previously that bio-oil contains, high moisture content which may reduce the cylinder gas temperature [8].

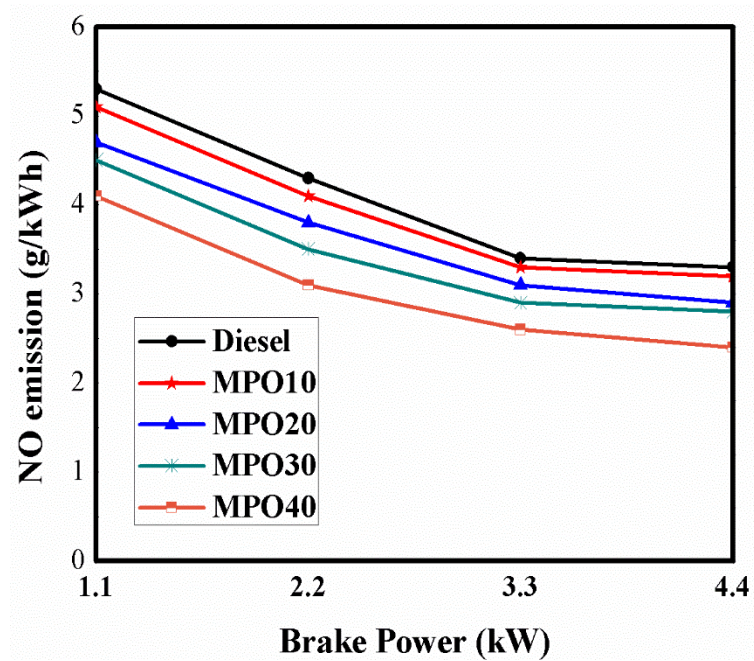


Fig. 6.8 Nitric oxide emission with brake power for diesel and the MPO-diesel blends

6.5.4 Smoke opacity

Smoke opacity is a strong function of oxygen availability in the cylinder and the amount of oxygen in the fuel. Smoke emission is formed mainly during the diffusion phase, at high load the combustion process is almost diffusive. Fig. 6.9 portrays the variation of smoke emission with brake power for the tested fuels in this study. Smoke is formed in the fuel rich regions of the combustion chamber [199]. The lower air fuel ratio, which is caused by the high fuel injection, results in a higher smoke emission. The fuel consumption also affects the smoke emission. The smoke values for diesel, MPO10, MPO20, MPO30 and MPO40 are 81%, 80%, 78%, 75% and 77%, respectively, at full load. The lower smoke opacity for the MPO-diesel blends than that of diesel may be due to the presence of oxygen in the fuel, which promotes smoke oxidation. The decrease in the smoke emission from the engine run on the blends is comparatively small due to the presence of aromatic compounds in the Mahua bio-oil. An increase in the BSEC for M40 results in a marginal increase in the smoke emission in the entire engine operation.

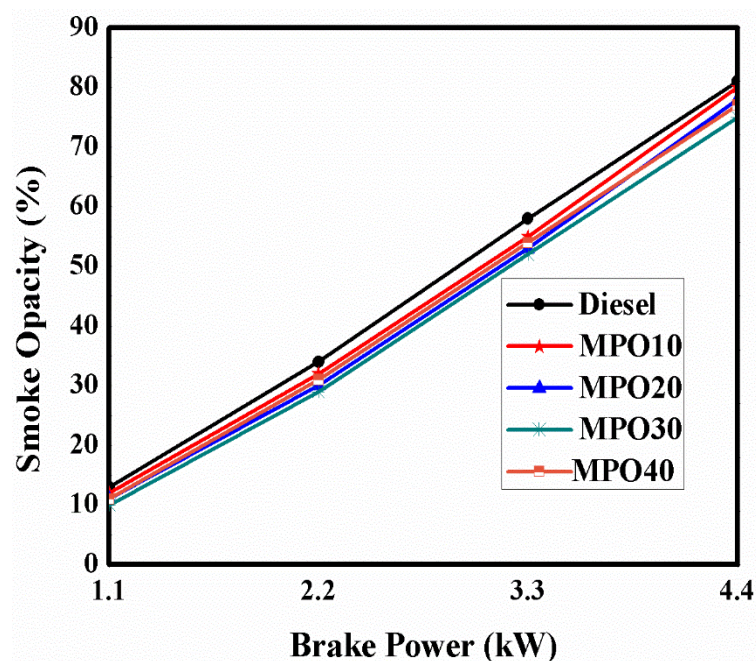


Fig. 6.9 Smoke opacity with brake power for diesel and the MPO-diesel blends

6.4 Conclusions

The performance, and emission characteristics of a DI diesel engine fuelled with the MPO-diesel blends were experimentally investigated. The pyrolysis experiments were carried out in between 450–600 °C with a heating rate of 20 °C/min. The optimum bio-oil yield of 48.65% was obtained at 525 °C. The GC-MS analysis of MPO shows a straight carbon number from C₈–C₁₉. The high viscous and low cetane MPO is not suitable for direct utilization in a diesel engine, but it can be used only in the blended form with diesel, without any engine modification. The HC and CO emissions were higher for the MPO-diesel blends than for diesel. The thermal efficiency was dropped by about 2% for MPO-diesel operation from no load to full load operation in comparison to diesel. The lower NO emission was found to be about 27% for MPO40, in comparison with diesel at full load. A marginal decrease in the smoke opacity (7.4%) was found for MPO30 in comparison with diesel at full load. From this study, it is recommended that up to 30% bio-oil blend can be used in the diesel engine for better performance.

Chapter 7

Application of co-pyrolysis oil in a diesel engine

7.1 Introduction

Energy is the vital source for human beings, and is highly used in the transportation sector. The huge consumption of energy in transportation sector greatly affects the world economy. On the other hand, fossil fuel resources are depleting, which is directly related to transportation sector. Recent technology pose a challenge to use new sustainable energy for the growth of world economy, as well as it can be able to play the role of conventional resources in the transportation sector. Biomass has been considered as one of the potential energy resources. However, biomass is the 4th largest energy resource and largely available throughout the world [200,201]. Various energy conversion processes are available to produce sufficient amount of energy from biomass. However at present thermochemical process, pyrolysis has been found more attractive to the researchers for the production of biofuel from biomass.

The pyrolysis process can convert the biomass into various forms of fuels such as liquid, solid and gaseous fuel. The product has a potentiality to use as a fuel either directly or after upgradation for various purposes, for transportation and power generation. The liquid fuel from pyrolysis of biomass is encouraging to use in both internal and external combustion engines, especially in internal (IC) engines [202]. There have been several literature works on the use of biomass pyrolysis oil in IC engine. Beld et al. studied the pyrolysis oil or pyrolysis derived fuels in diesel engine for development of combined heat and power (CHP) application. The authors have reported that the CO emission increased, and there was decrease in NO_x emission. Low peak temperatures were observed upon low heating value and high water content of pyrolysis oil [203]. Yang et al. studied the pyrolysis oil obtained from coffee bean residue and performed the engine test. The authors reported that coffee bean residue pyrolysis oil (CPO) CPO 5 and CPO 10 has showed the better performance than that of individual CPO 0 [124]. Pyrolysis oil produced from Japanese cedar has been used in diesel engine by blending the raw bio-oil with biodiesel fuel in 10%, 30%, and 50% volumetric ratios and resulted in the longer ignition delay when increasing the blend ratio due to the presence of high water content. The authors also reported that higher smoke, CO, THC emissions were observed due to the higher kinematic viscosity. They stated that the engine run on blend comparing 30% oil blend showed compatible operation with Japanese cedar pyrolysis oil [204]. Hossain et al. have studied the emission, performance and combustion

characteristics of de-inking sludge pyrolysis oil blended with biodiesel in an IC engine. From the results they have concluded that 20% blend gave a stable engine performance without addition of any ignition additives or surfactants [205]. The use of bio-oil in IC engine is not encouraged because of its acidic nature, low heating value and poor ignition properties. Hence, it is better to upgrade pyrolysis to a certain extent to simplify its use in engine. However, previously it was noted that due to the poor ignition characteristics, highly oxygenated compounds, high water content and low calorific value of pyrolysis bio-oil in an IC engine exhibited poor performance. Henceforth, there have been a few research works focused on upgradation of bio-oil by adding some additives and blending it with biodiesel to improve the characteristics of bio-oil [126,184,195,203,206]. Relatively, some research work has been focused to study the effect of adding plastic with biomass in pyrolysis to improve the quality of bio-oil. However, the obtained upgraded bio-oil has not been used for engine performance studies. Therefore, the aim of the present work is to use the upgraded pyrolysis oil as an alternative fuel in IC engine. Upgradation of pyrolysis oil by using co-pyrolysis technique, can enhance the stability of pyrolysis oil as a fuel since plastics can provide hydrogen that the biomass lacks. Plastics have higher hydrogen fraction than biomass and its pyrolysis produces liquid with no water content [77]. Recent investigations have shown that biomass and plastic co-pyrolysis achieved a synergistic effect with increment in liquid yield products and improvement in the overall process efficiency [15]. Kar et al., studied co-pyrolysis of walnut shell and tar sand in a fixed-bed reactor under specific operating conditions. The maximum bio-oil yield of 31.84 wt % was obtained from co-pyrolysis of walnut shell and tar sand which was 7.88 wt% compared to that of bio-oil yield from the pyrolysis of walnut shell alone. The physical and chemical properties of the co-pyrolysis oil were found to be different from the bio-oil obtained from walnut shell, the difference in physical and chemical properties may be due to the formation of some synergistic interactions during pyrolysis [207]. Rutkowski et al., observed the positive effect on co-pyrolysis product yield of polystyrene/cellulose mixture. The authors also stated that the influence of polystyrene during co-pyrolysis dominated the oxygen containing compounds and the addition of polystyrene to cellulose essentially changes the chemical structure of co-pyrolysis liquid product [82]. Co-pyrolysis of PS with synthetic polymer HDPE was proposed by Onal and his co-workers. The maximum yield of 56% pyrolysis oil was obtained at 500 °C. The oil obtained from co-pyrolysis produced higher amount of 2-alkenes, 1-alkenes and alkadienes, where the carbonyl, hydroxyl and aromatics compounds were dominated, however, these compounds were present in individual PS pyrolysis oil. The obtained pyrolysis oil from co-pyrolysis was found to be better in quality compared to that of the oil obtained from the individual biomass alone [87].

This research study was aimed to explore the possibility of using co-pyrolysis oil (CPO) in diesel engine. The bio-oil obtained from co-pyrolysis of Mahua seed and Polystyrene was blended with diesel at six different percentages from 10-60% on a volume basis in steps of 10% in the blend and used as fuels in a single cylinder, four stroke, and air cooled direct injection (DI) diesel engine. The blends were denoted as co-pyrolysis oil diesel blends (CPOD) of CPOD 10, CPOD 20, CPOD 30, CPOD 40, CPOD 50 and CPOD 60, where the numeric value indicates the percentage of CPOD in the blend. The performance and emission parameters of the engine run on the CPOD blends were evaluated, compared with those of diesel fuel operation and presented.

7.2 Materials and methods

7.2.1 Characterization of raw materials

The detailed materials and methods are explained in Chapter 3.

7.2.2 Co-pyrolysis oil production

The schematic diagram of the pyrolysis setup is shown in Fig.3.5. The specification and procedure detail explained in Chapter 3 section 3.3.3.2 Thermal co-pyrolysis of Mahua seed:Polystyrene blend.

7.2.3 Characterization of co-pyrolysis oil

The various physical and chemical characterization of the co-pyrolysis oil has been explained detailed in Chapter 3 section 3.4 Characterization of pyrolytic oil.

7.2.4 Engine experimental setup

The engine experimental setup and the specification details are explained in Chapter 6 in section 6.2. Materials and Methods.

7.3 Results and Discussion

7.3.1 Co-pyrolysis of Mahua seed:Polystyrene 1:1

7.3.1.1. Characterization of MSPS

The discussion about proximate and ultimate analysis of the feedstocks MSPS 1:1 blend and MS has previously explained in chapter 4 Section 4.3 Analysis of feedstock.

7.3.1.2 Co-pyrolysis of MSPS

Fig. 4.6 shows the MS:PS 1:1 blend pyrolysis yield with the various temperature ranges of 450-600 °C with a heating rate of 20 °C/min. The maximum of 74.25% of oil was obtained at 525 °C, which is attributed to the fact that polyolefin materials like PS plastic are a good hydrogen sources, which support to enhance the liquid yield, while co-processing with biomass. Biomass and plastic may have different decomposition mechanisms in the thermal pyrolysis process.

However, pyrolysis of biomass involves a series of exothermic and endothermic reactions, whereas the pyrolysis of plastic alone occurs by radical mechanisms initiation, Propagation, and termination [29]. Hence, the co-pyrolysis yielded more oil than pyrolysis of biomass alone, which also resulted in a decrease of char product. The reason for decreasing of char yield is due to the presence of hydrogen in plastic which partly inhibited the condensation reactions. Here we can also observe that the degree of polymerization has a strong influence on the thermal degradation of biomass [19].

7.3.2 Characterization of CPO

7.3.2.1 Physical characterization of CPO

Table 7.1 gives comparison of the physical properties of CPO and CPOD blend and diesel. The appearance of the CPO is dark brown in color with no phase separation. It is one of the important parameters to measure the volumetric output of pumps and injector needed to supply a given rate of delivered energy, because the heat of combustion is determined on a weight basic [35]. Density of the fuel is directly related to the engine performance since the injection system works principally on volume basis. As the density of the CPO is higher than that of diesel fuel therefore with the increase in the CPO percentage in diesel the density of blend increases. Flash point and fire point measure the volatility of the fuel [209]. In this study, the obtained flash point and fire point of CPO are marginally higher than those of diesel and CPOD blends which will not affect the characteristic of engine performances. Viscosity is also the parameter upon which the oil can be graded, lower the viscosity of the oil, the easier it is to pump and to atomize. The estimated kinematic viscosity of CPO is lower than that of the diesel, whereas with increase in the CPO percentage in diesel the viscosity of the CPOD blends also decreases as compared to diesel. The decrease in viscosity of the fuel will give better atomization during the engine performance [210]. Heating value of the CPO is 42.3 MJ/Kg, which is in the range of gasoline and diesel, therefore this fuel can give better performance when used in diesel engine [209]. High value of the carbon residue correlates with fuel injection nozzle clogging and combustion chamber deposits, which can affect the fuel injection and overall engine performance. However, the obtained carbon residue of CPO and its different blends are within the permissible limit of 0.35% [211,212] thus suitable for an engine performance test.

The cetane number is one of the most significant properties to specify the ignition quality of any fuel for IC engine. It measures the readiness of the fuel to auto ignite when injected into the engine. Higher cetane number can decrease the delay between injection and ignition. The cetane number of CPO is quite fair and useful for fuel application in IC engine [210]. The obtained

distillation range for CPO is in the range of gasoline, diesel. From the above results, it can be noted that these could be possible feedstock for further upgrading or use of lighter compounds as a diesel.[199].

Table 7.1 Physical properties of CPO

Property	ASTM method	Diesel	CPO	CPOD10	CPOD 20	CPOD30	CPOD40	CPOD50	CPOD60
Density (gm/ml)	ASTM D 1298	0.83	0.908	0.837	0.844	0.851	0.858	0.865	0.872
Kinematic viscosity at 40 °C Cst	ASTM D 445	2.58	1.943	2.516	2.45	2.38	2.324	2.26	2.19
Gross calorific value (MJ/kg)	ASTM D 4809-95	43.8	42.3	43.65	43.5	43.35	43.2	43.05	42.9
Flash Point (°C)	ASTM D 3828	50	58	56	55	53	51	50	48
Fire point (°C)	ASTM D 92	56	60	58	57	56	53	51	50
Carbon residue (%)	ASTM 4530	0.03	0.813	0.108	0.183	0.213	0.374	0.434	0.487
Cetane number	ASTM D 976	50	44	—	—	—	—	—	—
Distillation (°C)	ASTM D86								
Initial boiling point		173 °C	50 °C	—	—	—	—	—	—
Final Boiling point		370 °C	390 °C	—	—	—	—	—	—
C	(%)	86.5	74.07	—	—	—	—	—	—
H	(%)	13.2	12.24	—	—	—	—	—	—
N	(%)	Nil	0.72	—	—	—	—	—	—
S	(%)	0.3	0.18	—	—	—	—	—	—
O	(%) by difference	Nil	12.79	—	—	—	—	—	—

7.3.3 Chemical characterization of CPO

Chemical characterization such as FTIR and GCMS analysis are explained in chapter 4, section 4.5.3.

7.4 Performance parameter

7.4.1 Brake thermal efficiency

Brake thermal efficiency of a diesel engine is the efficiency in which the chemical energy of a fuel is turned into useful work. It can be determined by dividing the useful work by lower heating value of fuel [213]. Fig. 7.1 shows the variation of brake thermal efficiency with respect to load for diesel fuel and CPOD blends. It can be observed from the Fig that BTE increases with increase in load but decreases with increasing ratio of CPO in blends. The maximum brake thermal efficiency for diesel fuel at full load is 31.4%, which is higher than that of other tested fuels. In this study for CPOD 10%, CPOD 20%, CPOD 30%, CPOD 40%, CPOD 50% and CPOD 60%, the obtained thermal efficiency is found to be about 30.9%,30.2%, 29.65%,29% , 28.68% and 27.04%, respectively, at full load conditions. BTE is higher with increase in load due to the better combustion. The fuel consumption rate is higher for the blends and it is relatively higher for CPO-diesel 60% blend. Higher heat losses are observed for the blends compared to that of diesel. Thus, the BTE of CPO-diesel oil blends is lower than that of diesel fuel. This is also in a good agreement with the previous literature [197,214].

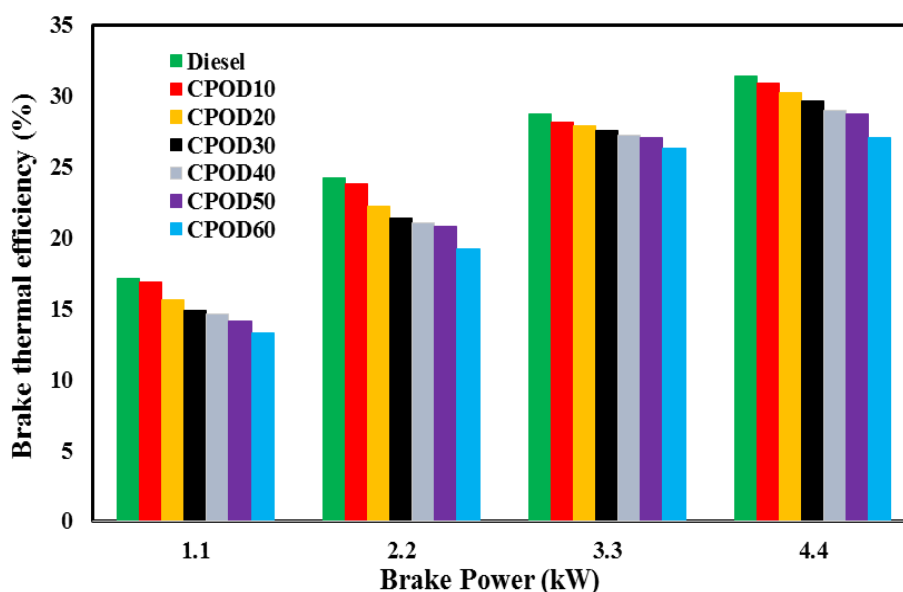


Fig. 7.1 Brake thermal efficiency with brake power for diesel and the CPO-diesel

7.4.2 Brake specific energy consumption

The brake specific energy consumption (BSEC) is a more reliable parameters, as compared to the brake specific fuel consumption. As BSEC is the product of BSFC and calorific value. So the fuels having same BSFC, will have different BSEC depending on their calorific value. The variation of BSEC with load for all the tested fuels is presented in the Fig. 7.2 The BSEC decreases sharply with increase in load for all the blends. Moreover, the BSEC was found to be 11.2 MJ/kWh for diesel at full load, but its values for CPOD 10%, CPOD 20%, CPOD 30%, CPOD 40%, CPOD 50% and CPOD 60%blends are 11.3, 11.69, 12.21, 12.78, 13.2 and 13.79 MJ/kWh, respectively. The main reason for lower BSEC for all the tested fuel at full load is due the percentage increase in the fuel required to operate the engine is less than the percent increase in brake power [190]. However, the BSEC for all the CPOD blends is higher than that of diesel fuel, the reason is that , the engine consumes more fuel with the CPO-diesel blends than that of diesel to develop the same power output and these fuels having lower calorific value as compared to the diesel [197].

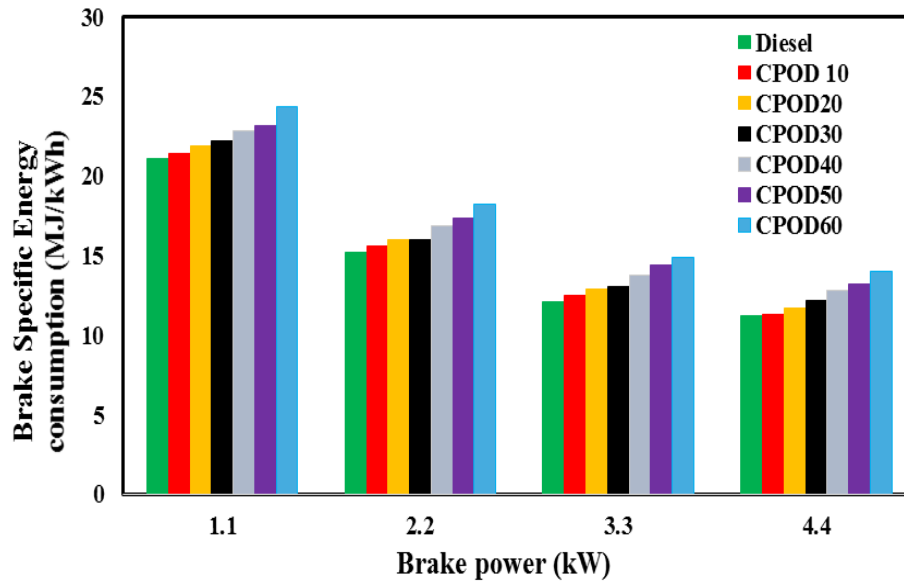


Fig. 7.2 Brake specific energy consumption with brake power for diesel and the CPO-diesel blends

7.5 Emission parameters

7.5.1 Carbon monoxide (CO) emission

CO emission is mainly formed due to insufficient oxygen, poor air entrainment mixture preparation and incomplete combustion during the combustion process. CO emission is toxic and it should be controlled. Fig. 7. shows the variation of CO emission with brake power for different test fuels. It can be observed from the Fig that CO emission increases with the increasing ratio of CPO in blends, at the same time it decreases with increasing load due to poor mixing and incomplete combustion. However, on the other hand, CO emission for CPO-diesel blend is higher than that of diesel, this may be due to the chemical composition of the CPO. The CO emission for diesel, CPO-diesel 10%, CPO-diesel 20%, CPO-diesel 30%, CPO-diesel 40%, CPO-diesel 50% and CPO-diesel 60% are 2.3%, 2.6%, 2.8%, 2.9%, 3%, 3.1% and 3.4%, respectively at full load.

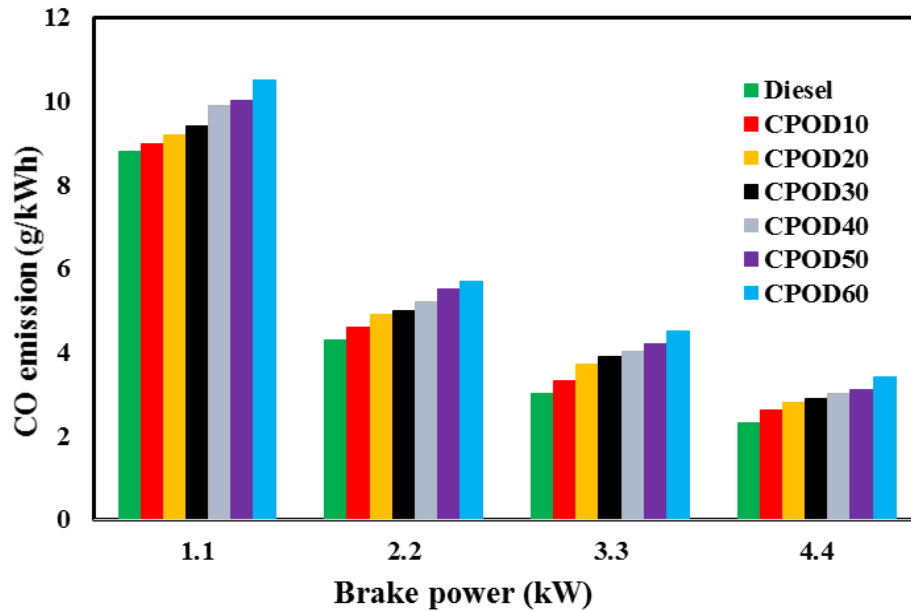


Fig. 7.3 Carbon monoxide emission with brake power for diesel and the CPO-diesel blends

7.5.2 Hydrocarbon (HC) emission

Hydrocarbon emission is basically formed due to incomplete combustion of the fuel, and it is one of the useful parameters to measure the combustion efficiency. Fig. 7. shows the variation of HC emission with brake power for diesel and the CPOD blends. It is apparent from the figure that the HC emission is higher for the CPOD blends compared to that of diesel at full load. A higher HC emission is noticed for the CPOD blends than for diesel, which may be due to the presence of unsaturated hydrocarbons in the CPO, which are unbreakable during the combustion process. The presence of more aromatic compounds is one of the reasons for the formation of higher emissions, incomplete combustion and poor atomization [206,208]. However, HC emission decreases with increasing load, but increases with increasing ratio of CPO in blends. The HC emission varies from 0.31 g/kWh at low load to 0.17 g/kWh at full load for CPOD 60% blend fuel

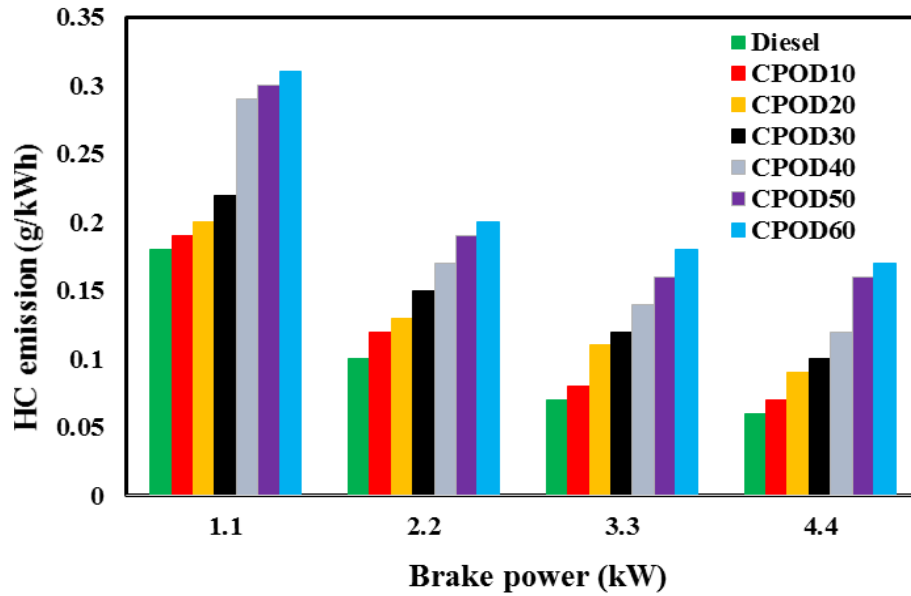


Fig. 7.4 HC emission with brake power for diesel and the CPO-diesel blends

7.5.3 Nitric oxide (NO) emission

The variations of the NO emission with brake power for diesel and the MSPS-diesel blends are shown in 7.5. In this study, the NO emission for diesel, CPOD 10%, CPOD 20%, CPOD 30%, CPOD 40%, CPOD 50% and CPOD 60% are 3.3, 3 2.8, 2.6, 2.3, 2, and 1.7 g/kWh respectively, at full load. The NO emission for the CPOD blends is lower than that of diesel. This may be due to the lower heat release rates than that of diesel [206]. Moreover, NO emission decreases with increasing ratio of CPO in the blend and at the same time it also decreases with load. A mixture of fuel and air reduced NO_x emissions. On the other hand, in-cylinder temperature is closely related to the formation of NO_x. Lower combustion temperature is one of the possible reasons for decreasing the NO_x emission [124].

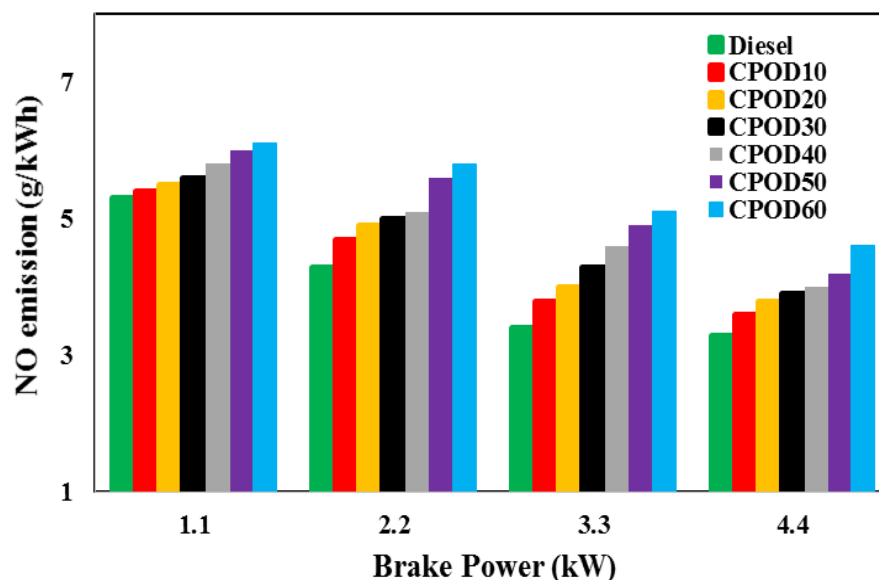


Fig 7.5 Nitric oxide emission with brake power for diesel and the CPO-diesel

7.5.4 Smoke opacity

Fig 7.6 represents the variation of smoke emission with brake power for the tested fuels in this study. Smoke emission is formed in the fuel rich regions of the combustion chamber[206]. The lower air to fuel ratio, which is caused by the high fuel injection, results in a higher smoke emission. The fuel consumption also affects the smoke emission. The smoke values for diesel, CPOD 10%, CPOD 20%, CPOD 30%, CPOD 40%, CPOD 50% and CPOD 60% are 81, 86, 90, 92, 94, 96 and 98% respectively, at full load. The higher smoke opacity for the CPOD blends than that of diesel occurs with the increase in the brake power. This may be due to air to fuel ratio which decreases as the fuel injected increases, and hence results in higher smoke. The presence of aromatic content in CPO is also one of the reasons for higher smoke.

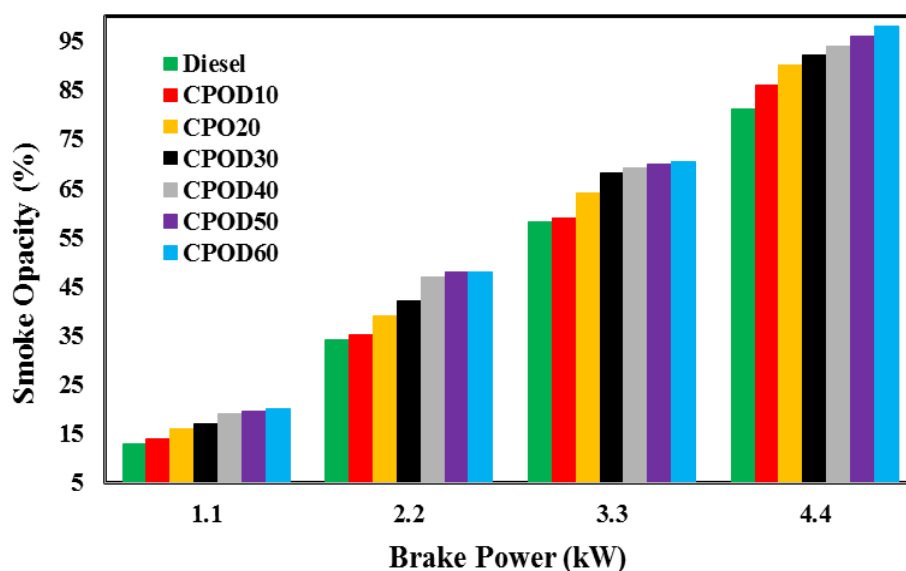


Fig 7.6 Smoke opacity with brake power for diesel and the CPO-diesel blends

7.6 Conclusions

The pyrolysis experiments were carried out the range of 450–600 °C with a heating rate of 20 °C/min. The optimum bio-oil yield of 74.25% was obtained at 525 °C. FTIR analysis shows the presence of higher aromatic compounds along with few aliphatic and oxygenated compounds, which present in CPO. The GC-MS analysis of CPO shows a straight carbon number from C₇–C₂₃. Further, the performance, and emission characteristics of a DI diesel engine fuelled with the CPO-diesel blends were experimentally investigated. The performance and emission studies concluded that high fuel flow rate and higher heat losses were observed for the CPO-diesel blends compared to those of diesel from no load to full load. Thus, the BTE of CPO-diesel blends is lower than that of diesel fuel from no load to full load. Due to the reduction of combustion rate, the CO emission increases with the addition of diesel to CPO. HC emission is higher for the CPOD blends compared to that of diesel. A higher HC emission is obtained for CPOD blends than that for diesel which may be due to the presence of unsaturated hydrocarbons in the CPO, which are unbreakable during combustion. The NO emission for the CPOD blends is lower than that of diesel due to the lower combustion temperature. The higher smoke opacity for the CPOD blends than that of diesel occurs with increase in the brake power. This is due to air to fuel ratio which decreases as the fuel injected increases, and hence it results in higher smoke. It is concluded that the CPO with diesel blend can be used as an alternative source in diesel engines.

Chapter 8

Conclusion and future scope

8.1 Conclusion

In this work, the main outcome is the development of upgradation process for bio-oil. We considered that co-pyrolysis is one of the upgradation processes to improve the bio-oil characteristics and properties. According to our first objective, the product obtained from Mahua seeds has been characterized. From the results the main conclusions are as follows: The maximum of 49% of bio-oil yield was obtained at an optimum temperature of 525 °C and 20 °C/min heating rate with the gas flow rate of 30 mL/min. Furthermore, the bio-oil and bio-char obtained at 525 °C are characterized as per their physical and chemical properties studies. Viscosity, flash point, pour point and the pH value are more. The obtained bio-oil could be used as an alternative fuel directly or mixed with other conventional fuels. Higher oxygen content and the acidic nature in bio-oil is disadvantageous in obtaining high quality bio-oil production. The inferior property and complex composition can be improved by further upgradation or refining. An important advantage of the bio-oil in application as a fuel is that it contains less amount of sulfur and therefore, emits almost no sulfur oxides into the atmosphere. From the chemical analysis studies like FTIR, GC-MS and ¹HNMR studies it can be concluded that, the most of the functional groups present in the bio-oil are oxygenated compounds. From the GC-MS analysis, it is concluded that the major chemical compounds present in Mahua bio-oil are tetradecanoic acid, hexadecanoic acid, octadecenoic acid etc which had combined relative composition of 37.36%. Out of these, hexadecanoic acid is used to produce soap/cosmetics agents and as a non-drying oil for surface coating. The IUPAC name of stearic acid is known as n-Octadecenoic acid, which is mainly used as emulsifying agent and solubilizing agent in aerosol products. But the purification of these fatty acids is limiting the application in laundry soaps or detergents. On the other hand, it has been considered that the presence of acid is an important issue for subsequent bio-oil treatment, since it is responsible for corrosion of the manifolds and potential chemical instability of bio-oil during the storage conditions. However, this problem has been reduced by the upgradation process. Most of the compounds present in Mahua bio-oil are aliphatic and oxygenated compounds. The Mahua bio-oil ascertained could be ranked as carbon chain range of C₇-C₂₇. The empirical formula of bio-oil was CH_{1.58}N_{0.03}S_{0.005}O_{0.19} and H/C ratio of bio-oil is 1.58, which lies between light and heavy petroleum products. Moreover, to improve the quality of bio-oil was our second objective of this study, where we used the upgradation process like co-pyrolysis of Mahua seed and polystyrene

which was studied with various ratios and various temperatures. The result of the co-pyrolysis study concluded that the addition of plastic with pyrolysis of biomass successfully improved the quantity and quality of pyrolysis oil. From the co-pyrolysis of Mahua seed and Polystyrene the maximum bio-oil yield of 74.25% was obtained at 525 °C with 1:1 blend. Also, it can be proposed that the addition of PS with MS had shown significant influence on enhancing the oil yield and decreasing the aqueous phase yield, and ratio of the feed was also a significant variable affecting liquid yield production. Elemental analysis study concluded that after applying the co-pyrolysis process, hydrogen and carbon content of oil increased to enhance the H and C content of biomass pyrolysis oil. The reason for the increment of H and C content of co-pyrolysis oil is due to the origin of plastic. The amount of nitrogen and sulphur content in the co-pyrolysis oil also decreased. Furthermore, the oxygen percentage was clearly decreased in the oil whereas the calorific value of oil is increased. By mixing of Polystyrene with Mahua seed 1:1 blend provided the suitable results. Therefore, further 1:1 blend co-pyrolysis has been characterized for its physical and chemical properties. Physical and chemical analysis studies concluded that the oil obtained from co-pyrolysis was improved in quality. Addition of plastic in biomass improved and lowered the acidic nature as the pH of plastic oil is neutral. From the study, it was concluded that influence of plastic in biomass pyrolysis provides effective results and improves the quality of bio-oil as compared to the individual biomass pyrolysis oil. FTIR analysis of co-pyrolysis oil concluded that there is a significant decrease of phenolic, acidic compounds, however most of the functional groups present in co-pyrolysis oil are aromatic compounds. The FTIR spectrum of the oil obtained from the co-pyrolysis closely resembled to that of PS pyrolysis oil rather than that of MS pyrolysis oil. From the GC-MS analysis studies it is concluded that most of the compounds present in MSPS pyrolysis oil is similar to that of PS pyrolysis oil. The aliphatic compound in co-pyrolysis are reduced as compared to the Mahua pyrolysis oil. The MSPS pyrolysis oil ascertained could be ranked as carbon chain range of C₆–C₁₈.

The result of the bio-char characterization studies concluded that the obtained calorific value of MSPS bio-char is more than that of MS bio-char, however both are more than that of Indian standard coal. The pH of MS and MSPS bio-char were 11.9 and 12.5 respectively which is probably good for acidic soils. From the SEM images of MS and MSPS bio-chars we can conclude that MSPS biochar is more porous than MS biochar. The obtained surface area of MSPS is more than that of MS bio-char. The bio-char could be used for the production of activated carbon after chemical and physical activation.

In addition from the result of the kinetic study we concluded that the co-pyrolysis characteristics of the blends are quite different to the combination of the individual materials, there exist

interaction and significant synergistic effects between plastic and biomass co-pyrolysis. The values of E_A and A are higher for mixtures than for individual components in Kissinger method, whereas the activation energy and pre-exponential factors obtained for FWO and KAS methods were lower than those of individual one. However, quantitatively, they do not vary significantly. Kinetic parameters obtained from three different methods are in good agreement, but KAS and FWO methods are more efficient in the description of the degradation mechanism of solid-state reactions.

The result of the engine performance test of Mahua bio-oil with diesel blend study concluded that the thermal efficiency was dropped by about 2% for MPO-diesel operation from no load to full load in comparison to diesel. The lower NO emission was found to be about 27% for MPO40, in comparison with diesel at full load. A marginal decrease in the smoke opacity (7.4%) was found for MPO30 in comparison with diesel at full load. From this study, it is recommended that up to 30% bio-oil blend can be used in the diesel engine for better performance.

Furthermore, the co-pyrolysis oil with diesel blend was also studied for engine performance test and it was concluded that BTE of CPOD blends is lower than that of diesel fuel from no load to full load. HC emission is higher for the CPOD blends compared to that of diesel. Whereas the NO emission for the CPOD blends is lower than that of diesel. It can also be concluded that CPO with diesel blend can be used as alternative sources in diesel engine.

In summary, the co-pyrolysis oil obtained from biomass and plastic can also be useful for various industrial and chemical applications and it can also be a good substitute for alternative fuel. The advantages of this process are less consumption of fossil fuels, solving some environmental issues, enhancing energy security and improving waste management systems. Apart from this, co-pyrolysis process also provides simplicity in design and feasibility with respect to economical point of view. Co-pyrolysis process can be done with low cost and no special equipment needed to be designed and constructed for this process. Some minor modification may be required for feed preparation system. Moreover, this process also benefits to enhance the calorific value of byproducts. One of the optional solutions to increase the energy security of the nation and reduce dependence on fossil fuel. From the above, it was observed that both bio-oil and bio-char obtained from co-pyrolysis have improved their quality. Consequently, this can be best upgradation process to improve the biofuel quality.

8.2 Future Scope

Based on the above results of the study, it can be concluded that the upgradation process like co-pyrolysis is one of the most suitable processes to obtain high grade fuel. Further studies are required to modify the process. The following are the recommendations for the future work:

- Other different types of plastic can also be used in co-pyrolysis process to improve the quality of bio-oil.
- Some modification of the pyrolysis system, design of reactor, and different types of reactor, will also be useful if the parameters of the pyrolysis system such as heating rate, temperature, and inert gas flow rate can be changed.
- The formation of non-condensable gases in this study is not used, so we recommended that it will be better to use some storage condition to store the gases for further analysis.
- There is a need to search for suitable catalysts, which can enhance the properties of the liquid fuel and produce more conversion.
- Optimization process application study can be done in future, especially RSM can be used in optimizing the pyrolysis process variables for several purposes. For example, for better understanding of co-pyrolysis yield from the relationship of the parameters.
- To further enhance the adsorption capacity of the bio-char, various activation processes such as steam activation and physical and chemical activation can be found to accelerate its positive effect on nutrient retention and uptake by plant relative to non-activated bio-char.
- Different kinetic models can also be used for better understanding of the kinetic mechanism of the biomass and plastic during co-pyrolysis.
- Modification of distillation process and IC engine setup are also required for direct use of liquid fuel obtained from pyrolysis in IC engine without blending with diesel.

References

- [1] Soetaert W, Vandamme EJ. Biofuels in perspective. *Biofuels* 2009;1–8.
- [2] Omer AM. Bioenergy for Energy or Materials: Future Perspective through Development of Management. *Glob J Technol Optim* 2014;5:2–16.
- [3] Babu B V. Biomass pyrolysis: a state-of-the-art review. *Biofuels, Bioprod Biorefining* 2008;2:393–414.
- [4] Demirbas A, Arin G. An Overview of biomass pyrolysis. *Energy Sources* 2002;24:471–482.
- [5] Isahak Wnrw, Hisham Mwm, Yarmo Ma, Yun Hin T. A review on bio-oil production from biomass by using pyrolysis method. *Renew Sustain Energy Rev* 2012;16:5910–5923.
- [6] Manzano-Agugliaro F, Alcayde A, Montoya FG, Zapata-Sierra A, Gil C. Scientific production of renewable energies worldwide: an overview. *Renew Sustain Energy Rev* 2013;18:134–143.
- [7] Jahirul MI, Rasul MG, Chowdhury AA, Ashwath N. Biofuels production through biomass pyrolysis—a technological review. *Energies* 2012;5:4952–5001.
- [8] Hossain AK, Davies PA. Pyrolysis liquids and gases as alternative fuels in internal combustion engines--A review. *Renew Sustain Energy Rev* 2013;21:165–189.
- [9] Eisentraut A. Sustainable production of second-generation biofuels 2010.
- [10] Xiu S, Shahbazi A. Bio-oil production and upgrading research: A review. *Renew Sustain Energy Rev* 2012;16:4406–4414.
- [11] Balat M, Ayar G. Biomass energy in the world, use of biomass and potential trends. *Energy Sources* 2005;27:931–940.
- [12] Vamvuka D. Bio-oil, solid and gaseous biofuels from biomass pyrolysis processes—An overview. *Int J Energy Res* 2011;35:835–862.
- [13] Bridgwater T. Biomass for energy. *J Sci Food Agric* 2006;86:1755–1768.
- [14] Vitolo S, Seggiani M, Frediani P, Ambrosini G, Politi L. Catalytic upgrading of pyrolytic oils to fuel over different zeolites. *Fuel* 1999;78:1147–1159.
- [15] Abnisa F, Daud WMAW. A review on co-pyrolysis of biomass: an optional technique to obtain a high-grade pyrolysis oil. *Energy Convers Manag* 2014;87:71–85.
- [16] Zhang Q, Chang J, Wang T, Xu Y. Review of biomass pyrolysis oil properties and upgrading research. *Energy Convers Manag* 2007;48:87–92.
- [17] Toba M, Abe Y, Kuramochi H, Osako M, Mochizuki T, Yoshimura Y. Hydrodeoxygenation of Waste Vegetable Oil over Sulfide Catalysts. *Catal Today* 2011;164:533–537.
- [18] Joshi N, Lawal A. Hydrodeoxygenation of pyrolysis oil in a microreactor. *Chem Eng Sci* 2012;74:1–8.
- [19] Abnisa F, Daud WMAW, Sahu JN. Pyrolysis of mixtures of palm shell and polystyrene: An optional method to produce a high-grade of pyrolysis oil. *Environ Prog Sustain Energy*

2014;33:1026–1033.

- [20] Dewangan A, Pradhan D, Singh RK. Co-pyrolysis of sugarcane bagasse and low-density polyethylene: Influence of plastic on pyrolysis product yield. *Fuel* 2016;185:508–516.
- [21] Panda AK, Singh RK, Mishra DK. Thermolysis of waste plastics to liquid fuel A suitable method for plastic waste management and manufacture of value added products—A world prospective. *Renew Sustain Energy Rev* 2010;14:233–248..
- [22] Brebu M, Spiridon I. Co-pyrolysis of LignoBoost® lignin with synthetic polymers. *Polym Degrad Stab* 2012;97:2104–2109.
- [23] Ye JL, Cao Q, Zhao YS. Co-pyrolysis of polypropylene and biomass. *Energy Sources, Part A* 2008;30:1689–1697.
- [24] Marin N, Collura S, Sharypov VI, Beregovtsova NG, Baryshnikov S V, Kutnetzov BN, et al. Copyrolysis of wood biomass and synthetic polymers mixtures. Part II: characterisation of the liquid phases. *J Anal Appl Pyrolysis* 2002;65:41–55.
- [25] V.I Sharypova, N.G Beregovtsova, B.N Kuznetsova, L Membradob, V.L Cebollab, N Marinc J. W. Co-pyrolysis of wood biomass and synthetic polymers mixtures. Part III: Characterisation of heavy products. *J Anal Appl Pyrolysis* 2003;67:325–340.
- [26] Sharypov VI, Beregovtsova NG, Kuznetsov BN, Baryshnikov S V, Cebolla VL, Weber J V, et al. Co-pyrolysis of wood biomass and synthetic polymers mixtures: Part IV: Catalytic pyrolysis of pine wood and polyolefinic polymers mixtures in hydrogen atmosphere. *J Anal Appl Pyrolysis* 2006;76:265–270.
- [27] Jeon MJ, Choi SJ, Yoo KS, Ryu C, Park SH, Lee JM, et al. Copyrolysis of block polypropylene with waste wood chip. *Korean J Chem Eng* 2011.
- [28] Aboulkas A, Makayssi T, Bilali L, Nadifiyine M, Benchanaa M, others. Co-pyrolysis of oil shale and High density polyethylene: Structural characterization of the oil. *Fuel Process Technol* 2012;96:203–208.
- [29] Önal E, Uzun BB, Pütün AE. Bio-oil production via co-pyrolysis of almond shell as biomass and high density polyethylene. *Energy Convers Manag* 2014;78:704–710.
- [30] Zhang H, Nie J, Xiao R, Jin B, Dong C, Xiao G. Catalytic co-pyrolysis of biomass and different plastics (polyethylene, polypropylene, and polystyrene) to improve hydrocarbon yield in a fluidized-bed reactor. *Energy and Fuels* 2014;28:1940–1947.
- [31] Gupta A, Chaudhary R, Sharma S. Potential applications of mahua (*Madhuca indica*) biomass. *Waste and Biomass Valorization* 2012;3:175–189.
- [32] Bardalai M. A Review of Physical Properties of Biomass Pyrolysis Oil. *Int J Renew Energy Res* 2015;5:277–286.
- [33] Lu Q, Li W-Z, Zhu X-F. Overview of fuel properties of biomass fast pyrolysis oils. *Energy Convers Manag* 2009;50:1376–1383.
- [34] Fahmi R, Bridgwater A V, Darvell LI, Jones JM, Yates N, Thain S, et al. The effect of alkali metals on combustion and pyrolysis of *Lolium* and *Festuca* grasses, switchgrass and willow. *Fuel* 2007;86:1560–9.
- [35] Özçimen D. An approach to the characterization of biochar and bio-oil. *Renew Energy Sustain Futur iConcept Press* 2013:41–58.

- [36] Gopakumar ST. Bio-oil Production through Fast Pyrolysis and Upgrading to “Green” Transportation Fuels. Auburn University, 2012.
- [37] Xu Y, Li W, Hu X, Shi Y. Preparation and characterization of bio-oil from biomass. Intech Open Access Publisher; 2011.
- [38] Lehto J, Oasmaa A, Solantausta Y, Kytö M, Chiaramonti D. Fuel oil quality and combustion of fast pyrolysis bio-oils. VTT Publ 2013;79.
- [39] Bridgwater A V, Meier D, Radlein D. An overview of fast pyrolysis of biomass. Org Geochem 1999;30:1479–1493.
- [40] Basu P. Biomass gasification and pyrolysis: practical design and theory. Academic press; 2010.
- [41] Bridgwater A V. Review of fast pyrolysis of biomass and product upgrading. Biomass and Bioenergy 2012;38:68–94.
- [42] Maher KD, Bressler DC. Pyrolysis of triglyceride materials for the production of renewable fuels and chemicals. Bioresour Technol 2007;98:2351–2368.
- [43] Wang Shu-Rong, Luo Zhong-Yang, Tan Hong, Hong Jun, Dong Liang-Jie, Fang Meng-Xiang, Cen Ke-Fa. The analyses of characteristics of bio-oil produced From Biomass By Flash Pyrolysis. J Eng Thermophys 2004;25:1049–1052.
- [44] Capunitan JA, Capareda SC. Assessing the potential for biofuel production of corn stover pyrolysis using a pressurized batch reactor. Fuel 2012;95:563–572.
- [45] S.-P. Zhang, Y.-J. Yan, Z.-W. Ren T-CL. Analysis of liquid product obtained by the fast pyrolysis of biomass. J East China Univ Sci Technol 2001;27:666–668.
- [46] Xiu S, Shahbazi A. Bio-oil production and upgrading research: A review. Renew Sustain Energy Rev 2012;16:4406–4414.
- [47] Tian Q, Li N, Liu J, Wang M, Deng J, Zhou J, et al. Catalytic Hydrogenation of Alkali Lignin to Bio-oil Using Fullerene-like Vanadium Sulfide. Energy & Fuels 2015;29:255–261.
- [48] Hester RE, Harrison RM. Waste as a Resource. Royal Society of Chemistry; 2013.
- [49] Bridgwater A V. Production of high grade fuels and chemicals from catalytic pyrolysis of biomass. Catal Today 1996;29:285–295.
- [50] Elliott DC. Historical developments in hydroprocessing bio-oils. Energy & Fuels 2007;21:1792–1815.
- [51] Huber GW, Iborra S, Corma A. Synthesis of transportation fuels from biomass: Chemistry, catalysts, and engineering. Chem Rev 2006;106:4044–4098.
- [52] Birtill J. Catalysis for renewables: From feedstock to energy production. Platin Met Rev 2008;52:229–30.
- [53] Guo X, Yan Y, Li T, Ren Z, Yuan C. Catalytic cracking of bio-oil from biomass pyrolysis. CHINESE J Process Eng 2003;3:95.
- [54] Horne PA, Williams PT. Upgrading of biomass-derived pyrolytic vapours over zeolite ZSM-5 catalyst: effect of catalyst dilution on product yields. Fuel 1996;75:1043–1050.

- [55] Olazar M, Aguado R, Bilbao J, Barona A. Pyrolysis of sawdust in a conical spouted-bed reactor with a HZSM-5 catalyst. *AIChE J* 2000;46:1025–1033.
- [56] Ortiz-Toral PJ. Steam reforming of bio-oil: Effect of bio-oil composition and stability. Digital Repository@ Iowa State University, 2008.
- [57] Czernik S, French R, Feik C, Chornet E. Hydrogen by catalytic steam reforming of liquid byproducts from biomass thermoconversion processes. *Ind & Eng Chem Res* 2002;41:4209–4215.
- [58] Galdámez JR, Garcia L, Bilbao R. Hydrogen production by steam reforming of bio-oil using coprecipitated Ni-Al catalysts. Acetic acid as a model compound. *Energy & Fuels* 2005;19:1133–42.
- [59] Chattanathan SA, Adhikari S, Abdoulmoumine N. A review on current status of hydrogen production from bio-oil. *Renew Sustain Energy Rev* 2012;16:2366–2372.
- [60] Cemek M, Küçük MM. Liquid products from *Verbascum* stalk by supercritical fluid extraction. *Energy Convers Manag* 2001;42:125–130.
- [61] Ogi T, Minowa T, Dote Y, Yokoyama S-Y. Characterization of oil produced by the direct liquefaction of Japanese oak in an aqueous 2-propanol solvent system. *Biomass and Bioenergy* 1994;7:193–199.
- [62] Ikura M, Stanciulescu M, Hogan E. Emulsification of pyrolysis derived bio-oil in diesel fuel. *Biomass and Bioenergy* 2003;24:221–232.
- [63] Peng J, Fan Z, Chen G. Thermochemical Conversion Technology on Lignocellulosic Biomass to Liquid Fuel: A Critical Review. *Power Energy Eng. Conf. (APPEEC)*, 2011 Asia-Pacific, 2011, 1–6.
- [64] Xu C, Etcheverry T. Hydro-liquefaction of woody biomass in sub-and super-critical ethanol with iron-based catalysts. *Fuel* 2008;87:335–345.
- [65] Patel RN, Bandyopadhyay S, Ganesh A. A simple model for super critical fluid extraction of bio oils from biomass. *Energy Convers Manag* 2011;52:652–657.
- [66] Xu J, Jiang J, Sun Y, LU Y. A novel method of upgrading bio-oil by reactive rectification. *J Fuel Chem Technol* 2008;36:421–425.
- [67] Ye J, Liu C, Fu Y, Peng S, Chang J. Upgrading bio-oil: Simultaneous catalytic esterification of acetic acid and alkylation of acetaldehyde. *Energy & Fuels* 2014;28:4267–72.
- [68] Junming X, Jianchun J, Yunjuan S, Yanju L. Bio-oil upgrading by means of ethyl ester production in reactive distillation to remove water and to improve storage and fuel characteristics. *Biomass and Bioenergy* 2008;32:1056–1061.
- [69] Milina M, Mitchell S, Pérez-Ram J. Prospectives for bio-oil upgrading via esterification over zeolite catalysts. *Catal Today* 2014;235:176–183.
- [70] Martinez JD, Veses A, Mastral AM, Murillo R, Navarro M V, Puy N, et al. Co-pyrolysis of biomass with waste tyres: upgrading of liquid bio-fuel. *Fuel Process Technol* 2014;119:263–271.
- [71] Brebu M, Ucar S, Vasile C, Yanik J. Co-pyrolysis of pine cone with synthetic polymers. *Fuel* 2010;89:1911–1918.

- [72] Zhang X, Lei H, Chen S, Wu J. Catalytic co-pyrolysis of lignocellulosic biomass with polymers: a critical review. *Green Chem* 2016.
- [73] Rotliwala YC, Parikh PA. Study on thermal co-pyrolysis of jatropha deoiled cake and polyolefins. *Waste Manag & Res* 2011;29:1251–1261.
- [74] Kuppens T, Cornelissen T, Carleer R, Yperman J, Schreurs S, Jans M, et al. Economic assessment of flash co-pyrolysis of short rotation coppice and biopolymer waste streams. *J Environ Manage* 2010;91:2736–2747.
- [75] Kunwar B, Cheng HN, Chandrashekar SR, Sharma BK. Plastics to fuel: a review. *Renew Sustain Energy Rev* 2016;54:421–428.
- [76] www.statista.com Global plastic production _ Statistic n.d.
- [77] Sharuddin SDA, Abnisa F, Daud WMAW, Aroua MK. A review on pyrolysis of plastic wastes. *Energy Convers Manag* 2016;115:308–326.
- [78] Panda AK. Studies on process optimization for production of liquid fuels from waste plastics. 2011.
- [79] Al-Salem SM, Lettieri P, Baeyens J. The valorization of plastic solid waste (PSW) by primary to quaternary routes: From re-use to energy and chemicals. *Prog Energy Combust Sci* 2010;36:103–129.
- [80] Sun J-P, Sui S-J, Zhang Z-J, Tan S, Wang Q-W. Study on the pyrolytic behavior of wood-plastic composites using Py-GC/MS. *BioResources* 2013;8:6196–6210.
- [81] Ojha DK, Vinu R. Fast co-pyrolysis of cellulose and polypropylene using Py-GC/MS and Py-FT-IR. *RSC Adv* 2015;5:66861–66870.
- [82] Rutkowski P, Kubacki A. Influence of polystyrene addition to cellulose on chemical structure and properties of bio-oil obtained during pyrolysis. *Energy Convers Manag* 2006;47:716–731.
- [83] Shadangi KP, Mohanty K. Co-pyrolysis of Karanja and Niger seeds with waste polystyrene to produce liquid fuel. *Fuel* 2015;153:492–498.
- [84] Cornelissen T, Jans M, Yperman J, Reggers G, Schreurs S, Carleer R. Flash co-pyrolysis of biomass with polyhydroxybutyrate: Part 1. Influence on bio-oil yield, water content, heating value and the production of chemicals. *Fuel* 2008;87:2523–2532.
- [85] Cornelissen T, Yperman J, Reggers G, Schreurs S, Carleer R. Flash co-pyrolysis of biomass with polylactic acid. Part 1: Influence on bio-oil yield and heating value. *Fuel* 2008;87:1031–41.
- [86] Cornelissen T, Jans M, Stals M, Kuppens T, Thewys T, Janssens GK, et al. Flash co-pyrolysis of biomass: The influence of biopolymers. *J Anal Appl Pyrolysis* 2009;85:87–97.
- [87] Önal E, Uzun BB, Pütün AE. An experimental study on bio-oil production from co-pyrolysis with potato skin and high-density polyethylene (HDPE). *Fuel Process Technol* 2012;104:365–370.
- [88] Demirbas A. Pyrolysis mechanisms of biomass materials. *Energy Sources, Part A* 2009;31:1186–1193.
- [89] Jakab E, Varhegyi G, Faix O. Thermal decomposition of polypropylene in the presence of

- wood-derived materials. *J Anal Appl Pyrolysis* 2000;56:273–285.
- [90] Jakab E, Blazs M, Faix O. Thermal decomposition of mixtures of vinyl polymers and lignocellulosic materials. *J Anal Appl Pyrolysis* 2001;58–59:49–62.
- [91] Johannes I, Tiikma L, Luik H. Synergy in co-pyrolysis of oil shale and pine sawdust in autoclaves. *J Anal Appl Pyrolysis* 2013;104:341–352.
- [92] Fei J, Zhang J, Wang F, Wang J. Synergistic effects on co-pyrolysis of lignite and high-sulfur swelling coal. *J Anal Appl Pyrolysis* 2012;95:61–67.
- [93] ICAR - Indian Institute of Oilseeds Research. Database on Area, Production and Productivity of Oilseeds from 1949-1450 to 2013-14 n.d.
- [94] Pradhan D, Singh RK, Bendu H, Mund R. Pyrolysis of Mahua seed (*Madhuca indica*) – Production of biofuel and its characterization. *Energy Convers Manag* 2016;108:529–38.
- [95] Gupta A, Kumar A, Sharma S, Vijay VK. Comparative evaluation of raw and detoxified mahua seed cake for biogas production. *Appl Energy* 2013;102:1514–1521.
- [96] Shadangi KP, Mohanty K. Comparison of yield and fuel properties of thermal and catalytic Mahua seed pyrolytic oil. *Fuel* 2014;117:372–380.
- [97] Raheem A, Wan Azlina WAKG, Taufiq Yap YH, Danquah MK, Harun R. Thermochemical conversion of microalgal biomass for biofuel production. *Renew Sustain Energy Rev* 2015;49:990–999.
- [98] Kader MA, Islam MR, Parveen M, Haniu H, Takai K. Pyrolysis decomposition of tamarind seed for alternative fuel. *Bioresour Technol* 2013;149:1–7.
- [99] Uçar S, Karagöz S. The slow pyrolysis of pomegranate seeds: The effect of temperature on the product yields and bio-oil properties. *J Anal Appl Pyrolysis* 2009;84:151–156.
- [100] Onay O, Koçkar OM. Pyrolysis of rapeseed in a free fall reactor for production of bio-oil. *Fuel* 2006;85:1921–1928.
- [101] Garg R, Anand N, Kumar D. Pyrolysis of babool seeds (*Acacia nilotica*) in a fixed bed reactor and bio-oil characterization. *Renew Energy* 2016;96:167–171.
- [102] Nayan NK, Kumar S, Singh RK. Production of the liquid fuel by thermal pyrolysis of neem seed. *Fuel* 2013;103:437–443.
- [103] Sinha R, Kumar S, Singh RK. Production of biofuel and biochar by thermal pyrolysis of linseed seed. *Biomass Convers Biorefinery* 2013;3:327–335.
- [104] Seal S, Panda AK, Kumar S, Singh RK. Production and characterization of bio oil from cotton seed. *Environ Prog Sustain Energy* 2015;34: 542-547
- [105] Singh RK, Shadangi KP. Liquid fuel from castor seeds by pyrolysis. *Fuel* 2011;90:2538–44.
- [106] Panda AK, Gouda N, Singh RK, Patel RK. Fast pyrolysis of Kaner (*Thevetia peruviana*) Seed to Fuel and Chemicals. *Int J Anal Appl Chem* 2015;1:7–20.
- [107] Nayan NK, Kumar S, Singh RK. Characterization of the liquid product obtained by pyrolysis of karanja seed. *Bioresour Technol* 2012;124:186–189.
- [108] Earth resources n.d. www.earthresource.org.

- [109] Gu R, Lee O, Salehzadah Y. An investigation into Polystyrene Recycling at UBC 2010.
- [110] Kositkanawuth K, Sattler ML, Dennis B. Pyrolysis of macroalgae and polystyrene: A review. *Curr Sustain Energy Reports* 2014;1:121–128.
- [111] United Nations Environment Programme. Converting Waste Plastics into a Resource Compendium of Technologies. 2009..
- [112] Total MSW, Total MSW. Municipal solid waste generation, recycling, and disposal in the United States: facts and figures for 2012 2007.
- [113] Siddiqui MN, Redhwi HH. Pyrolysis of mixed plastics for the recovery of useful products. *Fuel Process Technol* 2009;90:545–552.
- [114] Onwudili JA, Insura N, Williams PT. Composition of products from the pyrolysis of polyethylene and polystyrene in a closed batch reactor: Effects of temperature and residence time. *J Anal Appl Pyrolysis* 2009;86:293–303.
- [115] Slopiecka K, Bartocci P, Fantozzi F. Thermogravimetric analysis and kinetic study of poplar wood pyrolysis. *Appl Energy* 2012;97:491–497.
- [116] Khawam A. Application of solid-state kinetics to desolvation reactions 2007.
- [117] Khawam A, Flanagan DR. Complementary use of model-free and modelistic methods in the analysis of solid-state kinetics. *J Phys Chem B* 2005;109:10073–10080.
- [118] Opfermann JR, Kaisersberger E, Flammersheim HJ. Model-free analysis of thermoanalytical data-advantages and limitations. *Thermochim Acta* 2002;391:119–127.
- [119] Pinthong P, Duangchan A, Anantawaraskul S, Phanawadee P. Co-pyrolysis of Rice Husk, Polyethylene and Polypropylene Mixtures: A Kinetic Study. 2009.
- [120] Rotliwala YC, Parikh PA. Thermal degradation of rice-bran with high density polyethylene: A kinetic study. *Korean J Chem Eng* 2011;28:788–792.
- [121] Oyedun AO, Tee CZ, Hanson S, Hui CW. Thermogravimetric analysis of the pyrolysis characteristics and kinetics of plastics and biomass blends. *Fuel Process Technol* 2014;128:471–481.
- [122] Oyedun AO, Gebreegziabher TG, Hui CW. Co-pyrolysis of biomass and plastics waste: a modelling approach. *Chem Eng Trans* 2013;35:883.
- [123] Aboulkas A, others. Kinetic and mechanism of Tarfaya (Morocco) oil shale and LDPE mixture pyrolysis. *J Mater Process Technol* 2008;206:16–24.
- [124] Yang SI, Hsu TC, Wu CY, Chen KH, Hsu YL, Li YH. Application of biomass fast pyrolysis part II: The effects that bio-pyrolysis oil has on the performance of diesel engines. *Energy* 2014;66:172–80.
- [125] Volli V, Singh RK, Murugan S. The use of mustard cake pyrolytic oil blends as fuel in a diesel engine. *Waste and Biomass Valorization* 2014;5:661–668.
- [126] Yang Y, Brammer JG, Ouadi M, Samanya J, Hornung A, Xu HM, et al. Characterisation of waste derived intermediate pyrolysis oils for use as diesel engine fuels. *Fuel* 2013;103:247–57.
- [127] Bridgwater A V, Bridge SA. A review of biomass pyrolysis and pyrolysis technologies. *Biomass pyrolysis Liq. Upgrad. Util., Springer; 1991, 11–92.*

- [128] Ververis C, Georghiou K, Danielidis D, Hatzinikolaou DG, Santas P, Santas R, et al. Cellulose, hemicelluloses, lignin and ash content of some organic materials and their suitability for use as paper pulp supplements. *Bioresour Technol* 2007;98:296–301.
- [129] Kopsch H. Thermal methods in petroleum analysis. John Wiley & Sons; 2008.
- [130] Lapuerta M, Ballesteros R, Rodríguez-Fernández J. Thermogravimetric analysis of diesel particulate matter. *Meas Sci Technol* 2007;18:650–658.
- [131] Asadullah M, Rahman MA, Ali MM, Motin MA, Sultan MB, Alam MR, et al. Jute stick pyrolysis for bio-oil production in fluidized bed reactor. *Bioresour Technol* 2008;99:44–50.
- [132] Omar R, Idris A, Yunus R, Khalid K, Isma MIA. Characterization of empty fruit bunch for microwave-assisted pyrolysis. *Fuel* 2011;90:1536–1544.
- [133] Çepeliougullar Ö, Pütün AE. Thermal and kinetic behaviors of biomass and plastic wastes in co-pyrolysis. *Energy Convers Manag* 2013;75:263–70.
- [134] Onay O. Influence of pyrolysis temperature and heating rate on the production of bio-oil and char from safflower seed by pyrolysis, using a well-swept fixed-bed reactor. *Fuel Process Technol* 2007;88:523–531.
- [135] Lee K-H. Pyrolysis of waste polystyrene and high-density polyethylene. INTECH Open Access Publisher; 2012.
- [136] Oasmaa A, Czernik S. Fuel oil quality of biomass pyrolysis oils state of the art for the end users. *Energy & Fuels* 1999;13:914–921.
- [137] Demirbas A. Fuel properties of pyrolysis oils from biomass. *Energy Sources, Part A Recover Util Environ Eff* 2009;31:412–419.
- [138] Sarma AK, Tyagi SK, Yadav YK. Recent Advances in Bioenergy Research Volume III Editors Sachin Kumar 2014.
- [139] Litescu S-C, Tache A, Teodor ED, Radu G-L, Truica G-I. Fourier Transform Infrared Spectroscopy-Useful Analytical Tool for Non-Destructive Analysis. INTECH Open Access Publisher; 2012.
- [140] Kar Y. Co-pyrolysis of walnut shell and tar sand in a fixed-bed reactor. *Bioresour Technol* 2011;102:9800–9805.
- [141] Sinağ A, Sungur M, Güllü M, Canel M. Characterization of the liquid phase obtained by copyrolysis of Mustafa Kemal (MKP) lignite (Turkey) with low density polyethylene. *Energy & Fuels* 2006;5:2093–2098.
- [142] Nanda S, Mohanty P, Kozinski JA, Dalai AK. Physico-chemical properties of bio-oils from pyrolysis of lignocellulosic biomass with high and slow heating rate. *Energy Environ Res* 2014;4:21.
- [143] Leonardis I, Chiaberge S, Fiorani T, Spera S, Battistel E, Bosetti A. Characterization of bio-oil from hydrothermal liquefaction of organic waste by NMR spectroscopy and FTICR mass spectrometry. *ChemSusChem* 2013;6:160–167.
- [144] Bhattascharya P, Steele PH, El Barbary MH, Mitchell B, Ingram L, Pittman CU. Wood/plastic copyrolysis in an auger reactor: Chemical and physical analysis of the products. *Fuel* 2009;88:1251–60.

- [145] Duman G, Okutucu C, Ucar S, Stahl R, Yanik J. The slow and fast pyrolysis of cherry seed. *Bioresour Technol* 2011;102:1869–1878.
- [146] Duku MH, Gu S, Hagan E Ben. Biochar production potential in Ghana—A review. *Renew Sustain Energy Rev* 2011;15:3539–3551.
- [147] Sohi SP, Krull E, Lopez-Capel E, Bol R. A review of biochar and its use and function in soil. *Adv Agron* 2010;105:47–82.
- [148] Lehmann J, Rillig MC, Thies J, Masiello CA, Hockaday WC, Crowley D. Biochar effects on soil biota - A review. *Soil Biol Biochem* 2011;43:1812–1836.
- [149] Abdullah H, Wu H, Bio-char as a Fuel:1. Properties and grindability of biochars produced from the pyrolysis of mallee wood under slow-heating conditions *Energy & Fuels* 2009;23:4174–4181.
- [150] Rout T, Pradhan D, Singh RK, Kumari N. Exhaustive study of products obtained from coconut shell pyrolysis. *J Environ Chem Eng* 2016;4:3696-3705.
- [151] Brebu M, Vasile C. Thermal degradation of lignin—a review. *Cellul Chem & Technol* 2010;44:353.
- [152] Abnisa F, Arami-Niya A, Daud WMAW, Sahu JN, Noor IM. Utilization of oil palm tree residues to produce bio-oil and bio-char via pyrolysis. *Energy Convers Manag* 2013;76:1073–1082.
- [153] Hammes K, Smernik RJ, Skjemstad JO, Schmidt MWI. Characterisation and evaluation of reference materials for black carbon analysis using elemental composition, colour, BET surface area and ¹³C NMR spectroscopy. *Appl Geochemistry* 2008;23:2113–2122.
- [154] Speight JG. *Handbook of Coal Analysis*. A John Wiley & Sons. Inc, Publ USA 2005.
- [155] Tan KH. *Principles of soil chemistry*. CRC press; 2010.
- [156] Yuan J-H, Xu R-K, Zhang H. The forms of alkalis in the biochar produced from crop residues at different temperatures. *Bioresour Technol* 2011;102:3488–3497.
- [157] Nartey OD, Zhao B. Biochar preparation, characterization, and adsorptive capacity and its effect on bioavailability of contaminants: an overview. *Adv Mater Sci Eng* 2014;2014.
- [158] Viswanathan B, Neel PI, Varadarajan TK. *Methods of activation and specific applications of carbon materials*. India, Chennai 2009.
- [159] Ebrahimi-Kahrizsangi R, Abbasi MH. Evaluation of reliability of Coats-Redfern method for kinetic analysis of non-isothermal TGA. *Trans Nonferrous Met Soc China* 2008;18:217–221.
- [160] Zhou L, Wang Y, Huang Q, Cai J. Thermogravimetric characteristics and kinetic of plastic and biomass blends co-pyrolysis. *Fuel Process Technol* 2006;87:963–969..
- [161] Han B, Chen Y, Wu Y, Hua D, Chen Z, Feng W, et al. Co-pyrolysis behaviors and kinetics of plastics--biomass blends through thermogravimetric analysis. *J Therm Anal Calorim* 2014;115:227–35.
- [162] Suriapparao D V, Ojha DK, Ray T, Vinu R. Kinetic analysis of co-pyrolysis of cellulose and polypropylene. *J Therm Anal Calorim* 2014;117:1441–51.
- [163] Chin BLF, Yusup S, Al Shoaibi A, Kannan P, Srinivasakannan C, Sulaiman SA. Kinetic

- studies of co-pyrolysis of rubber seed shell with high density polyethylene. *Energy Convers Manag* 2014;87:746–753.
- [164] Aboulkas A, Nadifiyine M, Benchanaa M, Mokhlisse A, others. Pyrolysis kinetics of olive residue/plastic mixtures by non-isothermal thermogravimetry. *Fuel Process Technol* 2009;90:722–728.
- [165] Brigewater A V. Innovative technologies for conversion of biomass. *Energy Fuels* 1992;6:113–120.
- [166] Williams PT, Ahmad N. Influence of process conditions on the pyrolysis of Pakistani oil shales. *Fuel* 1999;78:653–662.
- [167] Ebrahimi Kahrizsangi R, Abbasi MH, Saidi A. Model-fitting approach to kinetic analysis of non-isothermal oxidation of molybdenite. *Iran J Chem Chem Eng* 2007;26:119–123.
- [168] Blaine RL, Kissinger HE. Homer Kissinger and the Kissinger equation. *Thermochim Acta* 2012;540:1–6.
- [169] Ozawa T. A new method of analyzing thermogravimetric data. *Bull Chem Soc Jpn* 1965;38:1881–6.
- [170] Flynn JH, Wall LA. A quick, direct method for the determination of activation energy from thermogravimetric data. *J Polym Sci Part B Polym Lett* 1966;4:323–328.
- [171] Radhakumari M, Prakash DJ, Satyavathi B. Pyrolysis characteristics and kinetics of algal biomass using tga analysis based on ICTAC recommendations. *Biomass Convers Biorefinery* 2016;6:189–195.
- [172] Chen C, Ma X, He Y. Co-pyrolysis characteristics of microalgae *Chlorella vulgaris* and coal through TGA. *Bioresour Technol* 2012;117:264–273.
- [173] Kissinger HE. Variation of peak temperature with heating rate in differential thermal analysis. *J Res Natl Bur Stand (1934)* 1956;57:217–221.
- [174] Akahira T, Sunose T. Joint convention of four electrical institutes. *Res Rep Chiba Inst Technol* 1971;16:22–31.
- [175] Sharara MA, Holeman N, Sadaka SS, Costello TA. Pyrolysis kinetics of algal consortia grown using swine manure wastewater. *Bioresour Technol* 2014;169:658–666.
- [176] Babu B V. Biomass pyrolysis: a state-of-the-art review. *Biofuels, Bioprod Biorefining* 2008;2:393–414.
- [177] Chhiti Y, Kemiha M. Thermal conversion of biomass, pyrolysis and gasification: a review. *Int J Eng Sci* 2013;2:75–85.
- [178] Solantausta Y, Nylund N-O, Westerholm M, Koljonen T, Oasmaa A. Wood-pyrolysis oil as fuel in a diesel-power plant. *Bioresour Technol* 1993;46:177–188.
- [179] Cao L, Wang J, Liu K, Han S. Ethyl acetoacetate: A potential bio-based diluent for improving the cold flow properties of biodiesel from waste cooking oil. *Appl Energy* 2014;114:18–21.
- [180] Sambusiti C, Monlau F, Ficara E, Carrère H, Malpei F. A comparison of different pre-treatments to increase methane production from two agricultural substrates. *Appl Energy* 2013;104:62–70.

- [181] Singh VK, Soni a. B, Kumar S, Singh RK. Pyrolysis of sal seed to liquid product. *Bioresour Technol* 2014;151:432–435.
- [182] Giannelos PN, Zannikos F, Stournas S, Lois E, Anastopoulos G. Tobacco seed oil as an alternative diesel fuel: physical and chemical properties. *Ind Crops Prod* 2002;16:1–9.
- [183] Peters JF, Petrakopoulou F, Dufour J. Exergy analysis of synthetic biofuel production via fast pyrolysis and hydrouprgrading. *Energy* 2015;79:325–336.
- [184] Prakash R, Singh RK, Murugan S. Experimental investigation on a diesel engine fueled with bio-oil derived from waste wood–biodiesel emulsions. *Energy* 2013;55:610–618.
- [185] Yang SI, Wu MS, Wu CY, Chen KH, Wu TM, Hsu YL, et al. The Performance of a diesel engine blended with coffee bean residue pyrolysis oil. *Adv. Mater. Res* 2012;593:325–32.
- [186] Dauenhauer PJ. Handbook of Plant-Based Biofuels. Edited by Ashok Pandey. *ChemSusChem* 2010;3:386–387.
- [187] Ghadge SV, Raheman H. Biodiesel production from mahua (*Madhuca indica*) oil having high free fatty acids. *Biomass and Bioenergy* 2005;28:601–605.
- [188] Saponins in *Madhuca Longifolia* as undesirable substances in animal feed. *EFSA J* 2009;7.
- [189] Yadav S, Suneja P, Hussain Z, Abraham Z, Mishra SK. Prospects and potential of *Madhuca longifolia* (Koenig) J.F. Macbride for nutritional and industrial purpose. *Biomass and Bioenergy* 2011;35:1539–1544.
- [190] Godiganur S, Murthy CHS, Reddy RP. 6BTA 5.9 G2-1 Cummins engine performance and emission tests using methyl ester mahua (*Madhuca indica*) oil/diesel blends. *Renew Energy* 2009;34:2172–7.
- [191] Yadav S, Suneja P, Hussain Z, Abraham Z, Mishra SK. Genetic variability and divergence studies in seed and oil parameters of mahua (*Madhuca longifolia* Koenig) JF Macbride accessions. *Biomass and Bioenergy* 2011;35:1773–1778.
- [192] Murugan S, Gu S. Research and development activities in pyrolysis--contributions from Indian scientific community--a review. *Renew Sustain Energy Rev* 2015;46:282–95.
- [193] Volli V, Singh RK. Production of bio-oil from mahua de-oiled cake by thermal pyrolysis. *J Renew Sustain Energy* 2012;4:13101.
- [194] Eyres L. Processing contaminants in edible oils: MCPD and glycidyl esters; *Food New Zeal* 2014;14:36.
- [195] Prakash R, Singh RK, Murugan S. Experimental studies on combustion, performance and emission characteristics of diesel engine using different biodiesel bio oil emulsions. *J Energy Inst* 2015;88:64–75.
- [196] Bendu H, Murugan S. Homogeneous charge compression ignition (HCCI) combustion: Mixture preparation and control strategies in diesel engines. *Renew Sustain Energy Rev* 2014;38:732–746.
- [197] Kumar S, Prakash R, Murugan S, Singh RK. Performance and emission analysis of blends of waste plastic oil obtained by catalytic pyrolysis of waste HDPE with diesel in a CI engine. *Energy Convers Manag* 2013;74:323–331.
- [198] Enweremadu CC, Rutto HL. Combustion, emission and engine performance characteristics

- of used cooking oil biodiesel—A review. *Renew Sustain Energy Rev* 2010;14:2863–2873.
- [199] Murugan S, Ramaswamy MC, Nagarajan G. Performance, emission and combustion studies of a DI diesel engine using Distilled Tyre pyrolysis oil-diesel blends. *Fuel Process Technol* 2008;89:152–159.
- [200] Sahin B, Demirbase A, Oèzdemir T, Guellue D, Cieaglar A, Akdeniz F, Upgrading of biomass materials as energy sources: Liquefaction of mosses from Turkey. *Energy Sources* 2000;22:403–8.
- [201] Dahlquist E. Technologies for converting biomass to useful energy: combustion, gasification, pyrolysis, torrefaction and fermentation. CRC Press; 2013.
- [202] Goyal HB, Seal D, Saxena RC. Bio-fuels from thermochemical conversion of renewable resources: A review. *Renew Sustain Energy Rev* 2008;12:504–517.
- [203] Beld B, Holle E, Florijn J. The use of pyrolysis oil and pyrolysis oil derived fuels in diesel engines for CHP applications. *Appl Energy* 2013;102:190–197.
- [204] Lee S, Chen L, Yoshida K, Yoshikawa K. Application of waste biomass pyrolysis oil in a direct injection diesel engine: For a small scale non-grid electrification. *J Energy Power Eng* 2015;9:929–943.
- [205] Hossain AK, Ouadi M, Siddiqui SU, Yang Y, Brammer J, Hornung A, et al. Experimental investigation of performance, emission and combustion characteristics of an indirect injection multi-cylinder CI engine fuelled by blends of de-inking sludge pyrolysis oil with biodiesel. *Fuel* 2013;105:135–42.
- [206] Sharma A, Murugan S. Investigation on the behaviour of a DI diesel engine fueled with *Jatropha Methyl Ester* (JME) and Tyre Pyrolysis Oil (TPO) blends. *Fuel* 2013;108:699–708.
- [207] Park DK, Kim SD, Lee SH, Lee JG. Co-pyrolysis characteristics of sawdust and coal blend in TGA and a fixed bed reactor. *Bioresour Technol* 2010;101:6151–6.
- [208] Nihanthaluvadi, P Vijay, Rishi venkat ram Puli, Yogeswar dadi CVVNP. Diesel engine performance improvement by using cetane improver. *Int J Eng Innov Technol* 2013; 2:179–182.
- [209] Bridgwater A V, Boocock DGB. *Developments in Thermochemical Biomass Conversion: Volume 1. vol. 2.* Springer Science & Business Media; 2013.
- [210] Imtenan S, Masjuki HH, Varman M, Arbab MI, Sajjad H, Fattah IMR, et al. Emission and performance improvement analysis of biodiesel-diesel blends with additives. *Procedia Eng* 2014;90:472–477.
- [211] Schmidt PF. *Fuel oil manual.* vol. 10. Industrial Press Inc.; 1985.
- [212] Boruff PA, Schwab AW, Goering CE, Pryde EH. Evaluation of diesel fuel—ethanol microemulsions. *Trans ASAE* 1982;25:47–53.
- [213] Canakci M, Ozsezen AN, Turkcan A. Combustion analysis of preheated crude sunflower oil in an IDI diesel engine. *Biomass and Bioenergy* 2009;33:760–777.
- [214] Gogoi TK, Baruah DC. The use of Koroch seed oil methyl ester blends as fuel in a diesel engine. *Appl Energy* 2011;88:2713–2725.

Dissemination

Internationally indexed journals

1. **Debalaxmi Pradhan**, R. K. Singh, “Analysis of Bio-Oil Produced by Co-Pyrolysis of Mahua Seed and Polystyrene”, Applied Mechanics and Materials Vol. 787 771-775 2015.
2. **Debalaxmi Pradhan**, R.K. Singh, Harisankar Bendu, Rachna Mund, “Pyrolysis of Mahua seed (*Madhuca indica*) – Production of biofuel and its characterization”, Energy Conversion and Management Vol. 108 529–538 2016.
3. **Debalaxmi Pradhan**, R.K. Singh, Harisankar Bendu, S. Murugan Mahua seed pyrolysis oil blends as an alternative fuel for light-duty diesel engines” Energy 2016. Volume 118, 600-612, 2017.

Other related publication

1. Ashish Dewangan, **Debalaxmi Pradhan**, R.K. Singh,” Co-pyrolysis of sugarcane bagasse and low-density polyethylene: Influence of plastic on pyrolysis product yield” Fuel 185 (2016) 508–516.
2. Tanmya Rout, **Debalaxmi Pradhan**, R.K. Singh, Namrata Kumari, “Exhaustive study of products obtained from coconut shell pyrolysis”, Journal of Environmental Chemical Engineering Vol. 4 3696–3705 2016.

Conferences and Workshop

1. **Debalaxmi Pradhan**, R. K. Singh, “Bio-oil from biomass: Thermal pyrolysis of mahua seed” IEEE International Conference on Energy Efficient Technologies for Sustainability (ICEETS’13) 10-12 April, 2013 at Kanyakumari (India).
2. **Debalaxmi Pradhan** R.K.Singh, “Optimizing The Production Of Liquid Fuel From Co-Pyrolysis Of Mahua Seed And Polystyrene” (ICFCE-2013) 9-11 Dec at NIT, Rourkela
3. **Debalaxmi Pradhan**, R. K. Singh, Co-pyrolysis of Biomass and plastic: An optional method to obtain a high-grade pyrolysis Oil” International Conference on Chemical engineering: Emerging Dimensions and Challenges Ahead 27-30 December 2014, Chandigarh, India.
4. Participated in five Day short term course on “Distributed Multimode Renewable Energy Systems (DMRES-2016)” from 11th -15th April 2016 organized by the Department of Mechanical Engineering, National Institute of Technology Rourkela.

Communicated

1. **Debalaxmi Pradhan**, R.K Singh. S. Murugan Liquid fuel production from co-pyrolysis of biomass/plastic waste and its application in a Diesel engine communicated in Energy Conversion Management.
2. **Debalaxmi Pradhan**, R.K Singh Upgraded bio-oil from co-pyrolysis of Mahua indica and waste polystyrene: Influence of operating conditions on product yield communicated in Energy conversion management.
3. **Debalaxmi Pradhan**, R.K Singh Kinetics study on co-pyrolysis of biomass and plastic waste communicated in Journal of Analytical and Applied pyrolysis